

ISSN 2255-9124 print  
ISSN 2255-9132 online



Scientific Journal  
of Riga Technical University

# **BOUNDARY FIELD PROBLEMS AND COMPUTER SIMULATION**

2014 / 53

Editor-in-Chief Aivars Spalvins

**RTU Press  
RIGA – 2014**

## Editor-in-Chief

Aivars Spalvins, *Dr. sc. ing.*, Riga Technical University, Latvia

## Editorial Board

Andrey Kolyshkin, *Dr. math.*, Riga Technical University, Latvia  
Inta Volodko, *Dr. math.*, Riga Technical University, Latvia  
Ilmars .Iltins, *Dr. sc. ing.*, Riga Technical University, Latvia  
Marija Iltina, *Dr. sc. ing.*, Riga Technical University, Latvia  
Rémi Vaillancourt, *Dr. math.*, University of Ottawa, Canada  
Delfim F. M. Torres, *Dr. math.*, University of Aveiro, Portugal  
Alexander Plakhov, *Dr. math.*, University of Aveiro, Portugal  
Igor Teplyakov, *Dr. sc. ing.*, Joint Institute for High Temperatures, Russia  
Alex Pedchenko, *Dr. sc. ing.*, Coventry University, United Kingdom  
Peter Greber, *Dr. hab. ing.*, Dresden Institute of Technology, Germany  
Roger Thunvik, *Dr. hab. ing.*, Royal Institute of Technology, Sweden  
Olena.V. Mul, *Dr. math.*, Ternopol State Technical University, Ukraine

---

## Managing Editor

Irina Eglite, *M. sc. ing., Mg. math.*, Riga Technical University, Latvia

## Technical Editor

Vladislavs Kremeneckis, *Dr. phys.*, Riga Technical University, Latvia

## Editorial Board Address

Environment Modelling Center  
Faculty of Computer Science and Information Technology  
Riga Technical University

1/4 Meza Street  
Riga, LV-1007  
Latvia

Tel.: +371 67089511  
Fax.: +371 67089531  
E-mail: emc@cs.rtu.lv

## From the Editorial Board

This volume is issued by RTU since 1966. The volume may be of importance to specialists and students interested in computer simulation of various environmental phenomena formulated as boundary field problems.

**Abstracted&Indexed:** *EBSCO, ProQuest and VINITI databases.*

All rights are reserved. No part of this publication may be reproduced, stored, transmitted or disseminated in any form or by any means without prior written permission from Riga Technical University represented by RTU Press to whom all requests to reproduce copyright material should be directed in writing.

## TABLE OF CONTENTS

<i>V. Doroshenko, O. Mul, O. Kravchenko</i> Prospects for Computer-Aided Design of Castings.....	4
<i>V. Koliskina</i> Calculation of Eigenvalues for Eddy Current Testing Problems .....	9
<i>A. Spalvins, J. Slangens, I. Lace, O. Aleksans, K. Krauklis, V. Skibelis, I. Eglite</i> Hydrogeological Model of Latvia After Increasing Density of its Hydrographical Network .....	12
<i>K. Krauklis, J. Slangens</i> Special Software Used for Implementing Elements of Hydrographical Network Into Hydrogeological Model of Latvia .....	25
<i>M. Remizov</i> Forced Oscillations in the System of Anisotropic Stripe-half-plane with Hard and Sliding Connection of the Media. Comparative Characteristics of Properties of Energy Fields .....	30
<i>G. Burov</i> The Optimization Algorithms of the Objective Control of Technical Objects.....	36
<i>A. Spalvins, I. Lace</i> Appliance of Pumping Data of Wells for Obtaining Transmissivity Distributions of Aquifers for Hydrogeological Model of Latvia .....	42
<i>S. Cernajeva</i> Improvement of Teaching Methodology of Mathematics in RTU by Using Video Lectures .....	49



# Prospects for Computer-Aided Design of Castings

Volodymyr Doroshenko<sup>1</sup>, Olena Mul<sup>2</sup>, Olena Kravchenko<sup>3</sup>,

<sup>1</sup>*Physico-Technological Institute of Metals and Alloys,*

<sup>2</sup>*Ternopil National Ivan Puluj Technical University,*

<sup>3</sup>*International Research and Training Center for Information Technologies and Systems*

**Abstract** – In the study on limiting possibilities of a casting process in terms of resource saving it is considered which solid-state constructions can optimally fill the space of the mold. The possibility of designing patterns for the Lost Foam Casting process in accordance with mathematical concepts is shown. The examples of patterns of frame cellular castings are described. The examples of cellular castings, designed with the help of computer technologies, are shown that often inherit structures of nature. Such castings allow expanding of the existing range of properties of metal products.

**Keywords** – Cellular castings, computer simulation, engineering castings, foam patterns, gyroid, lost foam casting, mathematical concepts, minimal surfaces, structures of nature, quasicrystals.

## I. INTRODUCTION

Lost Foam Casting (LFC) into a vacuumized sand mold provided a new look at the metal casting design.

On the one hand, the material of the used foam pattern on a thin section looks under a microscope like a small-cell foam, wherein air is "packed" into thin polystyrene shells and the metal, poured onto the pattern, gasifies these shells and replaces the pattern.

On the other hand, dry sand under vibro- and/or pneumo-impact during the molding process is similar in properties to the "pseudo-liquid", which flows around the pattern. Then the casting pattern can be considered as a construction for the impact of two fluids: the first is the metal, which replaces the pattern from the inside while pouring; the second is the "pseudo-liquid" of sand, which flows around the pattern surface outside during molding.

During research of limiting possibilities of the casting process and optimization of casting constructions in terms of resource saving the following question arose: which solid-state constructions could optimally fill the space, occupy the volume of the mold sand and "spill" in it?

The first clues for the answer are the constructions observed in animate and inanimate nature, as well as models of microstructures of organic and inorganic substances in the form as they are represented in the modern natural sciences.

The main difference between the engineering constructions, proposed by human, and those created by nature is the high energy efficiency of the last ones. Also, in many cases, the difference between them is in the presence of such characteristic properties as repeatability of identical elements in different directions, combinatority (fractality) and cellularity.

In particular, bionics studies the use of organization principles, properties, functions and structures of animate

nature in technical devices. However, in engineering, i.e. creating a prototype of some supposed or possible object, there can be used not only images of animate and inanimate nature but also imaginary, ideal, for example, mathematical models, which in general case do not necessarily have accordance with something in the physical world.

## II. ANALYSIS OF THE LATEST INVESTIGATIONS

This article continues the coverage of examples of both engineering cast frame cellular products and the search for ways to optimize their structure. That includes borrowing "technical solutions" from nature, which solved problems of the space "conquest" by constructions with high efficiency and resource saving.

Earlier the possibility of copying the structures of the simplest crystal lattices in cast products using volumetric prefabricated structures with repetitive unified elements has been described in [1]. The foam patterns of such elements can be produced at automatic formation machines or 3D-mills with the help of computer programs. The simplest and most noticeable in their properties structures were taken as the analogs for engineering the above cast constructions.

At present, computer simulation helps to reflect our conceptions about the world structure and borrow from it some of the details for our own man-made constructions. The basis of our knowledge of chemistry, physics, materials science, earth sciences and others is mainly the knowledge about the substance structure, which largely determines the substance properties. Thus, there arose the problem of creating new materials by calculating their structures on the computer.

Until recently, the problem of predicting the crystal structures on the basis of the chemical composition was considered unsolvable. Traditionally, inventions of new materials for the needs of engineering occurred either by the trial and error method, or just by chance. At present, thanks to the sufficiently high level of development of the quantum theory of materials, creation of new materials with the help of computers has become possible [2].

The stable crystal structure is characterized by the lowest energy. This problem can be solved by investigating all possible relative positions of atoms, calculating the energy for each of them and in this way determining the lowest energy and the optimal structure.

Complexity of the problem lies in the fact that the number of variants in the structure is astronomically large. Directly, this problem is unsolvable. However, it can be solved without exhaustive search but by directing calculations, with the help of self-training, to the global minimum of energy. In this vein,

the approach is developed, based on the ideas of evolution, which is a multidimensional minimization for the search of any thermodynamically stable states [2].

Creation of data analysis methods led crystallographers to the field of multidimensional geometry. Also, similar data analysis, in fact by means of multi-dimensional geometry, is carried out by anthropologists and literary critics. Thus, similar methods are long used by literary critics to determine the authorship of texts as well as by geneticists and anthropologists to determine the kinship among nations based on DNA.

### III. DISCUSSION AND RESULTS

At a junction of different sciences, similar ideas can be applied to a variety of scientific fields. If programs of designing structures of new materials from atoms are created, then by copying the atomic lattices analogically to the examples in [1] one can get their macro-sized foam patterns for spatial lattice castings and develop methods of casting such cellular metal products.

Expanding the range of castings designs and LFC-process allows to open a new direction of casting cellular, volume-cellular and skeletal lattice metal products. Such products have the potential for use as lightweight carriers, reinforcing, insulating, protecting and damping loads spatial constructions, which can absorb or pass through their cells some flow of matter or energy.

The concept of simplification of assembly of cellular casting foam patterns into volumetric structures by using repetitive unified elements of serial production has analogues in various mathematical models.

The whole class of periodical minimal surfaces (MS) can be obtained by repetition of some unit cell. The unit cells of many of such minimal surfaces, in turn, can be "assembled" from the copies of some fundamental element and its specular reflection.

The theory of MS is one of the classical and at the same time developing areas of mathematics at the junction of geometry, topology and calculus of variations. A soap film is the obvious realization of MS: it tightens the contours of different configuration and takes the shape, corresponding to the minimum of potential energy (surface tension energy), which is directly proportional to its area.

One of the remarkable examples of infinitely connecting and repetitive in three dimensions structure with MS is gyroid. It was first described in 1970 by the American physicist Alan Schoen from NASA, who was looking for the ultra-light and durable material for spacecrafts [3].

The surface of the gyroid is described by the following equation:

$$\cos(x) \cdot \sin(y) + \cos(y) \cdot \sin(z) + \cos(z) \cdot \sin(x) = 0.$$

Its sample, obtained in bronze by the investment casting method by sculptor and mathematician Bathsheba Grossman [4], is shown in Fig. 1a).

The reduced jewelry version of the same authorship is

produced using a 3D-printer.

Bodies with the gyroid structure are present in the cells of plants and animals in separate block copolymers at condensation of oligomers.

Scientists explain patterns on the palms, swollen of water, by the gyroid organization of the "skeleton" of the folds from the keratin fibers, which are laid in the skin as if they were in the gyroid cavities.

The gyroid structure (Fig. 1b)) is shown on the website of the Institute of Polymer Science of the University of Ulm [5].

The pattern for the casting in Fig. 1a) is obtained by the assembly from repetitive plates in the form of regular hexagons with a contoured surface, having convex and concave parts. Such plates can be called the fundamental elements. Their shape of a regular hexagon allows it to make them of two, three or six pieces as of repetitive elements in combination with copies of their "specular reflections".

The pattern with the gyroid surface can be assembled without size limitations, using such fundamental elements of only one type.

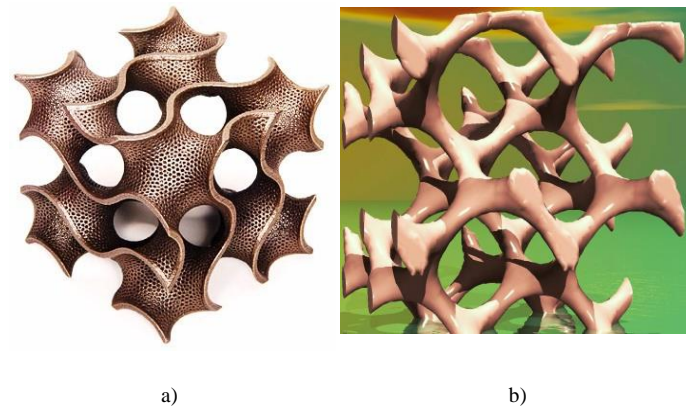


Fig. 1. Samples of constructions with the gyroid structure:  
a) metal casting; b) polymer structure.

For the small-scale production of foam patterns such plates or their above mentioned components can be performed flat and only after being bent by the method [6].

For the serial production of the described patterns it is more effective to produce their repetitive elements at automatic formation machines or in press molds by the autoclave method and then assemble by the known methods: by gluing, by the tongue and groove system and by others.

The casting pattern with MS during molding interacts with sand on the minimum area of its surface, rubbing against the sand, which contributes to the uniform sand compaction.

The MS presence for single patterns increases the number of options for their technological arrangement in the sand of the container mold without the risk of getting undercuts and channels, unfilled by sand.

With decreasing the surface of the mold cavity, there decreases the contact area of the poured metal with this surface, through which the heat from the metal is removed into the sand environment. This improves the fillability of the mold by the metal.

For the same reasons the minimal surfaces principle is effective for designing patterns of gating systems. Oval

outlines of the casting reduce the probability of cracking because of the hindered shrinkage of the casting.

On the website [4] it is indicated that the gyroid model is built using the freely available software Surface Evolver, created by Kenneth Brakke. The search of the minimum area surface or the total energy of the surface tension is only the simplest application of this software.

With its help, when designing castings or optimizing the constructions to improve their processability for any type of molding, it is possible to build the "minimal" surfaces in terms of more complex functionals. Such functional can be a combination of surface tension energy, gravitational energy, flexural deformation energy, etc., as well as arbitrary user-defined surface integrals [7]. This makes it possible to obtain not only the drawing of the pattern with the MS on the computer, but also the MS in combination with the specified service characteristics of the casting.

In particular, during LFC such drawing can be sent directly to a computer-controlled 3D-mill. The latter in the automatic mode will produce the casting pattern or the pattern of its press mold from the foam blocks, for example, from two halves, for the further serial production of casting patterns or their parts with the help of an autoclave or an automatic formation machine.

Surface Evolver, when designing castings, can process objects with arbitrary topology, which are subordinate to various volumetric and boundary connections.

For example, it is possible to fix the volume covered by the surface (isoperimetric problems) or the contact angle on the lines of intersection of the desired surface with some given surface.

For searching the configuration with the minimum energy, this software uses the gradient descent method. It is one of the examples of software that can be used for the MS construction and their combination with other surfaces when engineering the casting patterns or gating systems for various casting processes [7].

Minimal surfaces are analytical, i.e. each of their points in space is determined by an analytical function. This improves processability of: designing and producing the patterns, as well as the equipment for them; the pattern quality control; the casting quality control; the further casting processing with the help of modern equipment with software.

Investigation of the possibility of copying the crystal lattice structure in cast frame cellular constructions using volumetric prefabricated structures with repetitive unified elements [1] has the following sequel. In modern crystallography, when summarizing new studies, the increasing attention is paid not only to traditional crystal structures but also to quasicrystals. Professor Dan Shechtman was awarded the Nobel Prize in Chemistry 2011 for the discovery of quasicrystals.

The structural perfection of thermodynamically stable quasicrystals puts them on a par with the best of ordinary crystals and allows to classifying them as a subclass of crystals. Also, artificial materials with a structure similar to the

structure of quasicrystals were created and they were called quasicrystalline metamaterials. Quasicrystals have very low thermal conductivity and a low coefficient of friction.

A model of the quasicrystal structure may be created based on the Penrose tiling with two "elementary cells" connected to each other according to definite rules of matching [8]. At present, the three-dimensional generalization of the Penrose tiling is being developed, which is the Ammann–Mackay structure. It is composed of narrow and wide rhombohedrons, i.e. hexahedral figures, each face of which is a rhombus.

The "thin" and "thick" rhombuses from the Penrose tiling are shown in Fig. 2, above. In Fig. 2, below, one can see the drawings of the frame patterns of rhombohedrons, filling the space by which analogously to the quasicrystal structure gives the spatial pattern [9]. The examples of ways of mounting for similar frame cellular patterns are shown in [1].

Investigations of quasicrystals stimulated the revival of interest in the ideas and methods of constructing mosaics, which were the subject of study of the mathematical theory, called the "theory of tilings of unbounded plane or volume" [8]. This theory studies isoperimetric problems for polyhedra, finite and infinite partitions into rhombuses, periodical minimal surfaces, 3D-puzzles, fractal trees and others.

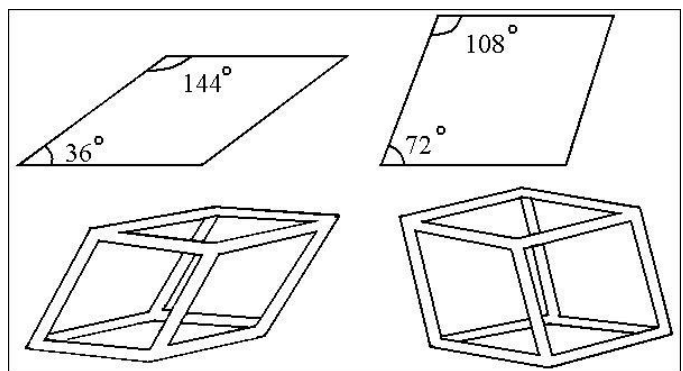


Fig. 2. Above: Rhombs from the Penrose tiling; Below: The frame patterns of rhombohedrons.

In particular, the computer graphics mastered the problems of tiling by the method of curves or surfaces of Bezier, who used them for computer-aided design of car bodies.

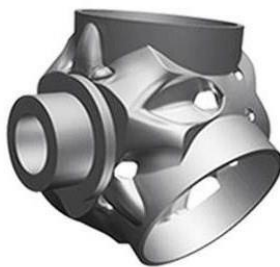
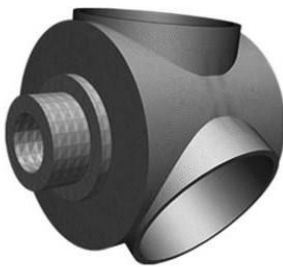
Technologies of software and virtual construction of spatial structures are intensively developing. Description of quasi-periodical structures is formed based on the integration of different disciplines, such as modern geometry, number theory, statistical physics, and also the concept of the golden ratio.

The unexpected appearance of the golden ratio in the structure of quasicrystals indicates the presence of the "living motive" in their symmetry, as far as, in contrast to non-living crystals, only living world accepts outstanding proportions of the golden ratio [8].

Fig. 3 shows the examples, taken from the open Internet sources, with the computer optimization of the construction of six castings.



a)



b)

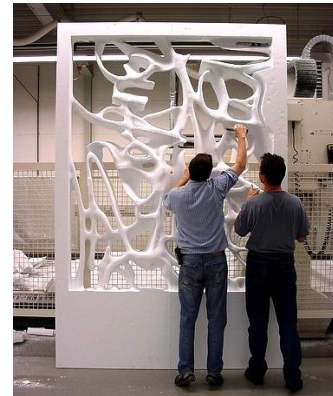
Fig. 3. Examples of computer optimization of the casting constructions.

In Fig. 3a) serial castings are presented at the top of the photo, and the designs of castings, "proposed" by computer,

are shown below. Most of such castings are meant for mounting in the movable structures.

In Fig. 3b) in each couple of images the serial casting is presented on the left, and the casting design, which is computer-optimized according to the requirements for its use, is shown on the right.

Thus, one can see how traditional monolithic constructions "turn" into the elegant frame cellular ones, serving as the illustrative examples of metal saving and appearance improving. The new constructions can be easily carried out by the LFC method.



a)



b)

Fig. 4. Examples of art castings as the architectural decoration: a) the gate pattern; b) sections of aluminium castings of the collage, assembled along the large building in New York.

The above mentioned 3D-mills are increasingly used for the production of single casting patterns from foam.

The examples of large-size patterns for art castings are presented in Fig. 4. Using such patterns, the "graffiti" collage was cast from aluminium as the architectural decoration of the many meters size for the apartment house in the luxury block of New York (the project Herzog & de Meuron, 2006). The prefabricated collage along the front side of the house consists of dozens of castings, including several gates, designed with the help of computer technologies with the thickness of walls, which is optimum for the casting process. In Fig. 4a) it is shown that the pattern of gates and the details of the 3D-mill

can be seen in the background. In Fig. 4b) sections of aluminium castings of the collage are presented.

A new step in obtaining metal products is their production by 3D-printers. The cellular constructions, obtained by 3D-printers according to computer programs, can have quite a fantastic look as it is shown, for example, in Fig. 5, taken from the open Internet sources.

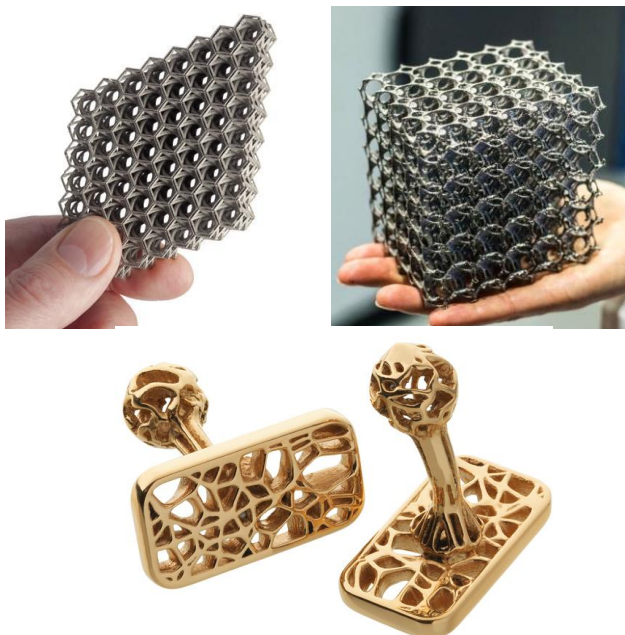


Fig. 5. Examples of constructions obtained by 3D-printing according to the computer programs.

Cellular castings can inherit properties of the nature structures and also can be created by human imagination with the help of computer design according to the human requirements. This significantly expands the existing range of metal products.

#### REFERENCES

- [1] V. S. Doroshenko, "Methods of Obtaining Frame and Cellular Cast Materials and Details by Gasified Patterns," (in Russian), *Liteinoye Proizvodstvo*, vol. 9, pp. 28–32, 2008.
- [2] A. R. Oganov, A. O. Lyakhov, and M. Valle, "How Evolutionary Crystal Structure Prediction Works – and Why," *Acc. Chem. Res.*, vol. 44, pp. 227–237, 2011. <http://dx.doi.org/10.1021/ar1001318>
- [3] A. H. Schoen, *Infinite Periodic Minimal Surfaces without Self-Intersections*. NASA Technical Note TN D-5541, Washington, D. C., 1970.
- [4] Bathsheba Sculpture [Online] Available: <http://www.bathsheba.com/math/gyroid/> [Accessed: Aug. 5, 2014].
- [5] University of Ulm, Institute of Polymer Science, Germany [Online] Available: [http://polymer.physik.uni-ulm.de/mol\\_graphics/](http://polymer.physik.uni-ulm.de/mol_graphics/) [Accessed: Aug. 5, 2014].
- [6] V. S. Doroshenko, "Spatial Cast Constructions, Obtained in a Volume of Sand (in Russian)," *Metal and Casting of Ukraine*, vol. 7–8, pp. 45–52, 2009.
- [7] V. Meshkov, "Minimal Surfaces and Surface Evolver of Kenneth Brakke (in Russian)," *Vestnik Molodykh Uchenykh*, vol. 1, p. 84, 2004.
- [8] V. S. Belyanyn, "Quasicrystals and the Golden Ratio," (in Russian) *Nauka i Zhizn*, vol. 10, pp. 68–76, 2005.
- [9] V. S. Cherednychenko, *Materials Science. Technology of Construction Materials* (in Russian). 2nd ed., Moscow: Omega-L, 2006.
- [10] V. S. Doroshenko, "Mathematical Design of Frame-Cellular Castings (in Russian)," *Liteinoye Proizvodstvo*, vol. 2, pp. 9–12, 2013.



**Doroshenko Volodymyr** received the Doctor's degree in Technical Sciences in 1990 from Kyiv Polytechnical Institute, Ukraine. The title of the Thesis was "Obtaining of Castings of Hydrodistributors from Cast Iron with Globular Graphite in Vacuum-processed Molds". Since 1982 he has been an Engineer (speciality: Foundry of Ferrous and Nonferrous Metals). He is currently a Senior Research Fellow with Physico-Technological Institute of Metals and Alloys, Ukraine.

Major areas of his scientific activity are: heat and mass transfer, gas and hydrodynamics of the interaction of a melt and a crystallizing metal with a sand casting mold, physics and chemistry of processes of sand casting molds production, particularly with the use of vacuumization; new methods of forming for foundry, which ensure environmental safety of production and improve the quality of metal castings; methods of casting into vacuum-processed molds; use of cryo-technologies in foundry, in particular, technological bases of accurate blanks obtained by single-use ice models. He is the author of more than 335 scientific and technical papers, including t 80 patents for inventions in Ukraine and Russia.

E-mail: dorosh@inbox.ru



**Mul Olena** received the Doctor's degree in Physics and Mathematics in 2001 from the Space Research Institute of NASU-NSAU, Kyiv, Ukraine. The title of her Thesis was "Analysis of Self-Oscillation Processes in the Complex Continuous and Discrete Systems". Since 1994 she has been an Engineer-mathematician (speciality: Applied Mathematics). She is currently an Associate Professor with the Computer-Integrated Department of Ternopil National Ivan Puluj Technical University.

Major areas of her scientific activity are: control theory on time scales with special emphasis on hybrid systems; controllability and optimality of nonlinear control systems; analysis and control of dynamical systems; numerical analysis; perturbation theory; theory of vibrations; mathematical physics and computational mathematics for nonlinear boundary value problems in PDE's and ODE's.

She is a member of IAMP.

She has received grants from INTAS, IUPAP, NATO, ESF, UNESCO, CIME, C.I.R.M., the Banach Center (Warsaw, Poland), Max Planck Institute of Physics of Complex Systems (Dresden, Germany) as well as 3-year FCT Post-doctoral fellowship "Analysis of Vibrations in Nonlinear Dynamical Systems" at Department of Mathematics, University of Aveiro, Portugal (2004-2007); 6 months scientific fellowship "Numerical and Asymptotical Methods for Highly Oscillatory Differential Equations" at the Department of Applied Mathematics and Theoretical Physics, Centre for Mathematical Sciences, University of Cambridge, UK (2012).

E-mail: ms.olena@gmail.com



**Kravchenko Olena** is a post-graduate student with International Research and Training Center for Information Technologies and Systems of NASU-MESU, Kyiv, Ukraine. She is a mathematician-programmer (speciality: Applied Mathematics). She is currently a software engineer with Glushkov Institute of Cybernetics of NASU, Ukraine.

Major areas of her scientific activity are: group method of data handling (GMDH) and other methods of inductive modeling under assumptions; robotics problems in using a mobile robot manipulator for repair and rescue works under extreme conditions of catastrophic situations in underground mining constructions; ecological problems in development of geoinformation systems for the prediction of natural meteorological disasters; interval method of telemetry information reliability control for monitoring the casting cooling in a sand mold; mathematical methods for assessing the quality of cast iron by temporal experimental data; monitoring and geoprocessing of the earth surface probing processes. She is the author of about 20 papers, published in scientific journals and presented at international and Ukrainian scientific conferences.

E-mail: len327@ukr.net

# Calculation of Eigenvalues for Eddy Current Testing Problems

Valentina Koliskina, Riga Technical University

**Abstract** – Semi-analytical solutions of eddy current testing problems require several computational steps. One of the steps where numerical methods are needed is calculation of complex eigenvalues without good initial approximation for the roots. In the presented paper we describe three eddy current testing problems with cylindrical symmetry where a cylindrical inclusion in a conducting medium is of finite size. In all three cases eigenvalue problem reduces to transcendental equations containing Bessel functions in a complex plane. The algorithm of the solution of such problems is described in the paper. Results of numerical computation are presented.

**Keywords** – Bessel functions, complex eigenvalues, eddy current testing, flaw detection, TREE method.

## I. INTRODUCTION

Eddy current method is widely used for quality testing of electrically conducting materials. The method is based on the principle of electromagnetic induction. If a conducting medium (for example, a metal plate) is located near a source of alternating current (for example, a coil) then eddy currents are induced in the medium. These currents, in turn, interact with the currents in the coil changing the impedance of the coil. If a flaw is present in a conducting medium then the parameters of the flaw are usually estimated solving the inverse problem, where the difference (in some norm) between experimental and theoretical data is minimized [1]. Thus, a reliable and accurate method for the solution of a direct problem is needed in order to solve the inverse problem.

The classical approach for solving direct problems is based on the assumption that a conducting medium is infinite in one or two spatial dimensions. Method of integral transforms (such as Hankel or Fourier transforms) is used in such cases to compute the change in impedance of the coil [2], [3]. In many cases, however, conducting medium is of finite size. Numerical methods such as finite element methods are usually used in cases of complex geometry of the conducting medium [4]. Applications include coin validation, estimation of the effects of corrosion and analysis of other flaws in a conducting medium.

Semi-analytical solutions for problems where a conducting medium is of finite size can be constructed by the TREE method [3], [5]. The basic assumption in the TREE method is that the electromagnetic field is assumed to be exactly zero at a sufficiently large distance from the coil. In this case the boundary conditions of the first or second kind are imposed on the artificial boundary (where the field is zero). This idea allows one to extend the class of problems which can be solved by analytical methods. Using the TREE method the solution is constructed by means of the method of separation of variables. However, some steps of the solution procedure

require the use of numerical methods. In particular, one of the steps in the TREE method is the calculation of complex eigenvalues. The eigenvalue problem reduces to the solution of the equation

$$\varphi(z) = 0, \tag{1}$$

where  $z$  is a complex which occurs in eddy current testing problems where the boundary conditions between media with different properties are used.

There are two important aspects of the solution of (1). First, no good initial guess for the roots of (1) is known. Second, relatively large number of eigenvalues needs to be computed since the change in impedance of an eddy current coil is represented by an eigenfunction expansion. The numerical procedure used to compute the roots of (1) is described in the presented paper. Preliminary results leading to this publication were reported at the international conference in Šibenik, Croatia, in 2013 [6].

## II. THREE TYPES OF EDDY CURRENT TESTING PROBLEM

In this section we describe three models where the solution of (1) represents an important computational step. The geometry of the first model is shown in Fig. 1.

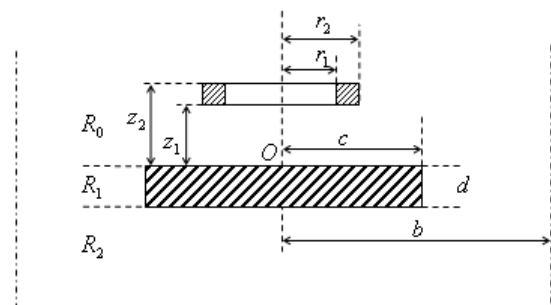


Fig. 1. Coil with alternating current above the conducting cylinder.

This model can be used in practice to analyze objects inserted in coin validators. Consider a coil with alternating current of frequency  $\omega$  located above the conducting cylinder. The inner and outer radii of the coil are  $r_1$  and  $r_2$ , respectively. The coil is located at a distance  $z_1$  from the conducting cylinder. The height of the coil is  $z_2 - z_1$ . The parameters describing the cylinder are as follows:  $c$  is the radius,  $d$  is the height and  $\sigma$  is the electrical conductivity (the cylinder is non-magnetic). We used the TREE method [3] to solve the problem. It was assumed that the electromagnetic

field is exactly zero at a sufficiently large radial distance  $b$  from the axis of the coil.

The problem was solved by method of separation of variables where the solution is expressed in terms of the vector potential. The finite size of the cylinder imposes some additional conditions. In particular, two sets of eigenvalues have to be calculated. One set of eigenvalues is obtained from the condition that the vector potential in regions  $R_0, R_1$  and  $R_2$  is equal to zero. The corresponding eigenvalues are given by

$$\lambda_i = \frac{\alpha_i}{b}, \quad i = 1, 2, \dots, n \quad (2)$$

where  $\alpha_i$  are the roots of the equation

$$J_1(\alpha) = 0. \quad (3)$$

Here  $J_1(\alpha)$  is the Bessel function of the first kind of order one. The roots  $\alpha_i$  can be easily computed with Mathematica. The corresponding Mathematica script is shown in Fig. 2 where the first ten zeros of (3) are shown.

```
<< NumericalMath`BesselZeros`
Ns = 10; alfa = BesselJZeros[1, Ns]
{3.83171, 7.01559, 10.1735, 13.3237, 16.4706,
19.6159, 22.7601, 25.9037, 29.0468, 32.1897}
```

Fig. 2. Mathematical code for the computation of the zeros of (3).

The corresponding eigenvalues  $p_i$  are the roots of the equation

$$pJ_1(qc)T_1'(pc) - qJ_1'(qc)T_1(pc) = 0, \quad (4)$$

where

$$T_1(p_i r) = J_1(p_i r)Y_1(p_i b) - J_1(p_i b)Y_1(p_i r),$$

$Y_i(x)$  is the Bessel function of the second kind of order one,

$$q_i = \sqrt{p_i^2 - j\omega\sigma\mu_0}, \quad j \text{ is the imaginary unit,}$$

$\omega = 2\pi f$  and  $\mu_0$  is the magnetic constant.

The second model is shown in Fig. 3.

The model can be used to analyze the effect of corrosion in metal plates. The corresponding eigenvalue relation in this case has the form

$$p_i T_1(q_i c) J_1'(p_i c) = q_i T_1'(q_i c) J_1(p_i c), \quad (5)$$

where  $T_1(q_i c) = J_1(q_i c)Y_1(q_i b) - J_1(q_i b)Y_1(q_i c)$ .

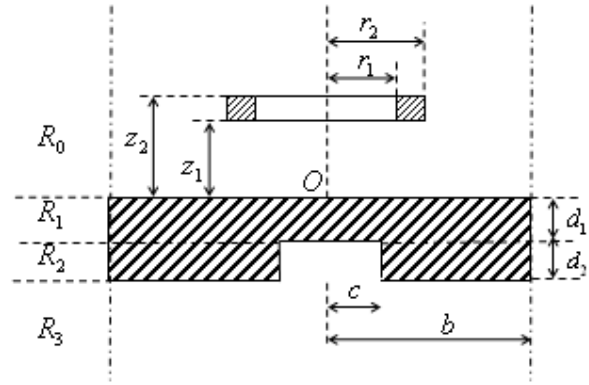


Fig. 3. Coil of finite dimensions above the conducting plate with a cylindrical hole.

The third model is shown in Fig. 4 and can be used to test the quality of spot welding. A cast core (represented by a cylinder of radius  $c$ ) is formed during the welding process. The conductivity  $\sigma_2$  of the cylinder is (as experimental data show) close to the conductivity  $\sigma_1$  of the surrounding medium (however, no restriction on  $\sigma_2$  is imposed in our analysis). The eigenvalue relation is given by (5), where

$$q_i = \sqrt{p_i^2 - j\omega\sigma_2\mu_0}.$$

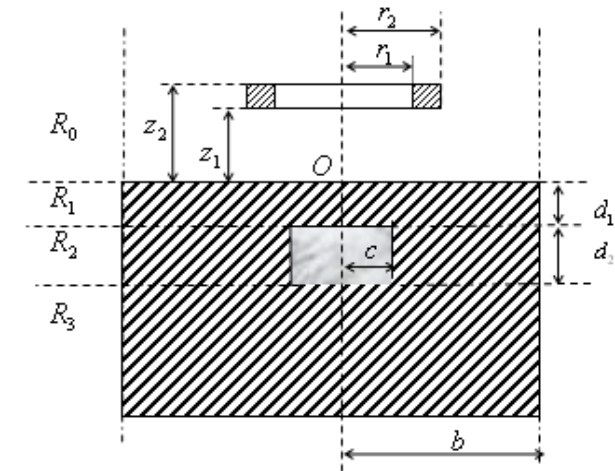


Fig. 4. Coil with finite dimensions above the half-space with a flaw.

### III. NUMERICAL PROCEDURE

The solution of eigenvalue problems (4) and (5) is based on the idea described in [7] and [8]. It is known from the theory of complex variables that the number of zeros  $n_0$ , of an analytic function  $\varphi(z)$  inside a closed contour  $C$  is equal to

$$n_0 = \frac{1}{2\pi} \oint_C \frac{\varphi'(z)}{\varphi(z)} dz. \quad (6)$$

In addition, it can be shown [7], [8] that

$$z_n = \frac{1}{2\pi i} \oint_C z^n \frac{\varphi'(z)}{\varphi(z)} dz = \sum_{i=1}^k \zeta_i^n, \quad (7)$$

where  $\zeta_i, i = 1, 2, \dots, k$  are zeroes (simple or multiple) of  $\varphi(z)$  inside  $C$  and  $n = 1, 2, \dots, k$ .

It is suggested in [7] and [8] that using (7) one can construct a polynomial of degree  $k$  roots of which are the same as the roots of  $\varphi(z)$ . The roots of the polynomial (and, therefore, the roots of  $\varphi(z)$ ) can be easily computed (for example, Mathematica command Roots can be used). However, the number  $k$  should not be too large since roots of a polynomial of high degree can be quite sensitive to the coefficients [9]. We developed an algorithm for the computation of roots of (1) for the case where there are at most two eigenvalues inside  $C$ . The contour  $C$  is a rectangle (which can easily be sub-divided into smaller rectangles, if necessary). If there are two eigenvalues inside  $C$  then the program divides the rectangle by smaller rectangles until there is only one root of (1) inside  $C$ . The eigenvalue is computed by formula (7) with  $n = 1$ . As an example we present here computational results for the first problem (detailed calculations for other cases can be found in [10]). The program for the computation of complex eigenvalues can also be found in [10].

The first 5 roots of (3) are shown in Fig. 5 for the following parameters of the problem  $\sigma = 9.6$  Ms/m,  $c = 19.75/2$  mm,  $b = 60$  mm,  $\omega = 1$  kHz.

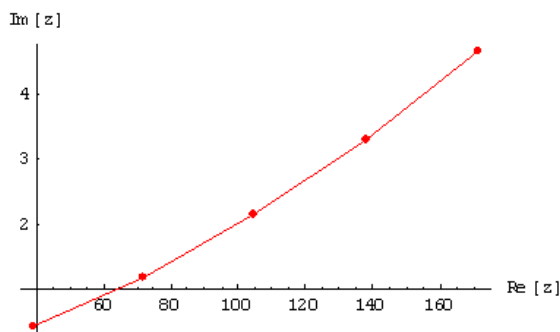


Fig. 5. First five roots of (3).

#### IV. CONCLUSION AND DIRECTION OF FUTURE WORK

An algorithm for the computation of complex eigenvalues for eddy current testing problems is described in the paper. The algorithm is implemented in Mathematica. Calculations show that the method is reliable and efficient (at least, for relatively low frequencies in the range from 1 kHz to 10 kHz). Determination of complex eigenvalues is one of the important steps in the TREE method (see examples in [11] and [12]). Recently asymmetric problems of eddy current testing problems were solved in [13]–[16]. Solutions were obtained using the second order vector potential formulation. The author is currently working on the application of the TREE

method and second order vector potential formulation to asymmetric problems in cylindrical coordinates.

#### REFERENCES

- [1] J. A. Tegopoulos and E. E. Kriezis, *Eddy currents in linear conducting media*. Amsterdam: Elsevier, 1985.
- [2] M. Ya. Antimirov, A. A. Kolyshekin, and R. Vaillancourt, *Mathematical models in eddy current testing*. Montreal: CRM, 1997.
- [3] T. P. Theodoulidis, and E. E. Kriezis, *Eddy current canonical problems (with application to nondestructive evaluation)*. Duluth: Tech Science, 2006.
- [4] N. Ida, *Numerical modeling for electromagnetic non-destructive evaluation*, Chapman & Hall, 1995.
- [5] T. P. Theodoulidis, and E. E. Kriezis, "Series expansions in eddy current nondestructive evaluation models," *Journal of materials processing technology*, vol. 161, pp. 343–347, 2005. <http://dx.doi.org/10.1016/j.jmatprotec.2004.07.048>
- [6] V. Koliskina and I. Volodko, "Determination of complex eigenvalues for axisymmetric problems in eddy current testing," 8<sup>th</sup> conference on applied mathematics and scientific computing, 2013.
- [7] L. M. Delves, and J. N. Lyness, "A numerical method for locating the zeros of an analytic function," *Mathematics of Computation*, vol. 21, pp. 543–560, 1967. <http://dx.doi.org/10.1090/S0025-5718-1967-0228165-4>
- [8] J. N. Lyness, "Numerical algorithms based on the theory of complex variable," *Proc. ACM*, pp. 125–133, 1967.
- [9] G.E. Forsythe, M.A. Malcolm, and C.B. Moler, *Computer methods for mathematical computations*, Prentice-Hall: Englewood Cliffs, 1977.
- [10] V. Koliskina, "Analytical and quasi-analytical solutions of direct problems in eddy current testing," PhD thesis, Riga Technical University, Latvia, 2014.
- [11] H. Sun, J.R. Bowler, and T.P. Theodoulidis, "Eddy currents induced in a finite length layered rod by a coaxial coil," *IEEE Transactions on Magnetics*, vol. 41, no. 9, 2005, pp. 2455–2461. <http://dx.doi.org/10.1109/TMAG.2005.855439>
- [12] T. Theodoulidis, and J. R. Bowler, "Eddy current interaction of a long coil with a slot in a conductive plate," *IEEE Transactions on Magnetics*, vol. 41, no. 4, 2005, pp. 1238–1247. <http://dx.doi.org/10.1109/TMAG.2005.844838>
- [13] A. Scarlatos, and T. Theodoulidis, "Impedance calculation of a bobbin coil in a conductive tube with eccentric walls," *IEEE Transactions on Magnetics*, vol. 46, no. 11, 2010, pp. 3885–3892. <http://dx.doi.org/10.1109/TMAG.2010.2064331>
- [14] T. Theodoulidis, and J. R. Bowler, "Interaction of an eddy current coil with a right-angled conductive wedge," *IEEE Transactions on Magnetics*, vol. 46, no. 4, 2010, pp. 1034–1042. <http://dx.doi.org/10.1109/TMAG.2009.2036724>
- [15] A. Scarlatos, and T. Theodoulidis, "Analytical treatment of eddy-current induction in a conducting half-space with a cylindrical hole parallel to the surface," *IEEE Transactions on Magnetics*, vol. 47, no. 11, 2011, pp. 4592–4599. <http://dx.doi.org/10.1109/TMAG.2011.2158550>
- [16] A. Scarlatos, and T. Theodoulidis, "Solution to the eddy-current induction problem in a conducting half-space with a vertical cylindrical borehole," *Proceedings of the Royal Society A: Mathematical, Physical and Engineering Sciences*, vol. 468(2142), 2012, pp. 1758–1777. <http://dx.doi.org/10.1098/rspa.2011.0684>



**Valentina Koliskina** defended her Doctoral Thesis "Analytical and quasi-analytical solutions of direct problems in eddy current testing" in the University of Latvia, Riga, Latvia in 2014. Presently she is a lecturer with the Department of Engineering Mathematics of Riga Technical University, Latvia. Her research interests are: analytical and semi-analytical solutions of direct problems in eddy current testing. Since 2007 she has participated in more than 20 international conferences. She is the author of more than 30 papers published in peer-reviewed journals and conference proceedings.

E-mail: valentina.koliskina@rtu.lv

# Hydrogeological Model of Latvia After Increasing Density of its Hydrographical Network

Aivars Spalvins<sup>1</sup>, Janis Slangens<sup>2</sup>, Inta Lace<sup>3</sup>, Olgerts Aleksans<sup>4</sup>,  
Kaspars Krauklis<sup>5</sup>, Viesturs Skibelis<sup>6</sup>, Irina Eglite<sup>7</sup>,  
<sup>1-7</sup> Riga Technical University

**Abstract** – In 2010 – 2012 the hydrogeological model (HM) of Latvia was developed and was named LAMO by scientists of Riga Technical University (RTU). The model comprises geological and hydrogeological information accumulated by the Latvian Environment, Geology and Meteorology Center (LEGMC). LAMO simulates the active groundwater zone that provides drinking water. To ensure compatibility with models of other countries, the worldwide used commercial program Groundwater Vistas (GV) is applied for running LAMO. In 2013 – 2014 LAMO was considerably upgraded and since 2012 three versions (LAMO1, LAMO2, LAMO3) of the HM have been developed. Density of the hydrogeological network was increased, transmissivity distributions for aquifers were refined and special software tools were developed to join the elements of hydrographical network (rivers, lakes, sea) with the HM body. In the paper the main innovations that have converted the LAMO2 into the next LAMO3 version are considered.

**Keywords** – Hydrogeological model, hydrographical network, transmissivity of aquifers.

## I. INTRODUCTION

The European Union (EU) countries are developing HM where by means of computer modeling the information necessary for groundwater management is obtained to implement the aims laid down by the EU Water Framework Directive [1] for sustainable use of water resources. In Latvia, the LEGMC team prepares plans for surface and groundwater management of four cross-border river basin districts: those of the Venta, Lielupe, Daugava and Gauja rivers. In 2010 – 2012 the HM LAMO was established by the scientists of RTU. The commercial program Groundwater Vistas (GV) was used for running LAMO [2]. The SURFER [3] and EXCEL [4] programs were applied to prepare the initial data for the GV system and to present the obtained results. In publications [5]–[9] novel methods and tools, used to establish LAMO, are considered.

In 2013 scientists of RTU using the results of LAMO prepared five reports [10]–[14] which were used by specialists of LEGMC for improving the management of groundwater bodies in the above mentioned four river basin districts of Latvia. The main items of the RTU reports are summarized in [15].

In 2013 – 2014 LAMO was considerably updated [16], [17] and due to the innovations four successive versions of LAMO can be distinguished. The comparison of LAMO versions is presented in the Appendix, Table IA. In 2012 the first version, LAMO1, was established and the report [10] revealed the

necessity for urgent improvements of the HM. In the first half of 2013 the following two upgrades were accomplished which converted LAMO1 into the LAMO2 version:

1. To avert unrealistic groundwater head distribution (shown for the profile 2W-2C in [10]), within the 24-th thick united aquifer D2ar#, the one was split into its natural parts: the aquifers D2brt, D2ar and the aquitard D2arz (Fig. 1) and the number of LAMO planes increased from 25 to 27;
2. River valleys were fully implemented into the HM body; for LAMO1 the valleys were immersed only into the Quaternary strata.

LAMO2 results were used to prepare the reports [11]–[14].

In 2014 LAMO 2 was turned into the LAMO3 version, due to the following upgrades:

1. The density of the hydrographical network of HM was increased (the number of rivers and lakes was changed from 199 to 469 and from 67 to 127, accordingly);
2. The transmissivity distribution for primary aquifers of HM were considerably refined [16];
3. To prepare the data for the hydrographical network special software was developed [17].

In 2014 the next LAMO4 version will appear because the following improvements of LAMO3 will be carried out:

1. The plane approximation step will be decreased from 500 meters to 250 meters;
2. To join the rivers of HM with its body more accurately, the measured flow of rivers will be accounted for;

In the paper the versions of LAMO2 and LAMO3 are compared. Due to considerable amount of complex maps and tables these materials are assembled in the Appendix.

## II. INCREASED DENSITY OF THE HM HYDROGRAPHICAL NETWORK

In Fig. 1a the “old” hydrographical network of LAMO2 and the “new” rivers and lakes included in the LAMO3 are shown. Evidently, in the LAMO3 the set of 469 rivers covers the land of Latvia much more evenly than the 199 rivers of the LAMO2. In LAMO3 sixty small lakes were added.

Hence the new rivers and lakes of LAMO3 are located mostly in the aquifer Q2, the groundwater flow regime of the Q-system changed considerably (Appendix, Table IIA):

- local inflow increased from 3 313 thous.m<sup>3</sup>/day to 7 270 thous.m<sup>3</sup>/day;
- the flow of rivers increased from 5 680 thous.m<sup>3</sup>/day to 9 436 thous.m<sup>3</sup>/day;

- the outflow through the ground surface decreased from 3 775 thous.m<sup>3</sup>/day to 1 804 thous.m<sup>3</sup>/day;
- the flow of lakes slightly increased from 426 thous.m<sup>3</sup>/day to 487 thous.m<sup>3</sup>/day;
- the outflow through the border decreased from 136 thous.m<sup>3</sup>/day to 100 thous.m<sup>3</sup>/day.

The outflow through the ground surface was partly reduced by minimizing (by 20 times) links of rivers and lakes with the relh plane of HM (Fig. 1). The links of lakes with the HM body were decreased by 500 times. The links of rivers with the HM body were only slightly adjusted in comparison with the ones of the LAMO2 version. The influence of the  $m = 0$  areas of aquitards, thickness of which is  $\varepsilon = 0.02$  meter, was decreased by 10 times (for the D3akz and D3elz aquitards by 100 times) by increasing their conductivity.

The total infiltration slightly increased from 11 194 thous.m<sup>3</sup>/day to 12 763 thous.m<sup>3</sup>/day which was very close to the value of 13 000 thous.m<sup>3</sup>/day given in [18].

For the LAMO3, due to increased intensity of groundwater processes for the  $Q$ -system, processes in the primary strata became slower. In Fig. 2A the distribution of groundwater flow and heads are shown for the primary aquifers of the LAMO2 and LAMO3 versions. Evidently, the LAMO3 discharge flow is smaller than the one of the LAMO2 version, but the head isoline pattern is similar in both versions. One can draw identical conclusions when observing Fig. 3a, where flow and heads of the D2ar aquifer of the LAMO2 and LAMO3 version are compared. In Fig. 2a and Fig. 3a simple color scales were applied, in order to distinguish the areas of discharge, transit and recharge flow. In Fig. 4a the LAMO3 infiltration flow for the primary and D2ar aquifers are shown where the full color scale for the infiltration flow was used.

In Fig. 5a the geological profile 4W-4E is shown for the LAMO2 and LAMO3 versions. For both HM versions the head isolines were drawn and one can conclude from comparing these profiles that the heads of the LAMO3 version are slightly lower (5 – 10 meters) than in the LAMO2. For the profile of LAMO3 the infiltration flow distribution picture was applied. In [8] the methods of creating profiles for the head and flow distributions ( $\varphi$  and  $q$ -maps) are explained. The isolines of heads and flow must be vertical, within aquifers and aquitards, accordingly. In Fig. 5a the SURFER color mode was used to show the flow distribution. The profile flow  $q$ -map assembles information (geological stratification, distributions of infiltration flows) carried by the vertical incision of the HM body. For example, the preQ and D2ar maps in Fig. 4a provide data, accordingly, for the top surface and the D3arz aquitard of the Fig. 5a profile. The flow profiles helped to find out and to correct some errors of HM, especially the ones related to joining rivers with the LAMO3 body.

### III. COMPARISON OF GROUNDWATER FLOW BALANCE OF THE LAMO2 AND LAMO3 VERSIONS

For the LAMO2 and LAMO3 version the flow balance of Latvia is presented in the Appendix, Table IIA. The scheme in Fig. 6a provides the graphical interpretation for the LAMO3 flow balance difference for Latvia between LAMO2 and LAMO3 version is given and the scheme in Fig. 7a explains

No of HM plane		Name of layer	Geological code	HM plane code
1.		Relief	relh	relh
2.		Aeration zone	aer	aer
3.		Unconfined Quaternary	Q4-3	Q2
4.		Upper moraine	gQ3	gQ2z
5.		Confined Quaternary or Jura	Q1-3 J	Q1#
6.		Lower moraine or Triass	gQ1-3 T	gQ1#z
7.		Perma Karbons Skerveles Ketleru	P2 C1 D3šķ D3ktl	D3ktl#
8.		Ketleru	D3ktl	D3ktlz
9.		Zagares Svetes Tervetes Muru	D3žg D3sv D3tr D3mr	D3zg#
10.		Akmenes	D3ak	D3akz
11.		Akmenes Kursas Jonisku	D3ak D3krs D3jn	D3krs#
12.		Elejas Amulas	D3el D3aml	D3el#z
13.		Stipinu Katlesu Ogres Daugavas	D3stp D3ktl D3og D3dg	D3dg#
14.		Daugavas Salaspils	D3dg D3slp	D3slp#z
15.		Plavinu	D3pl	D3pl
16.		Plavinu Amatas	D3pl D3am	D3am#z
17.		Amatas	D3am	D3am
18.		Upper Gauja	D3gj2	D3gj2z
19.		Upper Gauja	D3gj2	D3gj2
20.		Lower Gauja	D3gj1	D3gj1z
21.		Lower Gauja	D3gj1	D3gj1
22.		Burtnieku	D2brt	D2brtz
23.		Burtnieku	D2brt	D2brt
24.		Arikula	D2ar	D2arz
25.		Arikula	D2ar	D2ar
26.		Narvas Narvas	D2nr2 D2nr1	D2nr#z
27.		Pernavas	D2prn	D2pr

 - aquitard

# - united aquifer; #z – united aquitard

Fig. 1. Vertical schematization of LAMO.

graphically the Table IIIA of the Appendix. To compare the flow balance for Latvia of LAMO2 and LAMO3 version, the scheme in Fig. 7a reflecting their difference  $\Delta = q_{LAMO3} - q_{LAMO2}$  must be considered. The total local increase of LAMO3 is 3 564 thous.m<sup>3</sup>/day. It comprises four components (3 756 for rivers, 171 for lakes, 37 for wells, -400 for border). The well flow increase is formal, because in the D3pl aquifer the drainage system rate 37 thous.m<sup>3</sup>/day of the Riga HPS is added. The border flow decrease is considerable (936→536). The increase for the river flow for LAMO3 is caused mainly by the new rivers of the Q-system (3295→6627). It is possible that for the next LAMO4 version the river flow should be decreased.

The considerable increase of the lake flow for the primary strata (2→112) can be explained as follows:

- water reservoirs of the Riga, Kegums and Plavinu HPS are treated as lakes;
- some lakes are fully or partly linked with the primary aquifers D3zg#, D3gj1, D2brt.

In Appendix, Table IVA the relative difference  $\delta = 100 \Delta / q_{LAMO2}$  between the local balance of LAMO2 and LAMO3 is presented in the Appendix, Table IIIA and Table IIA (LAMO2). The relative difference enables to ascertain changes of groundwater flow if compared with the LAMO2 flow. In the Appendix, Table IVA its content may be much larger than 100%. For example, for the lake the relative difference is  $\infty$  if no lake is linked with the LAMO2 aquifer ( $q_{LAMO2} = 0$ ).

When considering the local balance of the D3gj1, D2brt and D2ar aquifers one can notice that their local inflow has decreased. For this reason the river and border flow there also is smaller. This decrease may be partly caused by nearly twofold reduced permeabilities of these aquifers (Table I) for the LAMO3 version.

#### IV. REFINEMENT OF TRANSMISSIVITY DISTRIBUTION OF AQUIFERS

For the GV-system the transmissivity of aquifers is controlled by changing the permeability  $k$ -maps. The  $k$ -map represents the product:

$$k = k_{\text{norm}} k_{\text{mean}}, \quad k_{\text{norm}} = k / k_{\text{mean}}$$

where  $k_{\text{norm}}$  and  $k_{\text{mean}}$  are accordingly normalized and denote permeabilities of a geological stratum.

It is explained in [15] how the data of well pumping were used to obtain  $k$ -maps for the LAMO3 version. Table I summarizes the results of this investigation:

- for LAMO2  $k_{\text{norm}} = 1$ , because constant values of  $k$  are applied;
- for LAMO3  $k_{\text{norm}}$  is variable and this feature partly causes considerable changes of the HM groundwater flow balance.

To calibrate HM, "theoretical" value  $k_{\text{meant}}$  was replaced by  $k_{\text{meanc}} > k_{\text{meant}}$ , because  $k_{\text{meant}}$  corresponded to the minimal transmissivity of an aquifer. It is possible to exploit the well pumping data more punctiliously by accounting for the well partial penetrating factor [15].

TABLE I  
COMPARISON OF  $K$ -MAPS FOR LAMO2 AND LAMO3 VERSION

Aquifer code	LAMO2		LAMO3		
	$k_{\text{norm}}$	$k_{\text{mean}}$	$k_{\text{norm}}$	$k_{\text{meant}}^*$	$k_{\text{meanc}}^*$
D3ktl	1.0	3.0	0.2–2.1	2.1	3.0
D3zg#	1.0	3.0	0.4–2.2	3.6	5.0
D3krs#	1.0	2.0	0.4–1.7	5.9	6.0
D3dg#	1.0	10.0	0.1–1.2	5.6	8.0
D3pl	1.0	10.0	0.2–1.9	7.8	12.0
D3am	1.0	10.0	0.3–1.8	4.7	7.0
D3gj2	1.0	10.0	0.4–1.8	5.6	8.0
D3gj1	1.0	14.0	0.3–1.9	5.2	8.0
D2brt	1.0	5.0	0.3–1.8	1.9	3.0
D2ar	1.0	5.0	0.3–1.9	2.1	3.0

\*  $k_{\text{meant}}$ ,  $k_{\text{meanc}}$  theoretical and calibrated mean permeability [metre/day] for LAMO3.

#### V. CONCLUSION

In 2014 the LAMO2 version was converted into the more efficient LAMO3 version due to the appliance of denser hydrographical network of HM to the refined aquifer transmissivity distribution and to the use of special software tools. The groundwater flow balance of Latvia for both HM versions differs considerably, especially in the river flow. For the LAMO3 version, the total discharge rate of rivers is larger than the one for the LAMO2 version. The enlargement of the river flow is caused by the increase of the number of rivers simulated by HM. It is possible that the river flow enlargement must be reduced by decreasing the strength of the links that join the rivers with the HM body. More accurate links will be found for the next LAMO4 version when the measured flow in rivers will be accounted for and the HM plane step will be changed from 500 meters to 250 meters.

#### ACKNOWLEDGMENT

In 2010–2012 the hydrogeological model of Latvia LAMO was developed within the framework of the project "The Creating of Hydrogeological Model of Latvia to be Used for Management of Groundwater Resources and for Evaluation of Their Recovery Measures." The project has been co-financed by the European Regional Development Fund.

#### APPENDIX

Table IA. Comparison of LAMO versions.

Fig. 1a. Hydrogeological network of LAMO2 (blue color) and the new rivers and lakes of LAMO3 (red color).

Fig. 2a. Distribution of groundwater flow and heads for primary preQ aquifers of LAMO2 and LAMO3.

Fig. 3a. Distribution of groundwater flow and heads for D2ar aquifer of LAMO2 and LAMO3.

Fig. 4a. Infiltration flow for primary (preQ) and D2ar aquifers of LAMO3.

Fig. 5a. Geological profile 4W-4E for LAMO2 and LAMO3.

Table IIa. Groundwater flow [thous.m<sup>3</sup>/day] balance of LAMO2 and LAMO3 for Latvia (preliminary data).

Table IIIa. Groundwater flow difference [thous.m<sup>3</sup>/day] balance between LAMO2 and LAMO3 for Latvia (preliminary data).

Table IVa. Groundwater flow relative difference [%] between local balance of LAMO2 and LAMO3.

Fig. 6a. Scheme of LAMO3 groundwater flow balance of Latvia for Table IIa

Fig. 7a. Scheme of LAMO2 and LAMO3 groundwater flow difference balance for Table IIIa

TABLE IA  
COMPARISON OF LAMO VERSIONS

Version	Years	Grid step [meter]	Number of layers	Number of cells×10 <sup>6</sup>	Number of rivers	Number of lakes	River valleys	River flow
LAMO1	2012	500	25	14.25	199	67	–	–
LAMO1	2013	500	27	15.43	199	67	+	–
LAMO1	2014	500	27	15.43	469	127	+	–
LAMO1	2015	250	27	61.56	469	127	+	+

c:\FIGDI1\LAMO\_3\LAMO\_geografija.srf



Fig. 1a. Hydrogeological network of LAMO2 (blue color) and the new rivers and lakes of LAMO3 (red color).

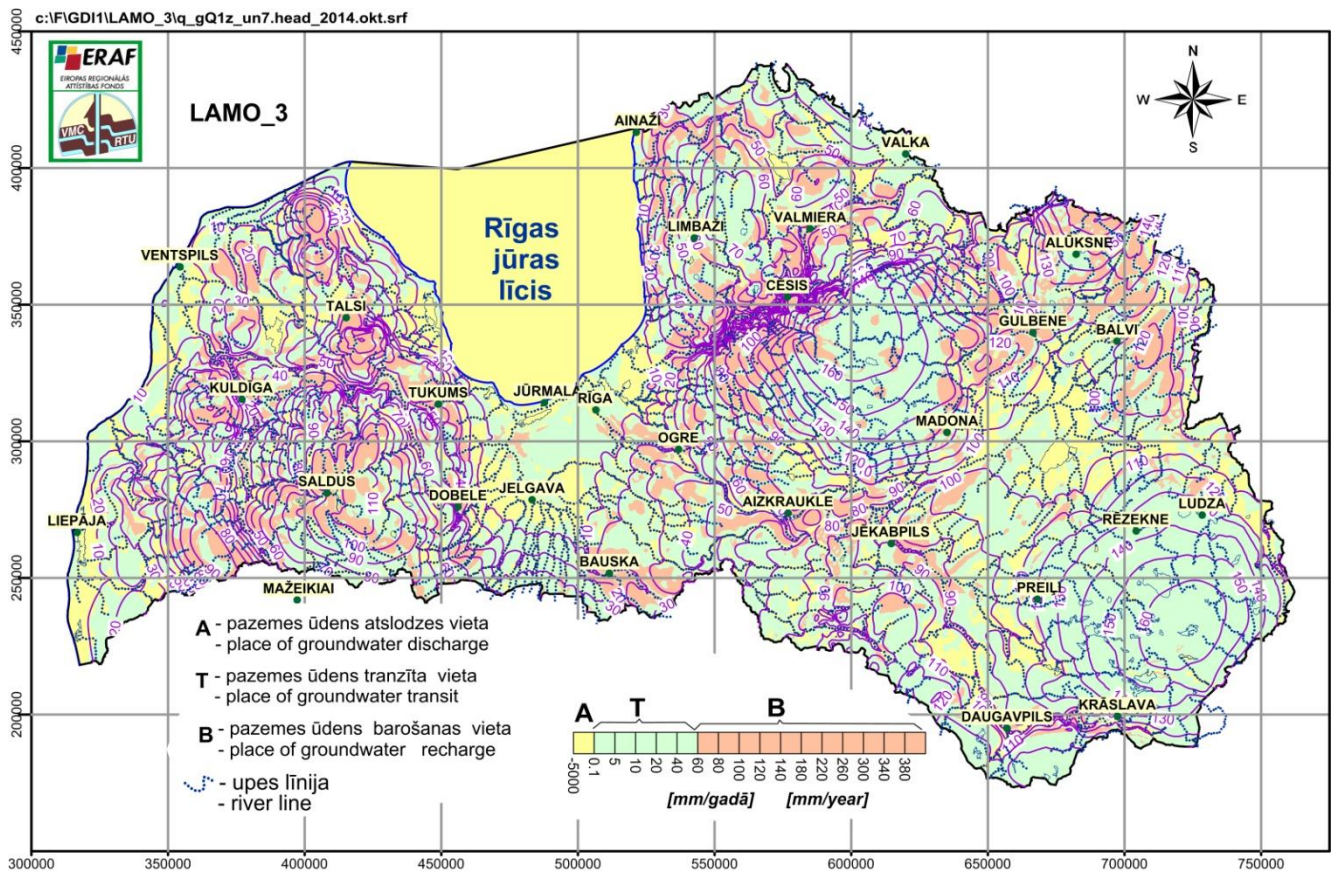
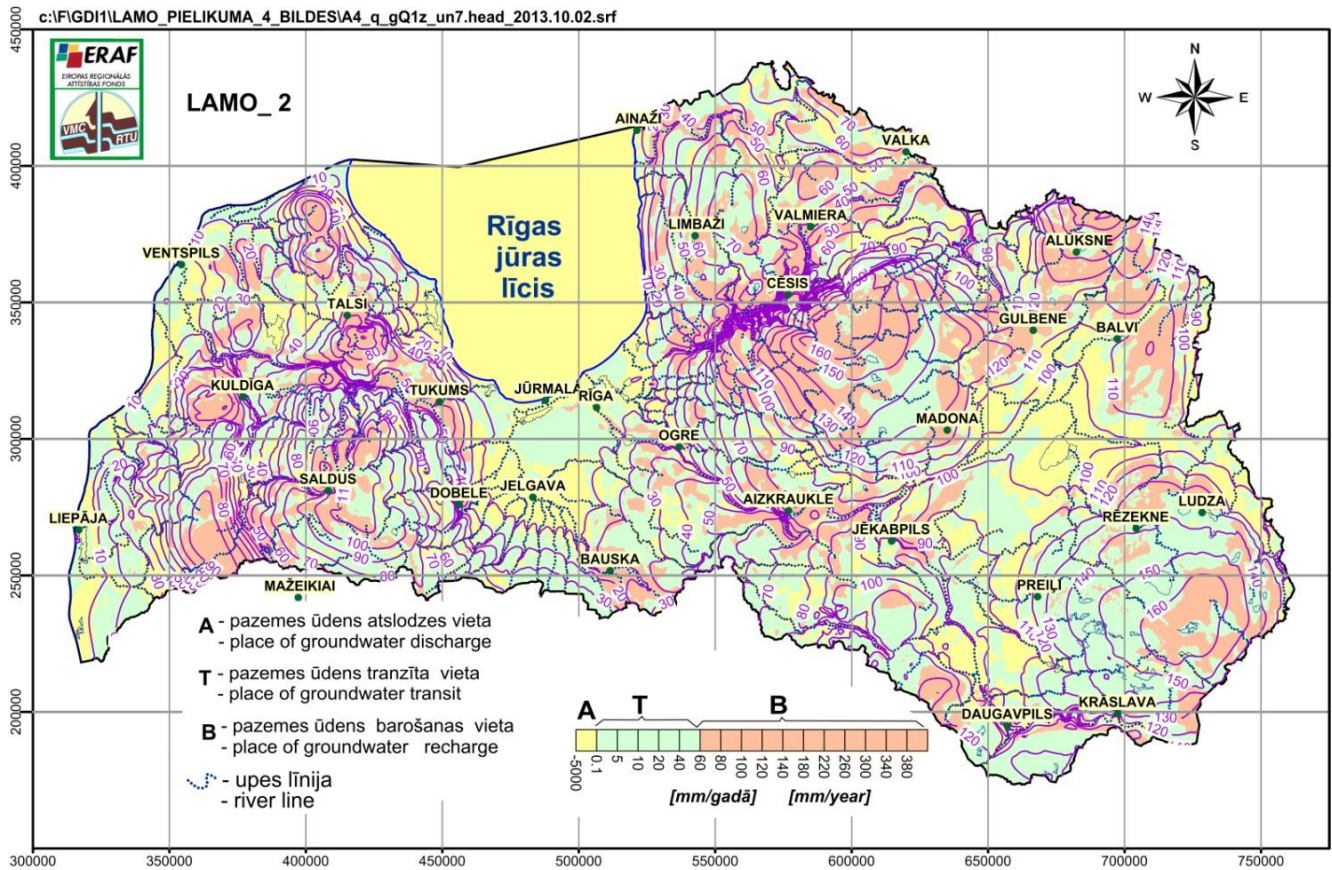


Fig. 2a. Distributions of groundwater flow and heads for primary preQ aquifers of LAMO2 and LAMO3.

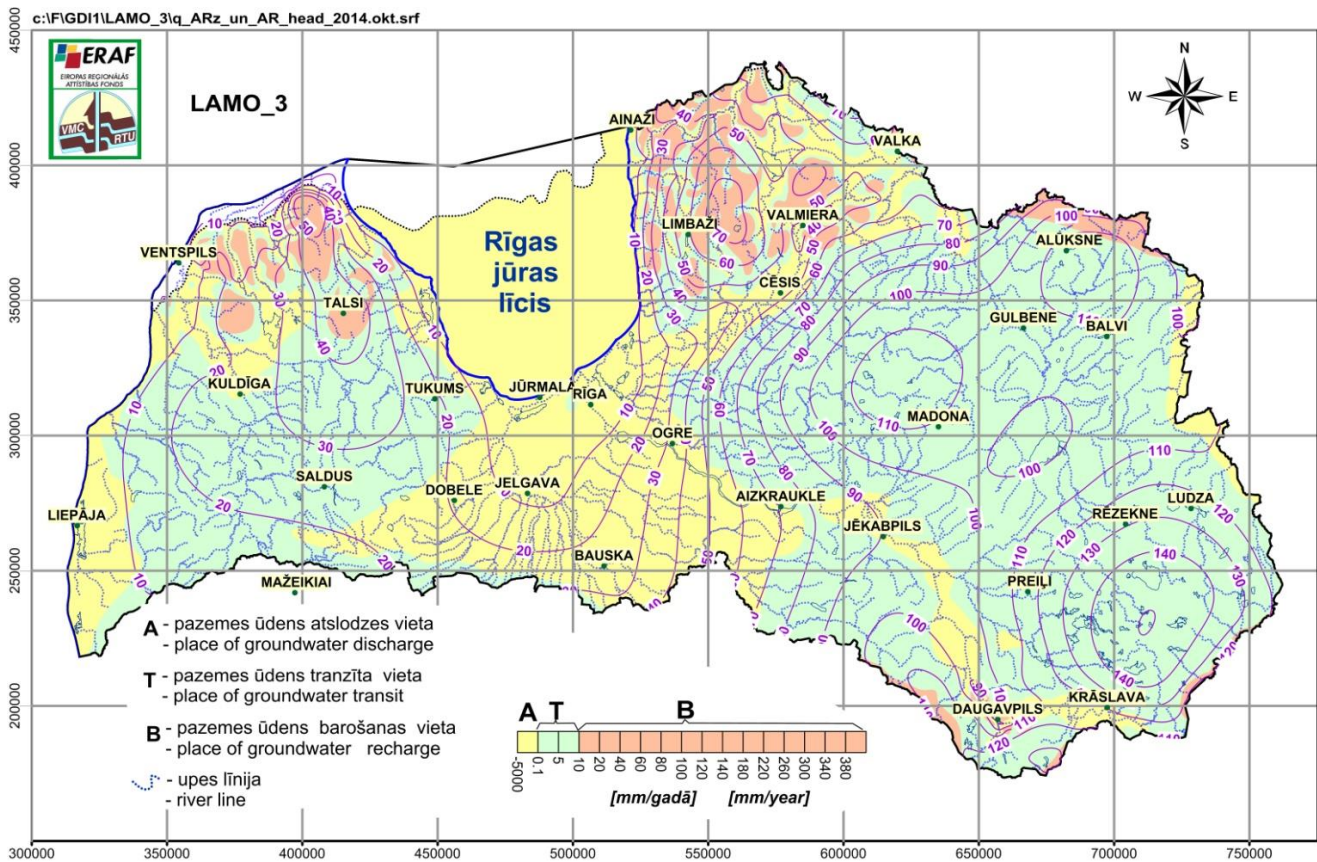
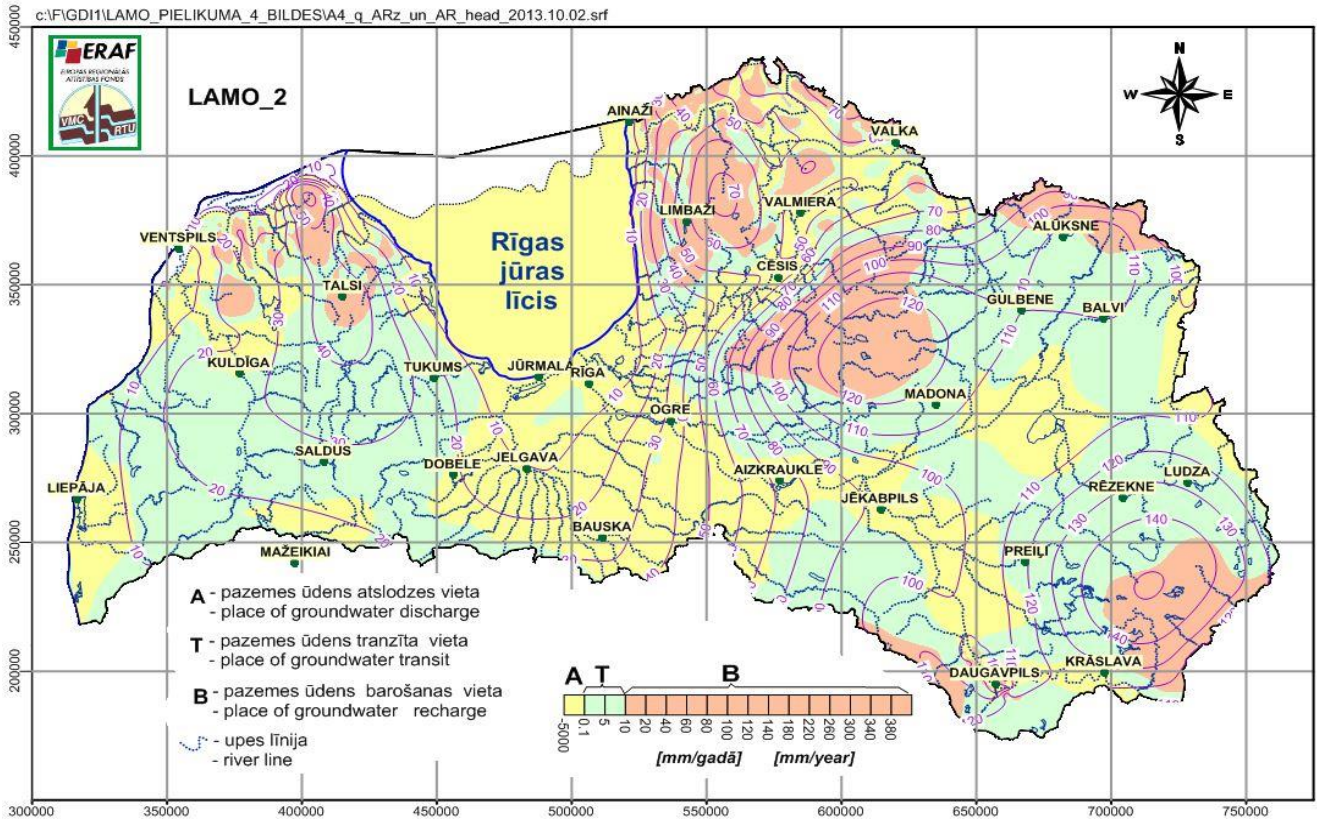


Fig. 3a. Distribution of groundwater flow and heads for D2ar aquifer of LAMO2 and LAMO3.

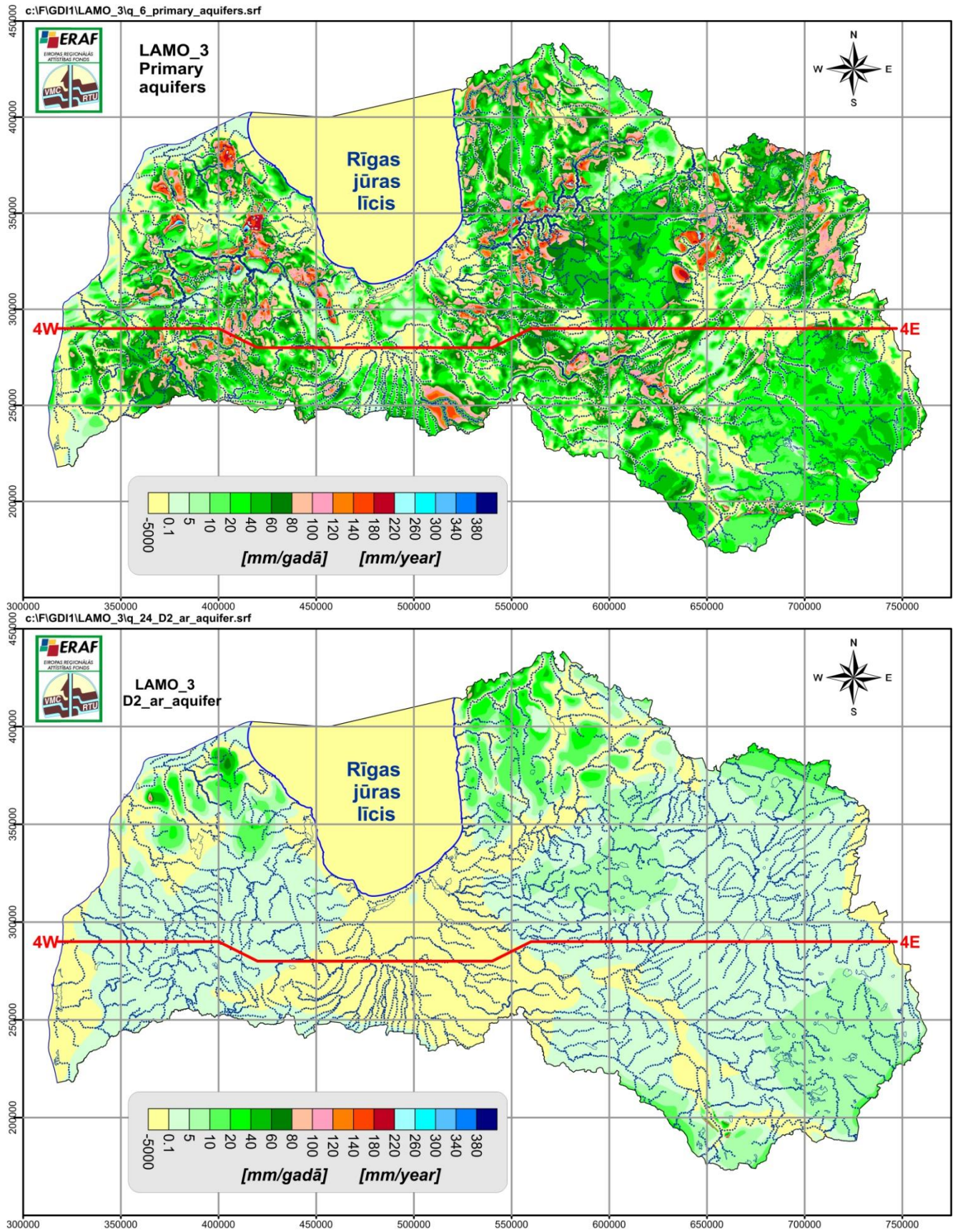


Fig. 4a. Infiltration flow for primary (preQ) and D2ar aquifers of LAMO3.

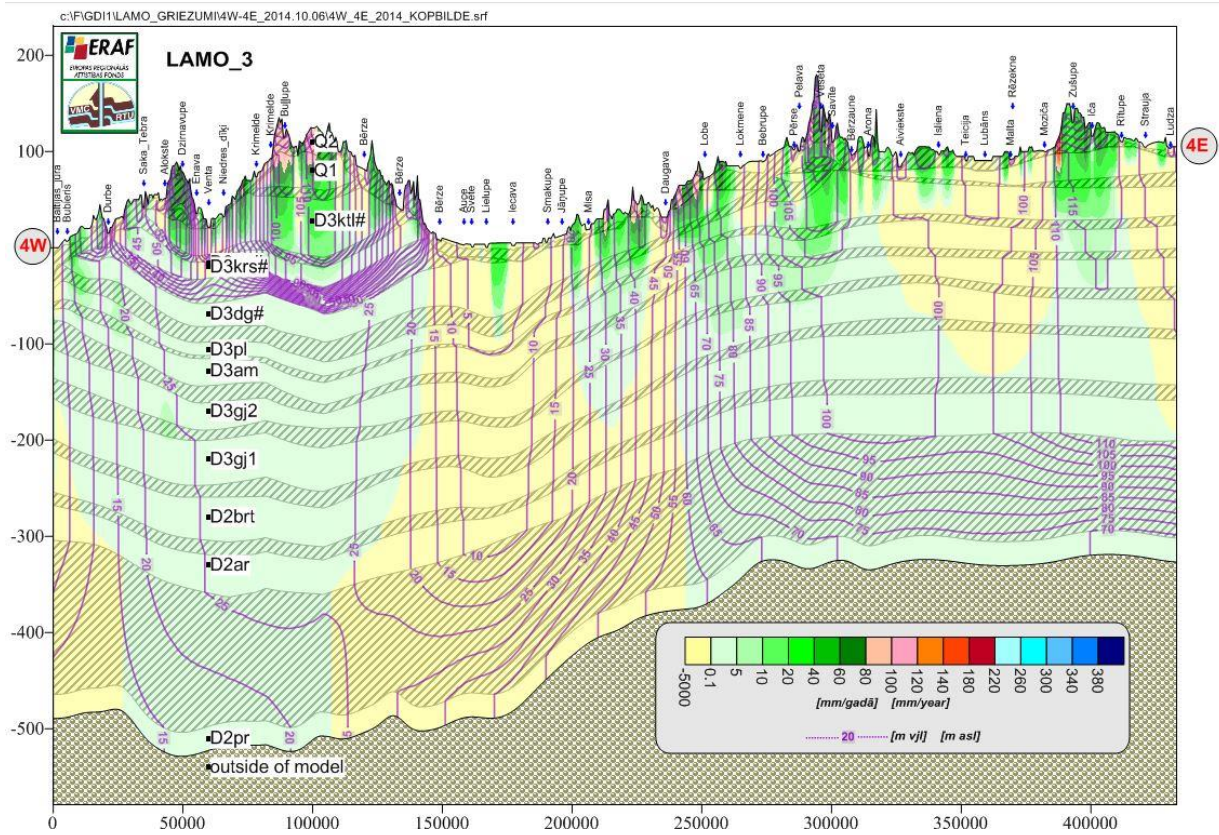
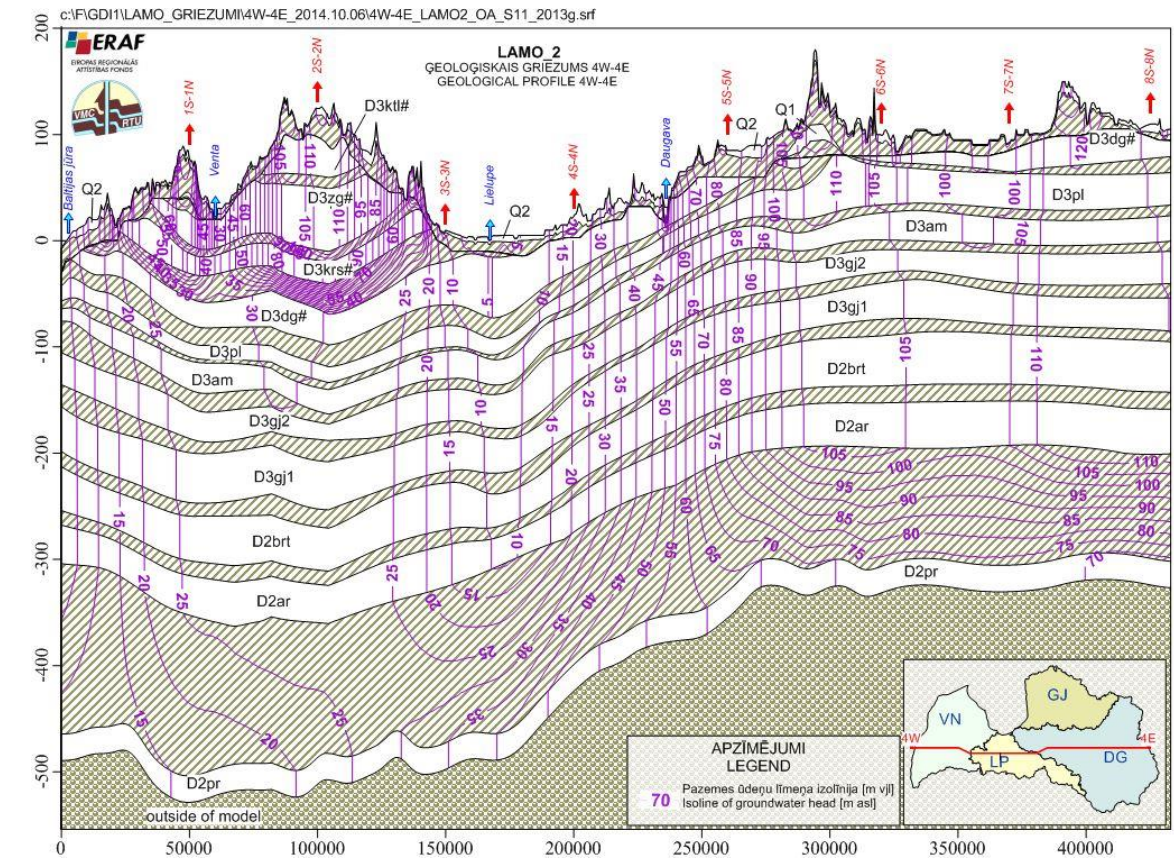


Fig. 5a. Geological profile 4W-4E for LAMO2 and LAMO3.

TABLE IIA

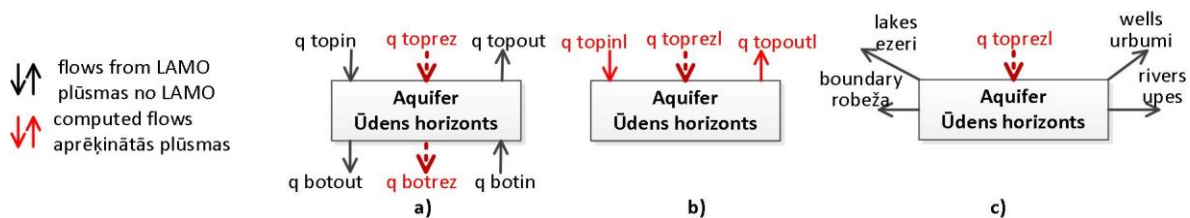
GROUNDWATER FLOW [THOUS.M<sup>3</sup>/DAY] BALANCE OF LAMO2 AND LAMO3 FOR LATVIA (PRELIMINARY DATA)

## LAMO2

Name of aquifer	$q_{topin}$	$q_{topout}$	$q_{toprez}$ (2+3)	$q_{botout}$	$q_{botin}$	$q_{botrez}$ (5+6)	$q_{topinl}$ (2+5)	$q_{topoutl}$ (3+6)	$q_{toprezl}$ (4+7) (8+9)	rivers	lakes	boundary	wells
1	2	3	4	5	6	7	8	9	10	11	12	13	14
Q2	11194	-3775	7419	-6992	3461	-3531	4202	-314	3888	-3288	-426	-118	-56
Q1	6992	-3461	3531	-6855	3349	-3506	137	-112	25	-7	0	-18	0
D3ktl#	6855	-3349	3506	-6524	3191	-3333	331	-158	173	-192	0	20	-1
D3zg#	6524	-3191	3333	-6284	3014	-3270	240	-177	63	-41	0	-18	-4
D3krs	6284	-3014	3270	-6233	2986	-3247	51	-28	23	-11	0	-8	-4
D3dg#	6233	-2986	3247	-4981	2333	-2648	1252	-653	599	-569	-10	-15	-5
D3pl	4981	-2333	2648	-3981	1849	-2132	1000	-484	516	-446	8	-70	-8
D3am	3981	-1849	2132	-3622	1634	-1988	359	-215	144	-93	0	-50	-1
D3gj2	3622	-1634	1988	-3041	1418	-1623	581	-216	365	-244	0	-96	-25
D3gj1	3041	-1418	1623	-2114	996	-1118	927	-422	505	-327	0	-154	-24
D2brt	2114	-996	1118	-852	423	-429	1262	-573	689	-462	0	-214	-13
D2ar	852	-423	429	-256	36	-220	596	-387	209	0	0	-195	-14
Model	11194	-3775	7419	-256	36	-220	10938	-3739	7199	-5680	-428	-936	-155
Q1+Q2	11194	-3775	7419	-6855	3349	-3506	4339	-426	3913	-3295	-426	-136	-56
Primary	6855	-3349	3506	-256	36	-220	6599	-3313	3286	-2385	-2	-800	-99

## LAMO3

Name of aquifer	$q_{topin}$	$q_{topout}$	$q_{toprez}$ (2+3)	$q_{botout}$	$q_{botin}$	$q_{botrez}$ (5+6)	$q_{topinl}$ (2+5)	$q_{topoutl}$ (3+6)	$q_{toprezl}$ (4+7) (8+9)	rivers	lakes	boundary	wells
1	2	3	4	5	6	7	8	9	10	11	12	13	14
Q2	12762	-1804	10958	-7125	3390	-3735	5637	1586	7223	-6596	-487	-84	-56
Q1#	7125	-3390	3735	-6960	3272	-3688	165	-118	47	-31	0	-16	0
D3ktl#	6960	-3272	3688	-6593	3166	-3427	367	-106	261	-277	0	17	-1
D3zg#	6593	-3166	3427	-6205	2860	-3345	388	-306	82	-64	-3	-11	-4
D3krs	6205	-2860	3345	-6027	2776	-3251	178	-84	94	-80	0	-10	-4
D3dg#	6027	-2776	3251	-4588	2137	-2451	1439	-639	800	-692	-90	-13	-5
D3pl	4588	-2137	2451	-3279	1302	-1977	1309	-835	474	-361	-8	-60	-45
D3am	3279	-1302	1977	-2872	1157	-1715	407	-145	262	-237	0	-24	-1
D3gj2	2872	-1157	1715	-2184	996	-1188	688	-161	527	-443	0	-59	-25
D3gj1	2184	-996	1188	-1554	688	-866	630	-308	322	-213	-5	-80	-24
D2brt	1554	-688	866	-596	287	-309	958	-401	557	-442	-6	-96	-13
D2ar	596	-287	309	-229	34	-195	367	-253	114	0	0	-100	-14
Model	12762	-1804	10958	-229	34	-195	12533	-1770	10763	-9436	-599	-536	-192
Q1+Q2	12762	-1804	10958	-6960	3272	-3688	5802	1468	7270	-6627	-487	-100	-56
Primary	6960	-3272	3688	-229	34	-195	6731	-3238	3493	-2809	-112	-436	-136



Legend of stages a), b), c) for obtaining the flow of Table IIA:

- a)  $q_{toprez}$ ,  $q_{botrez}$  computing of resulting flows;  
 b)  $q_{topinl}$ ,  $q_{topoutl}$ ,  $q_{toprezl}$  computing of local flows;  
 c) local balance of aquifer

TABLE IIIA  
GROUNDWATER FLOW DIFFERENCE [THOUS.M3/DAY] BALANCE BETWEEN LAMO2 AND LAMO3 FOR LATVIA (PRELIMINARY DATA)

Name of aquifer	$\Delta q_{\text{topin}}$	$\Delta q_{\text{topout}}$	$\Delta q_{\text{toprez}}$ (2+3)	$\Delta q_{\text{botout}}$	$\Delta q_{\text{botin}}$	$q_{\text{botrez}}$ (5+6)	$\Delta q_{\text{topinl}}$ (2+5)	$\Delta q_{\text{topoutl}}$ (3+6)	$\Delta q_{\text{toprezi}}$ (4+7) (8+9)	$\Delta$ rivers	$\Delta$ lakes	$\Delta$ boundary	$\Delta$ wells
1	2	3	4	5	6	7	8	9	10	11	12	13	14
Q2	1568	1971	3539	-133	-71	-204	1435	1900	3335	3308	61	-34	0
Q1#	133	71	204	-105	-77	-182	28	-6	22	24	0	-2	0
D3ktl#	105	77	182	-69	-25	-94	36	52	88	85	0	3	0
D3zg#	69	25	94	79	-154	-75	148	-129	19	23	3	-7	0
D3krs	-79	154	75	206	-210	-4	127	-56	71	69	0	2	0
D3dg#	-206	216	4	393	-196	197	187	14	201	123	80	-2	0
D3pl	-393	196	-197	702	-547	155	309	-351	-42	-85	16	-10	37
D3am	-702	547	-155	750	-477	273	48	70	118	144	0	-26	0
D3gj2	-750	477	-273	857	-422	435	107	55	162	199	0	-37	0
D3gj1	-857	422	-435	560	-308	252	-297	114	-183	-114	5	-74	0
D2brt	-560	308	-252	256	-136	120	-304	172	-132	-20	6	-118	0
D2ar	-256	136	-120	27	-2	25	-229	134	-95	0	0	-95	0
Model	1568	1971	3539	27	-2	25	1595	1969	3564	3756	171	-400	37
Q1+Q2	1568	1971	3539	-105	-77	-182	1463	1894	3357	3332	61	-36	0
Primary	105	77	182	27	-2	25	132	75	207	424	110	-364	37

Contents of Table IIIA are difference  $\Delta = q_{\text{LAMO3}} - q_{\text{LAMO2}}$  between contents of Table IIa for LAMO3 and LAMO2.

TABLE IVA  
GROUNDWATER FLOW RELATIVE DIFFERENCE [%] BETWEEN LOCAL BALANCES OF LAMO2 AND LAMO3

Name of aquifer	$\delta_{\text{toprez}}$	$\delta_{\text{river}}$	$\delta_{\text{lakes}}$	$\delta_{\text{border}}$	$\delta_{\text{wells}}$
1	2	3	4	5	6
Q2	85	100	14	-29	0
Q1#	88	243	0	-10	0
D3ktl#	51	44	0	15	0
D3zg#	11	12	$\infty$	-39	0
D3krs	308	627	0	25	0
D3dg#	33	21	800	-13	0
D3pl	-8	-19	200	-14	462
D3am	82	155	0	-52	0
D3gj2	44	81	0	-38	0
D3gj1	-36	-35	$\infty$	-48	0
D2brt	-19	-4	$\infty$	-55	0
D2ar	-45	0	0	-49	0
Model	2	66	40	-47	22
Q1+Q2	96	101	14	-26	0
Primary	6	18	550	-45	35

Contents of Table IVA are relative difference  $\delta = 100 \Delta / q_{\text{LAMO2}}$  that are computed as division of Table IIA / Table IIA (LAMO2)

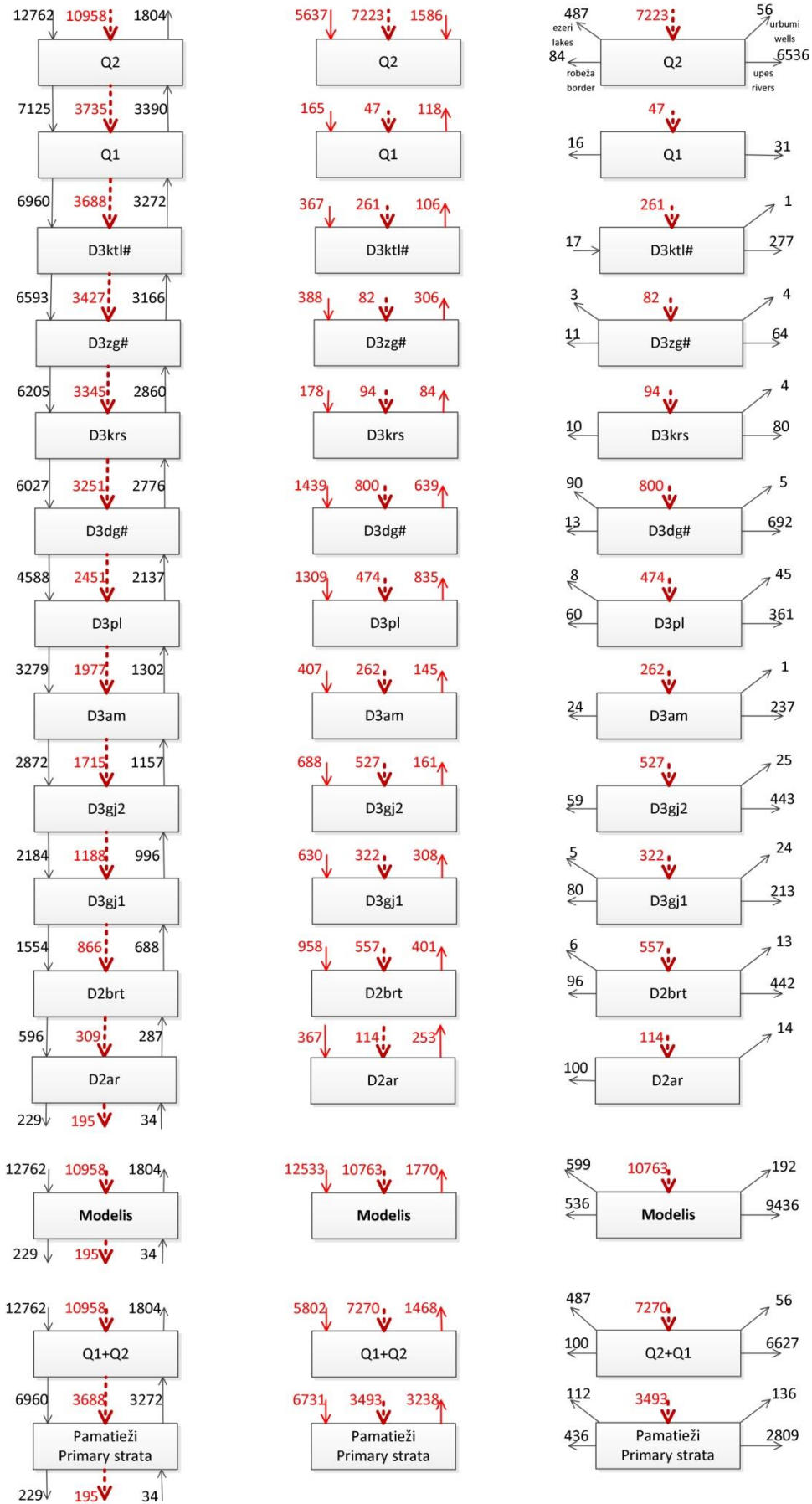


Fig. 6a. Scheme of LAMO3 groundwater flow balance of Latvia for Table IIa.

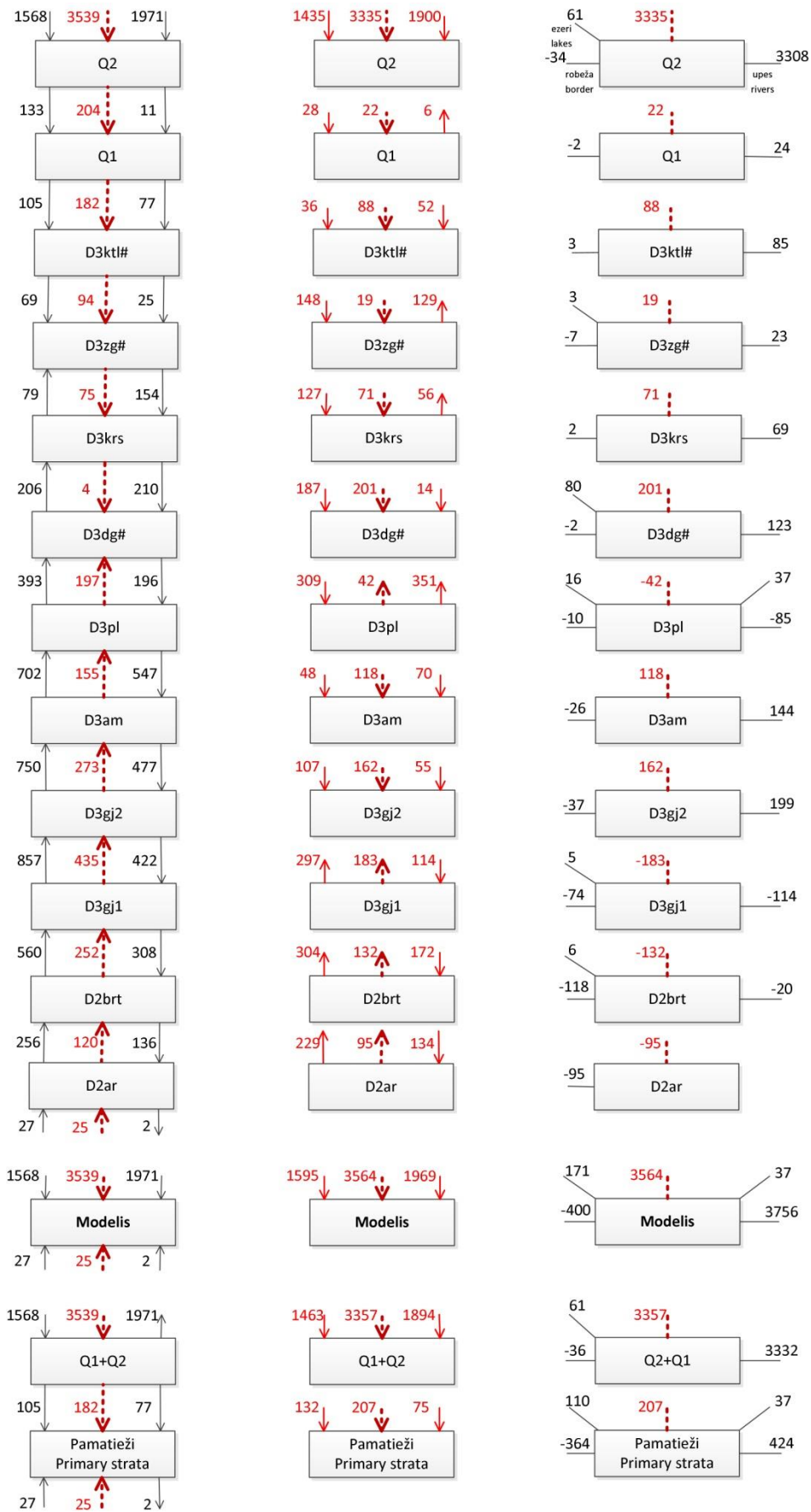


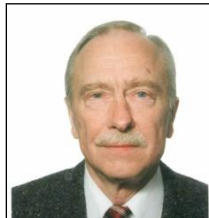
Fig. 7a. Scheme of LAMO2 and LAMO3 groundwater flow difference balance for Table IIIa.

## REFERENCES

- [1] "Water Framework Directive (2000/60/EC of the European Parliament and of the Council), Official Journal of the European Communities" L327, 22.12.2000, 2000.
- [2] A. Spalvins, J. Slangens, K. Krauklis, I. Lace, and O. Aleksans, "Novel methods used to develop hydrogeological model of Latvia," in *Proceedings of 27-th European Conference on Modelling and Simulation ECMS*, 2013, p. 136–143.
- [3] "Environmental Simulations, Inc. Groundwater Vistas – 6, Guide to using," 2011, [Online]. Available: [http://www.groundwatersoftware.com/groundwater\\_vistas.htm](http://www.groundwatersoftware.com/groundwater_vistas.htm) [Accessed May 15, 2014].
- [4] "Golden Software, SURFER – 9 for Windows, Users Manual," 2010, [Online]. Available: <http://www.goldensoftware.com/products/surfer> [Accessed May 20, 2014].
- [5] J. Walkenbach, *Excel 2007 Bibl*, Indianapolis, Indiana: Wiley Publishing, Inc., 2007.
- [6] A. Spalvins, J. Slangens, K. Krauklis, and I. Lace, "Methods and tools to be applied for creating of regional hydrogeological model of Latvia," in *25th European Conference on Modelling and Simulation*, 2011, pp. 132–141.
- [7] A. Spalvins, J. Slangens, O. Aleksans, K. Krauklis, and I. Lace, "Regional hydrogeological model of Latvia for management of its groundwater resources," in *5-th International scientific conference Applied information and communication technologies*, 2012, pp. 135–155.
- [8] A. Spalvins, J. Slangens, I. Lace, and K. Krauklis, "Geological profiles as efficient means for expounding results provided by hydrogeological model of Latvia," in *14th Geo Conference on Science and Technologies in Geology*, Exploration and Mining (SGEM), Conference Proceedings, vol. II, 2012, pp. 401–408.
- [9] A. Spalvins, J. Slangens, I. Lace, K. Krauklis, and O. Aleksans, "Efficient Methods Used to Create Hydrogeological Model of Latvia," *International Review on Modelling and Simulations*, (I.RE.MO.S), vol. 6, no. 5, pp. 1718–1726, Okt. 2013.
- [10] "Mapping of groundwater bodies of the Gauja-Koiva river basin district," Report on contract carried out by Riga Technical University, 25-maps (in Latvian), 2013. [Online]. Available: <http://www.emc.rtu.lv/> [Accessed May 20, 2014].
- [11] "Mapping for the Gauja river basin district by using results of hydrogeological model of Latvia," Riga Technical University, 12 p., 49 maps, 6 tables, (in Latvian), 2013. [Online]. Available: <http://www.emc.rtu.lv/> [Accessed May 20, 2014].
- [12] "Mapping for the Daugava river basin district by using results of hydrogeological model of Latvia," Riga Technical University, 12 p., 52 maps, 7 tables, (in Latvian), 2013. [Online]. Available: <http://www.emc.rtu.lv/> [Accessed May 20, 2014].
- [13] "Mapping for the Lielupe river basin district by using results of hydrogeological model of Latvia," Riga Technical University, 12 p., 55 maps, 7 tables, (in Latvian), 2013. [Online]. Available: <http://www.emc.rtu.lv/> [Accessed May 20, 2014].
- [14] "Mapping for the Venta river basin district by using results of hydrogeological model of Latvia," Riga technical University, 12 p., 57 maps, 7 tables, (in Latvian), 2013. [Online]. Available: <http://www.emc.rtu.lv/> [Accessed May 20, 2014].
- [15] A. Spalvins, J. Slangens, I. Lace, K. Krauklis, and O. Aleksans, "Survey of the first results provided by hydrogeological model of Latvia," in *9-th International Conference Environmental Engineering*, 2014.
- [16] A. Spalvins, and I. Lace, "Appliance of Pumping Data of Wells for Obtaining Transmissivity Distributions of Aquifers for Hydrogeological Model of Latvia," *Scientific Journal of Riga Technical University, Boundary Field Problems and Computer Simulation*, vol. 53, pp. 43–49, 2014.
- [17] K. Krauklis, and J. Slangens, "Special software used for implementing elements of hydrographical network into hydrogeological model of Latvia," *Scientific Journal of Riga Technical University, Boundary Field Problems and Computer Simulation*, vol. 53, pp. 25–29, 2014.
- [18] I. Dzilna, *Resources, composition and dynamics of groundwater for the middle part of the Baltic area*. Riga: Zinatne, 1970 (in Russian).



**Aivars Spalvins** was born in Latvia. In 1963, he graduated from Riga Polytechnical Institute (Riga Technical University since 1990) as a Computer Engineer. He is Head of the Environment Modeling Center of RTU. His research interests include computer modeling of groundwater flows and migration of contaminants.  
E-mail: emc@cs.rtu.lv



**Janis Slangens** was born in Latvia. In 1969, he graduated from Riga Polytechnical Institute (Riga Technical University, since 1990) as a Computer Engineer. He is a Senior Researcher with the Environment Modeling Center of RTU. His research interests include computer modeling of groundwater flows.  
E-mail: emc@cs.rtu.lv



**Inta Lace** was born in Latvia. In 1971, she graduated from Riga Polytechnical Institute (Riga Technical University, since 1990) as a Computer Engineer. In 1995, she received the Master's degree in Applied Computer Science. Since 1991, she has been a Researcher with the Environment Modeling Center, Faculty of Computer Science and Information Technology, RTU.  
E-mail: emc@cs.rtu.lv



**Olgerts Aleksans** was born in Latvia. In 1979, he graduated from Vilnius State University as a Hydrogeologist & Engineering Geologist. In 2011, he received the Doctor's degree in Geology. Since 2011, he is a Researcher with the Environment Modeling Center of Riga Technical University.  
E-mail emc@cs.rtu.lv



**Kaspars Krauklis** received a Master's Degree in Computer Systems from Riga Technical University in 2007 and the Certificate in Teaching of Engineering Sciences from the Institute of Humanities of RTU in 2005. Presently he is a Researcher with the Environment Modeling Center of Riga Technical University.  
E-mail: emc@cs.rtu.lv



**Viesturs Skibelis** was born in 1945 in Germany. In 1967, he graduated from Riga Polytechnical Institute (Riga Technical University, since 1990) as a Computer Engineer. In 2001, he received the Master's degree in Applied Computer Science. He is a Researcher with the Environment Modeling Center, Riga Technical University.  
E-mail: Viesturs.Skibelis@cs.rtu.lv



**Irina Eglite** received the Master's degree in Mathematics from the University of Latvia and the Master's degree in Applied Computer Science from Riga Technical University. Presently she is a PhD student with Riga Technical University, a Researcher with the Environment Modeling Center and a Lecturer with the Department of Engineering Mathematics, RTU.  
E-mail: Irina.Eglite@rtu.lv

# Special Software Used for Implementing Elements of Hydrographical Network into Hydrogeological Model of Latvia

Kaspars Krauklis<sup>1</sup>, Janis Slangens<sup>2</sup>,  
<sup>1-2</sup> Riga Technical University

**Abstract** – Hydrogeological model (HM) of Latvia (LAMO) is used for simulation of groundwater flow regime in its active zone. Surface waters – rivers, lakes and sea have great influence on groundwater flow. Current LAMO3 version contains 27 layers with  $610 \times 951 \times 27 = 15\,431\,877$  spatial grid nodes; the plane approximation step of LAMO3 is 500 meters. Rivers, lakes and sea form hydrographical network (HN) of LAMO3: 462 rivers in 42 680 nodes and 128 lakes and sea in 104303 nodes are attached to aquifers. Development, modifying and improving of HN is an iterative process. Adding or excluding of a particular river or lake must be performed in short time. It is impossible to do it without developing special software, which performs automation of creating the HN and including it into the model. This paper describes some algorithms and software, which were used for HN creation and its inclusion into LAMO3, such as the data interpolation of river and lake geometry, attaching HN to the model, immersion of river valleys into the HM body, creation of HN data for a model version with a different plane approximation step, joining of model surfaces for data input for Groundwater Vistas (GV) modelling system and software solution overview, which achieved all objectives of HN creation.

**Keywords** – Automation, hydrographical network, LAMO, modelling, software.

## I. INTRODUCTION

Problems of HN creation in LAMO3 [1]–[3] are common in HM development. An essential need for automation of this process is based on rapid evolution of IT hardware and software approaches, with growing opportunity of obtaining, processing and using huge amounts of data. Original software solutions of Environment Modelling Centre of Riga Technical University were adapted using the newest software compilers and by increasing data array sizes [4]. Notable amount of initial data were obtained which described geological layers. It was difficult to find faults in these data manually, because the checking was time consuming. In the creation of the LAMO relief surface [5] more than 1 million isolines were checked and the false level values were corrected.

It was impossible to obtain HN data for the regional model LAMO without software automation. The main reason was the complicated HN calculation algorithm, which had been developed and used for several years. This algorithm was previously described in [6] and it is improved in this paper. The second reason is the future development of LAMO4, which contained  $1201 \times 1901 \times 27 = 61\,643\,727$  spatial grid nodes. The number of lakes and rivers included in HN could

be increased by changing the initial set of HN data, too. All these problems need an automated solution.

LAMO uses modelling environment GV [7]. The automation of this environment is done basically on the input/output data file level by creating the input data or by processing the data of results. The main initial data for the implementation of HN into a model are surfaces of layers and attaching data for rivers and lakes to the HM grid nodes set. In Section „Algorithms and Methods” some algorithms are described which are used in creation of HN and its implementation into the model. In Section „Architecture of Automation” software solution is described, which realizes these algorithms.

## II. ALGORITHMS AND METHODS

### A. Creation of River Data

The EMC software GDI [8] interpolates the model surface set. The data for rivers should be interpolated as a long line profile with the water level value by the program CRP [8] on each river profile line intersection point with cell edge of the model. The first stage of the LAMO development interpolation levels of long line profile of rivers was performed. The levels were based on the river level post data with the following correction with only on elevation lines based relief surface data. According to the algorithm, which is described in [6], the river long line should be below the relief surface level. The first calculations of the LAMO river flow balance confirmed the collecting of groundwater by rivers and also losing it, mostly in rivers. Source interpolated data for rivers were unreliable, because they were based only on the relief elevation data. The assumption was made that in those places the level of river should be below groundwater level of the Q2 aquifer:

$$Z_i \leq \text{Head}_{Q2} - L \quad (1)$$

where  $Z_i$  – level of the river for a grid node;  $\text{Head}_{Q2}$  – groundwater level on the aquifer;  $Q2$ ,  $L$  – constant value, which describes minimal difference between the river level and the  $\text{Head}_{Q2}$ . The decreasing level values on river long line profile must be supported when (1) is applied.

The problem of river water loss to an aquifer was solved by this correction. Obtaining of levels on river long line profile was realized as iterative process, because these levels were

dependent on the groundwater levels formed in previous model simulation. The correction of the Gauja river long line profile is shown in Fig. 1. The main correction was realized near the river source that could be originated by the lack of the river level post data there and by the imperfection of the used linear interpolation algorithm. The river width value was computed by linear interpolation of the available river width data.

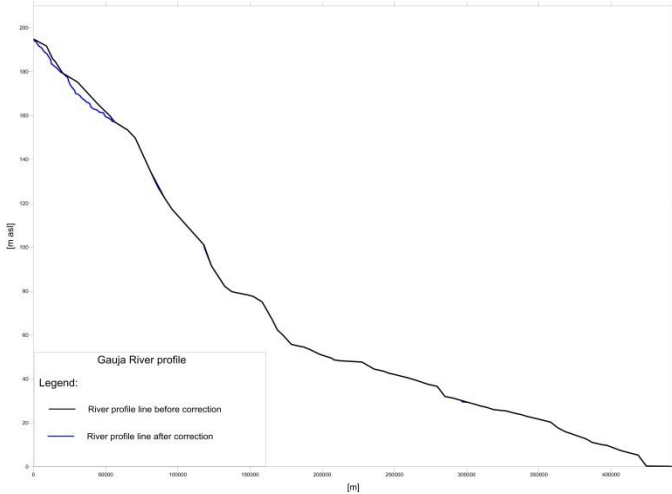


Fig. 1. Correction of levels on the Gauja river.

**B. Creation of River Attaching Data**

The rivers were incorporated into LAMO by attaching them to it. The attaching algorithm was performed by the GV Modflow module. The .RIV file (Fig. 2) shows how a river was attached to HM. The file had the address of the river attached node as row and column indexes. These addresses were converted to the model coordinates. The river was linked with the two nearest nodes and to the grid cell edge intersection point.

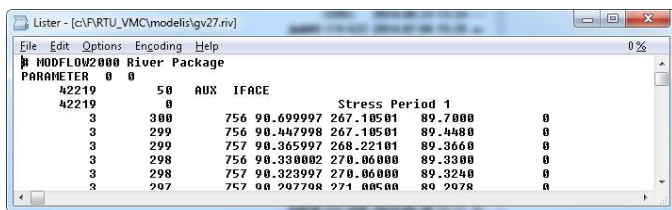


Fig. 2. Modflow River package file.

The conversion from the model cell address to the HM coordinates was given by the formula:

$$\begin{aligned}
 x_i &= (column_i - 1) \times step + startx \\
 y_i &= (rowcount - row_i + 1) \times step + starty
 \end{aligned}
 \tag{2}$$

where  $x_i, y_i$  -coordinate of the node;  $column$  - column number;  $step$  - model plane approximation step;  $rowcount$  - row count in model layer;  $startx, starty$  the coordinate of the left bottom corner of HM.

Some additional parameters are needed for the creation of river attaching data to HM, such as the river width, attachment aquifer number and the coordinates of the two nearest model nodes to the intersection point.

The coordinates of the two nearest nodes can be calculated by the following formulas:

$$\begin{aligned}
 x_i &= INT\left(\frac{x_p}{step}\right) \times step \\
 x_{i+1} &= INT\left(\frac{x_p}{step} + 1\right) \times step \\
 y_i, y_{i+1} &= y_p
 \end{aligned}
 \tag{3}$$

where  $x_p$  and  $y_p$  are the coordinates of the intersection point and  $step$  denotes the plane approximation step. These formulas are for the case when the intersection point is on the Y edge of the grid cell.

The attaching data file (Fig. 3) contains: coordinate X, coordinate Y, attaching layer, river id, river level and width, thickness of sediments and the river name. The attaching layer values are obtained by the algorithm described in Subsection ‘‘Immersion of Valleys of Rivers Into the HM Body’’.

	0	10	20	30	40	50	60	70	80
1	X_coord,	Y_coord,	Layer_Nr,	River_id,	Relh_2,	River_width,	thickness_of_sed		
2	603000.0000,	327000.0000,	3,	46,	194.7000,	241.1530,	1,	Gauja	
3	603000.0000,	327500.0000,	3,	46,	194.7000,	241.1530,	1,	Gauja	
4	603500.0000,	327000.0000,	3,	46,	194.5400,	595.2680,	1,	Gauja	
5	603500.0000,	327500.0000,	3,	46,	194.6390,	595.2680,	1,	Gauja	
6	604000.0000,	327000.0000,	3,	46,	194.1830,	29.8390,	1,	Gauja	

Fig. 3. Example of river attaching file.

The lake attaching data file has a similar structure (Fig. 3) to the attaching data file of a river. The main difference is in the lake node set, because the river node set is based on a line, but the lake node set is based on an area. To include all nodes, which are located within the lake area, the blanking operation ‘‘Grid Blank’’ of the Surfer software is used. After the blanking every masked node value was changed to the  $id$  value of the lake.

In the case, when the lake area is narrow, this algorithm obtained only a few nodes (Fig. 4a). It was necessary to enlarge the number of nodes for narrow lakes.

To provide adequate number of the lake data, the described algorithm for lakes was merged with the algorithm for rivers, where the lake coast line was used as the river line. Then the nearest node outside the lake was added to the lake. In the Ciecere lake case (Fig. 4) the attaching node number increased from 10 to 40.

The lake level was obtained from the LAMO relief with HN included. The calculation of the lake attaching layer was realized by the algorithm described in Subsection ‘‘Immersion of River Valleys Into the HM Body’’. The fragment of the lake attaching file is shown in Fig. 5. It contains X and Y coordinates of the lake node, attaching layer number, id, level, width, thickness of sediments and the lake name.

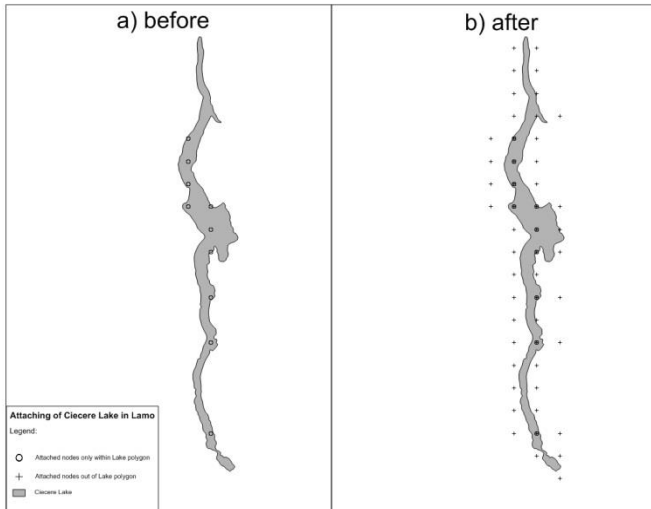


Fig. 4. Attaching of the Cicere lake in LAMO.

0	10	20	30	40	
1	X_coord	Y_coord	Layer_Nr	Lake_id	Relh_Z
2	443500	354500	3 1	0.7501 50	1 Engures
3	444000	354500	3 1	0.75 50	1 Engures
4	444000	354000	3 1	0.75 50	1 Engures
5	444500	354000	3 1	0.705 50	1 Engures
6	444000	353500	3 1	0.75 50	1 Engures

Fig. 5. Example of lake attaching file.

### C. Immersion of River Valleys Into the HM Body

Including of HN data into the relief was done by the GDI interpolation software [8]. Sometimes the river valley cuts through geological layers. Then geological layers should be changed by accounting for presence of the valley. In the planes where the layer is cut, its thickness is set to 0.02 meter, but for aquifer  $Q_2$  – 1 meter.

Surfaces of layers were used as the input data without accounting for valleys of rivers. Only for nodes of river attaching files data (Fig. 3) were processed to account for incised valleys. Data on all layers were compared by using the following formula:

$$Layer_i \leq Layer_{(i-1)} - thickness\_of\_layer \quad (4)$$

where  $Layer_i$  denotes the current layer node of the surface elevation and  $thickness\_of\_layer$  is the minimal thickness of the current layer.

All surfaces below the relief were changed and surfaces of layers were immersed below the incised part of the river by this algorithm. In the example (Fig. 6) of the cross section 2W–2E, which intersects the Gauja river twice, the incisions of the river were not done. After applying the immersion algorithm, the full Gauja river valley was formed (Fig. 7).

## II. ARCHITECTURE OF AUTOMATION

### A. Architecture

Automation software for HN creation and incorporation into LAMO contains a set of programs and scripting files that are united in modules, which can be dependent from each other on the input/output data level. Basically algorithms are implemented in the Fortran programming language with some scripts written in the Surfer [9] BASIC and in the VBScript language. The scripting approach enables to use several algorithms for manipulations with surface data and for changing of the data format. The description of modules and names of main programs are given in Fig. 8.

Main programs:

- 1) CRP – processes data linear interpolation with the given plane approximation step;
- 2) GDI – interpolates prepared data as surface with the given plane approximation step;
- 3) izoliniju\_vertibas\_upei – adds new points for the river geometry with the same level as in point attribute data. The program allows adding of river level values only in decreasing order;
- 4) dig\_dck\_rez\_to\_bln – obtains river data correction points, where the river long line is above the surface level i.e., the relief surface level;
- 5) izoliniju\_izvide – joins the geometry of isolines with their attribute – level;
- 6) grd\_vistas\_river\_level\_former – creates the river attaching data;
- 7) lamo\_lakes\_blank\_2014 – creates the lake attaching data;
- 8) grd\_on\_river\_correction – realizes incision of rivers on the geometry of HM;
- 9) grd\_to\_gvw\_matrix – merges and changes the format of all layer surfaces to the GV Matrix file format.

Additional scripts for data type conversion, blanking and other mathematical operations on grid surfaces are used. The module control, data exchange and the union of modules is realized by MS-DOS BAT command scripts.

Unified approach used in batch files enables to change the plane approximation step and to use input data sets for HN. In the example (Fig. 9) names of input and output data files are declared as variables in rows 1–8, which are used as parameters for calling two other batch files in rows 9 and 11. This fragment describes the HN incorporation into relief and representation of results as the Surfer map.

```

1 set omenbuf=relh4.buf
2 set maska=LV_ezeri_msk.msk
3 set vide=nav
4 set urbumi=relh_A.dck
5 set izolin=LV_ezeri.krp+%mpe%\LV_upes.krp
6 set dck=relh2_vissMOD.dck
7 set grd=relh2_vissMOD.grd
8 set masketle=nav
9 call GDI.bat %mpe% %omenbuf% %maska% %vide% %urbumi% %izolin% %dck% %grd% %masketle%
10 :T3
11 call DRAW.BAT %mpe% %omenbuf% %grd%

```

Fig. 9. Using parameters in the batch file.

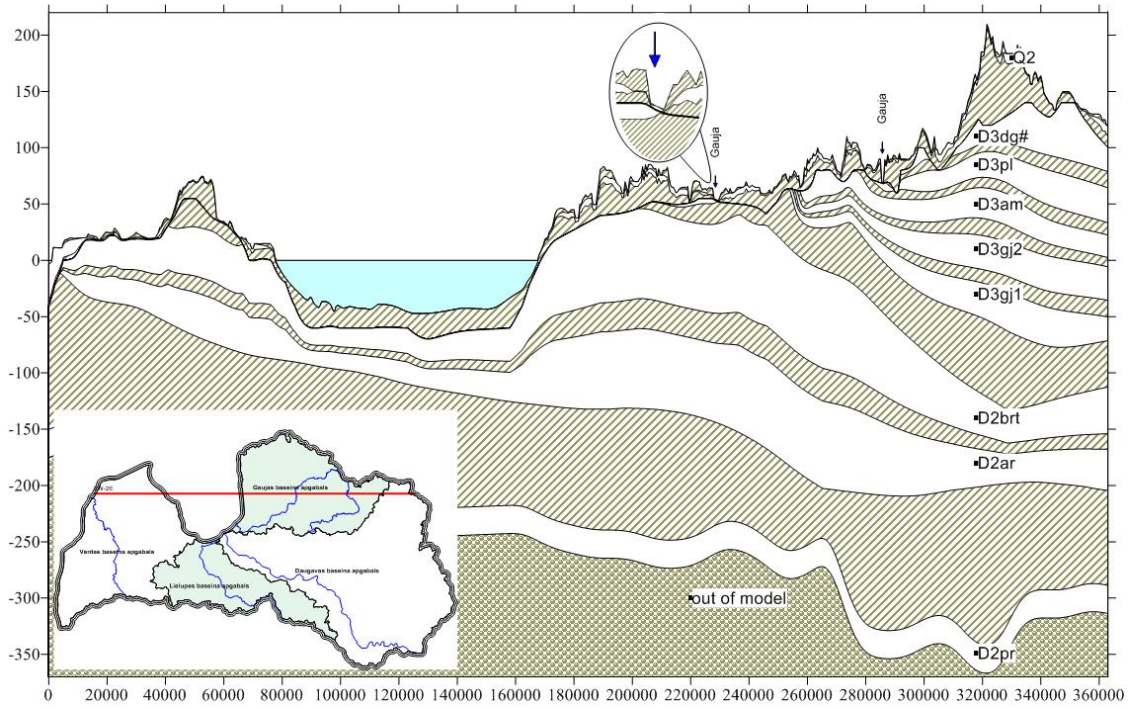


Fig. 6. Cross section 2W-2E before correcting the geometry.

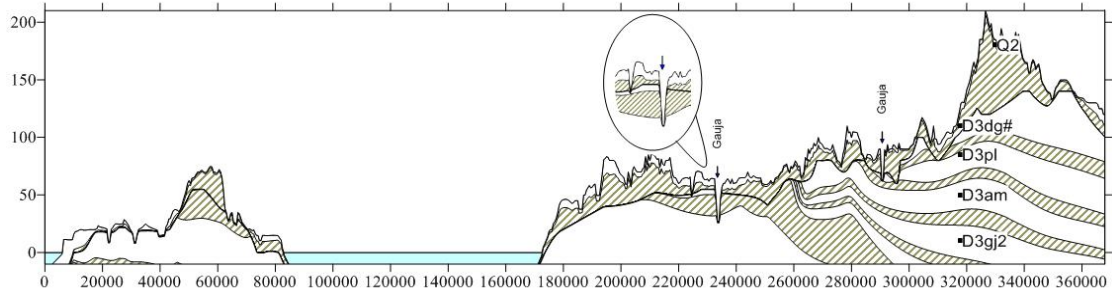


Fig. 7. Part of cross section 2W-2E after correcting the geometry.

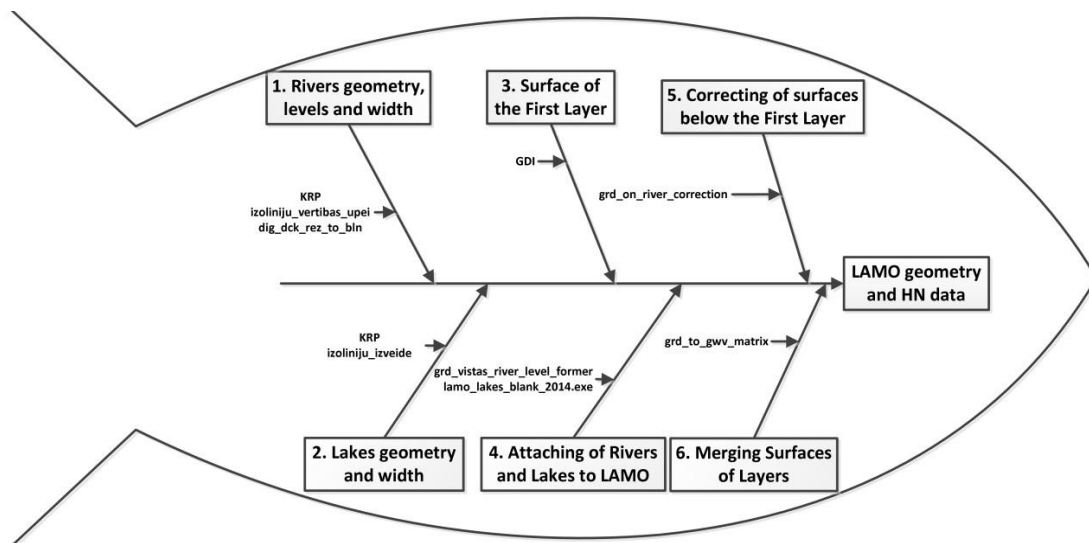


Fig. 8. Structure of important modules and programs for HN creation.

### B. Performance

This module set prepares LAMO3 geometry, HN attaching data and some other data for boundary conditions of HM in two hours. In the case of LAMO4 it will be approximately 8 hours.

Definitely, optimization of the software is possible – by minimizing conversion operations for data, by using data bases as storage, by combining more tasks under one, main program, by using parallelization approach for the software and by optimizing algorithms. The main advantages of the current solution are: the possibility of rapid change in every module and easy data control in each stage.

### III. CONCLUSION

The described algorithms and methods were used in practice in creation of the LAMO data. The algorithms of river level calculation guarantee changing of values in decreasing way, integrity of level data between rivers of the same basin, between the river and the relief surface and between the river and groundwater head. Immersion of river valleys was realized by decreasing the level and thickness of LAMO surfaces in places, where the incision existed. Two algorithms were developed and implemented for attaching rivers and lakes to HM. Unifying of all LAMO surfaces in one file saved a lot of time when the HM geometry had to be changed.

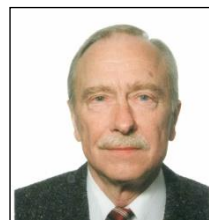
The current software solution is very fragmentary and needs a lot of time to perform it. All modules can work uninterruptedly, without user's involvement. The prepared data can be checked in each stage on the file level. Parametric approach for the batch files enables to create HN data for different models with a different plane approximation step and different initial HN data without significant changes. This statement will be proved by the next model LAMO4, which will be with different plane approximation step – 250 m. The main directions of the future development for this solution will be the improvement of algorithms and of software performance.

### ACKNOWLEDGEMENT

In 2010–2012 the hydrogeological model of Latvia called LAMO was developed within the framework of the project “The Creating of Hydrogeological Model of Latvia to be used for Management of Groundwater Resources and for Evaluation of Their Recovery Measures”. The project was co-financed by the European Regional Development Fund.

### REFERENCES

- [1] A. Spalvins, J. Slangens, I. Lace, O. Aleksans, K. Krauklis, V. Skibelis, and I. Eglite, “Hydrogeological model of Latvia after increasing density of its hydrographical network,” *Scientific Journal of Riga Technical University, Boundary Field Problems and Computer Simulation*, vol. 53, pp. 12–24, 2014.
- [2] Environment Modelling Centre, “Latvian Model,” February 2013. [Online]. Available: <http://www.emc.rtu.lv/lamo.htm> [Accessed Oct. 28, 2014].
- [3] A. Spalvins, and U. Nulle. “Hydrogeological model for management and recovery of groundwater resources of Latvia,” (in Latvian), *Scientific Journal of Riga Technical University, Boundary Field Problems and Computer Simulation*, vol. 49, pp. 7–13, 2011
- [4] A. Spalvins, J. Slangens, and K. Krauklis, “Updating of Geological Data Interpolation Programs,” *Scientific Proceedings of Riga Technical University in series Computer Science*, vol. 33, pp. 118–129, 2007.
- [5] J. Slangens, and K. Krauklis, “Creating of Digital Relief Map for Regional Hydrogeological Model of Latvia,” *Scientific Journal of Riga Technical University, Boundary Field Problems and Computer Simulation*, vol. 49, pp. 21–26, 2011.
- [6] J. Slangens, K. Krauklis, and I. Eglite, “Incorporation of the Hydrographical Network into the Digital Map of the Ground Relief,” *Scientific Journal of Riga Technical University, Boundary Field Problems and Computer Simulation*, vol. 45, pp. 45–52, 2010.
- [7] Groundwater Modeling Software Specialists, “Environmental Simulations Incorporated,” 2014. [Online]. Available: <http://groundwatermodels.com>, [Accessed Oct. 27, 2014].
- [8] A. Spalvins, J. Slangens, R. Janbickis, and I. Lace, “Interpolation as an Important Tool for Creating Credible Hydrogeological Models,” in *Proc. of the 4th International Conference on Calibration and Reliability in Groundwater Modelling, ModelCARE'2002*, 2002, pp. 84–87. [Online]. Available: <http://www.emc.rtu.lv/PragaPoster2002.pdf>, [Accessed Oct. 27, 2014].
- [9] Golden Software Inc., “Surfer® 12,” 2014. [Online]. Available: <http://www.goldensoftware.com/products/surfer> [Accessed Oct. 28, 2014].



**Janis Slangens** was born in Latvia. In 1969, he graduated from Riga Polytechnical Institute (Riga Technical University since 1990) as a Computer Engineer. He is a Senior Researcher with the Environment Modeling Center. His research interests include computer modeling of groundwater flows.

E-mail: [emc@cs.rtu.lv](mailto:emc@cs.rtu.lv)



**Kaspars Krauklis** received the Master's degree in Computer Systems from Riga Technical University in 2007 and the Certificate in Teaching of Engineering Sciences in 2005 from the Institute of Humanities, RTU. He is currently a Researcher with the Environment Modeling Center of Riga Technical University.

E-mail: [emc@cs.rtu.lv](mailto:emc@cs.rtu.lv)

# Forced Oscillations in the System of Anisotropic Stripe-half-plane with Hard and Sliding Connection of Media. Comparative Characteristics of Properties of Energy Fields

Michael Remizov, Rostov-on-Don State University of Civil Engineering

**Abstract** – This is the first research which considered the problem of forced oscillations strip connected with the half-plane where both scopes were supposed to be different anisotropy to the orthorhombic crystal system. Researchers used the method of contour integration in the fields of displacements and a comparative analysis of the properties of the energy flows in hard and sliding connection of these medium.

**Keywords** – Anisotropic medium, contour integration, distribution of energy flow, flow of energy, Fourier transforms, half-plane, rigid and slide connection, strip.

## I. INTRODUCTION

The influence of different pads located along the edge of the semi-infinite environment, was seen repeatedly. For anisotropic models of semi-infinite substrates the influence of the properties of border discontinuities on the dispersion curves and surface waves was investigated [1], [2]. The authors of [3] and [4] studied the acoustic effects observed in the elastic wave propagation in layered anisotropic media.

However, analysis of the energy transferred by anisotropic medium with overlay, was presented in smaller publications, among them [5] can be mentioned, where the energy characteristics of wave fields in multilayered anisotropic composites and estimation of the distribution of the portable power mod was investigated.

It is the first time that the researchers considered the problem of forced oscillations of strip connected with the half-plane, where both scopes were supposed to be of different anisotropy up to the orthorhombic crystal system inclusive of their hard and sliding connections. The defining move for each of the areas addressed issues associated with energy transfer and dependence of this characteristic length of the segment action of surface loading. The study first showed the relationship between the flows of energy transmitted in each of the medium separately, with respect to the total flow supplied to the infinite layer in the half-plane through the area dimension of loading of different lengths. A comparative analysis of properties of energy flows in hard and sliding connection is given. For numerical studies and examples, we used the following anisotropic material of strip and half-plane, respectively: titanate barium and beryllium.

## II. FORMULATION OF THE PROBLEM

The following dynamic problem is considered. In fields  $V^{(1)} = \{x_1 | \leq \infty, -h \leq x_3 \leq 0\}$ ,  $V^{(2)} = \{x_1 | < \infty, x_3 \geq 0\}$  we will seek the solution of the differential equations of motion, transformed by Fourier in the assumption of the existence of the mode steady-state oscillations (time-dependent factor  $e^{i\alpha t}$  is omitted):

$$\begin{cases} (-C_{11}^{(k)}\alpha + C_{55}^{(k)}\partial_3^2 + \rho^{(k)}\omega^2)U_1^{(k)} - i\alpha(C_{55}^{(k)} + C_{13}^{(k)})\beta_3 U_3^{(k)} = 0, \\ -i\alpha(C_{55}^{(k)} + C_{13}^{(k)})\beta_3 U_1^{(k)} + (-C_{55}^{(k)}\alpha^2 + C_{33}^{(k)}\partial_3^2 + \rho^{(k)}\omega^2)U_3^{(k)} = 0, \end{cases} \quad (1)$$

where  $k = 1, 2$  defines the system for strip and half-plane, respectively.

Boundary conditions and the conditions that characterize the type of interaction of these media are the following:

1) The case of rigid connection:

$$\left. \begin{cases} U_1^{(1)}(x_1, \alpha) = U_1^{(2)}(x_1, \alpha) \\ U_3^{(1)}(x_1, \alpha) = U_3^{(2)}(x_1, \alpha) \\ \sigma_{13}^{(1)}(x_1, \alpha) = \sigma_{13}^{(2)}(x_1, \alpha) \\ \sigma_{33}^{(1)}(x_1, \alpha) = \sigma_{33}^{(2)}(x_1, \alpha) \end{cases} \right\} x_3 = 0; \quad (2)$$

$$\left. \begin{cases} \sigma_{13}^{(1)}(x_1, \alpha) = 0 \\ \sigma_{33}^{(1)}(x_1, \alpha) = F(\alpha) \end{cases} \right\} x_3 = -h, \quad x_1 \in [-a; a].$$

2) The case of sliding connection:

$$\left. \begin{cases} U_3^{(1)}(x_1, \alpha) = U_3^{(2)}(x_1, \alpha) \\ \sigma_{13}^{(1)}(x_1, \alpha) = \sigma_{13}^{(2)}(x_1, \alpha) = 0 \\ \sigma_{33}^{(1)}(x_1, \alpha) = \sigma_{33}^{(2)}(x_1, \alpha) \end{cases} \right\} x_3 = 0; \quad (3)$$

$$\left. \begin{cases} \sigma_{13}^{(1)}(x_1, \alpha) = 0 \\ \sigma_{33}^{(1)}(x_1, \alpha) = F(\alpha) \end{cases} \right\} x_3 = -h, \quad x_1 \in [-a; a].$$

The statement of the problem completes the selection condition of the only solution, which here is the limiting absorption principle [10].

After that the standard technique of solution is applied. Imagine Fourier transforms for strip and half-plane in the form

$$\underline{U}^{(1)}(\alpha, x_3) = \underline{A}e^{\gamma x_3}, \quad \underline{U}^{(2)}(\alpha, x_3) = \underline{B}e^{-i\beta x_3}, \quad (4)$$

and substituting (4) with (1) where  $k = 1, 2$ , respectively. There will be two systems of homogeneous algebraic equations for the component vectors  $\underline{A}$ ,  $\underline{B}$ . A nontrivial solution of these systems turns to a zero specifier. These conditions determine the expression of characteristic numbers  $\gamma_m, \beta_m, m = 1 - 4$ .

Omitting the details of calculations, we give the expression  $\gamma_k(\alpha), \beta_k(\alpha)$  to dimensionless forms. For this we introduce the dimensionless elastic constants

$$b_{mn}^{(1)} = C_m^{(1)} / C_{33}^{(1)}, \quad m, n = 1, \dots, 6.$$

Then the formula for the roots takes the form of

$$\tilde{\beta}_{1,3}(\tilde{\alpha}) = \pm \sqrt{G_1^{(2)}(\tilde{\alpha})}, \quad \tilde{\beta}_{2,4}(\tilde{\alpha}) = \pm \sqrt{G_2^{(2)}(\tilde{\alpha})}, \quad (5)$$

$$\tilde{\gamma}_{1,3}(\tilde{\alpha}) = \pm i \sqrt{G_1^{(1)}(\tilde{\alpha})}, \quad \tilde{\gamma}_{2,4}(\tilde{\alpha}) = \pm i \sqrt{G_2^{(1)}(\tilde{\alpha})}, \quad (6)$$

where

$$G_1^{(k)}(\tilde{\alpha}) = 1 + b_{55}^{(k)} - \tilde{\alpha}^2 d^{(k)} + \sqrt{D_k(\tilde{\alpha})};$$

$$G_2^{(k)}(\tilde{\alpha}) = 1 + b_{55}^{(k)} - \tilde{\alpha}^2 d^{(k)} - \sqrt{D_k(\tilde{\alpha})}$$

$$\tilde{\alpha} = \alpha / \Omega, \quad \Omega = \omega \sqrt{\frac{\rho^{(k)}}{c_{33}^{(k)}}}, \quad b_{km}^{(k)} = \frac{C_{km}^{(2)}}{C_{33}^{(k)}}, \quad \tilde{\rho}^{(k)} = \frac{\rho^{(k)}}{c_{33}^{(k)}};$$

$$\tilde{\beta}_k = \beta_k \sqrt{\frac{2b_{55}^{(2)}}{\tilde{\rho}^{(2)}}}, \quad \tilde{\gamma}_k = \gamma_k \sqrt{\frac{2b_{55}^{(1)}}{\tilde{\rho}^{(1)}}};$$

$$d^{(k)} = b_{11}^{(k)} - 2b_{55}^{(k)} b_{13}^{(k)} - [b_{13}^{(k)}]^2.$$

Thus the discriminant  $D_k(\tilde{\alpha})$  is expressed by formulas

$$D_k(\tilde{\alpha}) = (1 - b_{55}^{(k)}) + \tilde{\alpha}^4 d_2^{(k)} - 2\tilde{\alpha}^2 d_3^{(k)};$$

$$d_2^{(k)} = [d^{(k)}]^2 - 4b_{11}^{(k)} [b_{55}^{(k)}]^2; \quad (7)$$

$$d_3^{(k)} = d^{(k)}(1 + b_{55}^{(k)}) - 2b_{55}^{(k)}(b_{11}^{(k)} + b_{55}^{(k)}).$$

For convenience, the tilde over  $\gamma_k, \beta_k$  further will be omitted.

When considering characteristic functions (5) and (6) in complex plane  $\zeta = \sigma + i\eta$  ( $\sigma = \tilde{\alpha}$ ) further it is assumed that the branches of the roots are selected according to the conditions

$$\operatorname{Re} \sqrt{D_k(\zeta)} > 0, \quad \operatorname{Re} \sqrt{G_m^{(k)}(\zeta)} > 0, \quad k, m = 1, 2. \quad (8)$$

In contrast, the solutions for stripes, involving all four roots of the characteristic equation, the half-plane must choose two values  $\beta_m$  that satisfy the attenuation of the waves at infinity ( $x_3 \rightarrow \infty$ )

$$\operatorname{Im} \beta_m < 0; \quad m = 1, 2. \quad (9)$$

It is easy to carry it out for those  $\beta_m$ , which take complex values. If  $\beta_m$  is real, the limiting absorption principle is used, which allows to build the only solution for the half-plane. This principle, as it is known, is that instead of the parameter  $\omega$ ,  $\omega - i\varepsilon$ ,  $\varepsilon > 0$  is introduced and the roots  $\beta_m$ , satisfying the condition (9) are taken.

Note that under the values of  $\beta_1, \beta_2$ , one should understand a couple of roots involved in the solution with the required sign before their external radicals from (5) in order to meet the condition (9).

So, we get the general expression of the transformant solution for strip and half-plane, respectively:

$$\begin{aligned} \underline{U}^{(1)}(\alpha, x_3) &= \sum_{k=1}^4 C_k \underline{A}^{(k)} e^{\gamma_k x_3}, \\ \underline{U}^{(2)}(\alpha, x_3) &= \sum_{k=1}^4 \tilde{C}_k \underline{B}^{(k)} e^{-i\beta_k x_3}. \end{aligned} \quad (10)$$

Now we will use the boundary conditions to determine the unknown constants  $C_k, \tilde{C}_k$ , included in (10) for each type of connection. The advanced matrix of these heterogeneous systems takes the following forms:

1) The case of rigid connection:

$$\begin{pmatrix} a_{11} & a_{12} & a_{13} & a_{14} & 0 & 0 & 0 \\ a_{21} & a_{22} & a_{23} & a_{24} & 0 & 0 & F \\ A_1^{(1)} & A_1^{(2)} & A_1^{(3)} & A_1^{(4)} & -B_1^{(1)} & -B_1^{(2)} & 0 \\ 1 & 1 & 1 & 1 & -1 & -1 & 0 \\ a_{51} & a_{52} & a_{53} & a_{54} & a_{55} & a_{56} & 0 \\ a_{61} & a_{62} & a_{63} & a_{64} & a_{65} & a_{66} & 0 \end{pmatrix} \quad (11)$$

2) The case of sliding connection:

$$\begin{pmatrix} a_{11} & a_{12} & a_{13} & a_{14} & 0 & 0 & 0 \\ a_{21} & a_{22} & a_{23} & a_{24} & 0 & 0 & F \\ 0 & 0 & 0 & 0 & -a_{55} & -a_{56} & 0 \\ 1 & 1 & 1 & 1 & -1 & -1 & 0 \\ a_{51} & a_{52} & a_{53} & a_{54} & 0 & 0 & 0 \\ a_{61} & a_{62} & a_{63} & a_{64} & a_{65} & a_{66} & 0 \end{pmatrix}, \quad (12)$$

where

$$\begin{cases} a_{1k} = (-i\alpha A_3^{(k)} + A_1^{(k)}\gamma_k) b_{55}^{(1)} e^{\gamma_k h}; \\ a_{2k} = (-i\alpha b_{13}^{(1)} A_1^{(k)} + A_3^{(k)}\gamma_k) e^{\gamma_k h}; \\ a_{5k} = (-i\alpha A_3^{(k)} + A_1^{(k)}\gamma_k) b_{55}^{(1)}; \\ a_{6k} = -i\alpha b_{13}^{(1)} A_1^{(k)} + A_3^{(k)}\gamma_k; \\ a_{55} = i b_{55}^{(2)} [\alpha B_3^{(1)} + \beta_1 B_1^{(1)}]; \\ a_{56} = i b_{55}^{(2)} [\alpha B_3^{(2)} + \beta_2 B_1^{(2)}]; \\ \\ \left\{ \begin{aligned} a_{65} &= i [\alpha B_1^{(1)} b_{13}^{(2)} + \beta_1 B_3^{(1)}] \\ a_{66} &= i [\alpha B_1^{(2)} b_{13}^{(2)} + \beta_2 B_3^{(2)}] \end{aligned} \right. \quad (13) \\ k = \overline{1,4}, \quad \gamma_1 = \gamma_1, \gamma_2 = -\gamma_1, \gamma_3 = \gamma_2, \gamma_4 = -\gamma_2. \end{cases}$$

Solving the system (11) and (12) relative to  $C_k, \tilde{C}_k$ , will provide solutions for both media in the form of the following transformant:

$$\underline{U}^{(1)} = \sum_{n=1}^4 \frac{\tilde{D}_n(\alpha)}{D_0^\varepsilon(\alpha, \omega)} A^{(n)} e^{\gamma_n x_3}, \underline{U}^{(2)} = \sum_{k=1}^2 \frac{\hat{D}_k(\alpha)}{D_0^\varepsilon(\alpha, \omega)} B^{(k)} e^{-i\beta_k x_3}. \quad (14)$$

Applying the inverse transform to (14) we can write the solution to the strip and half-plane  $x_3 \geq 0$  in the integral form used below.

$$\underline{u}^{(1)} = \frac{1}{2\pi} \int_{-\infty}^{\infty} \left\{ \sum_{n=1}^4 \frac{\tilde{D}_n(\alpha)}{D_0^\varepsilon(\alpha, \omega)} A^{(n)} e^{\gamma_n x_3 - i\alpha x_1} \right\} d\alpha, \quad (15)$$

$$\underline{u}^{(2)} = \frac{1}{2\pi} \int_{-\infty}^{\infty} \left\{ \sum_{k=1}^2 \frac{\hat{D}_k(\alpha)}{D_0^\varepsilon(\alpha, \omega)} B^{(k)} e^{-i\beta_k x_3 - i\alpha x_1} \right\} d\alpha. \quad (16)$$

Further applied known approach to the calculation of improper integrals (15) and (16) is based on the method of contour integration in complex plane. The feasibility of this process stems from the fact that for the elastic field asymptotic effective evaluation can be obtained far from sources of the disturbance area, for large  $R = \sqrt{x_1^2 + x_3^2}$ . For performing contour integration and cuts, on the banks of which the sheets of the Riemann surface are connected, where the functions  $\beta_k(\alpha), k = 1, 2, 3, 4$  are uniquely identified, the limiting absorption principle is used.

Integrand expression in (15) and (16), after the introduction according to the principle of limiting absorption of small friction  $\varepsilon > 0$ , will have four branch points

$$\zeta_k = \pm(\alpha_k - i\eta_k), \eta_k > 0; |\alpha_k| \gg |\eta_k|, k = 1, 2 \quad (17)$$

and a finite number of poles  $\overset{\circ}{\zeta}_n = \pm(\overset{\circ}{\alpha}_n - i\overset{\circ}{\eta}_n)$ :

$$D_0(\overset{\circ}{\zeta}_n, \omega_0), \quad n = 1, 2, \dots, N.$$

Positive branch points are shifted in the lower complex half-plane, negative on the top. If we consider the shift from real axis poles, then imagine implicit function  $\tilde{D}_0(\overset{\circ}{\alpha}_n, \omega_0) = 0$  in the form

$$\overset{\circ}{\alpha}_n = \chi(\omega_0).$$

Then, when you replace  $\omega_0 \Leftrightarrow \omega_0 - i\varepsilon$ , the new pole takes the form

$$\overset{\circ}{\zeta}_n = \chi(\omega_0 - i\varepsilon) = \chi(\omega_0) + \chi \frac{\partial \chi}{\partial \varepsilon};$$

$$\frac{\partial \chi}{\partial \varepsilon} = \chi(\omega_0) + \frac{\partial \chi(\omega_0 - i\varepsilon)}{\partial(\omega_0 - i\varepsilon)} \cdot \frac{\partial(\omega_0 - i\varepsilon)}{\partial \varepsilon} = \overset{\circ}{\alpha}_n - i \frac{\partial \overset{\circ}{\alpha}_n}{\partial \omega_0};$$

$$\overset{\circ}{\zeta}_n = \overset{\circ}{\alpha}_n - i \frac{\partial \overset{\circ}{\alpha}_n}{\partial \omega_0}. \quad (18)$$

From (18) we see that the shift of the pole with real axis is determined by the sign of the derivative of  $\frac{\partial \overset{\circ}{\alpha}_n}{\partial \omega_0}$ .

The next step is the deciding on the choice of spending cuts in the complex plane  $\zeta$ , allowing to select definite branch functions from (15) and (16), corresponding to the limiting absorption principle: when considering  $\beta_n \in C$ , choose roots that satisfy the attenuation of waves at infinity  $x_3 \rightarrow \infty$ , so,

$$\beta_n: \quad \text{Im } \beta_n < 0, \quad n = 1, 2.$$

Before proceeding to further discussion, let us pay attention to the following. The numerical results presented in this work belong to such a half-plane anisotropy, when in terms of dimensionless parameters of elasticity  $\alpha, \beta, \gamma$  and the dimensionless constant  $b_{mn}$ , introduced for the half-plane above,

$$\alpha = \frac{b_{55}}{b_{11}}, \beta = b_{55}, \gamma = \frac{b_{11} - 2b_{55}b_{13} - (b_{13})^2}{b_{11}} = \frac{d}{b_{11}}, \quad (19)$$

this type is defined as the second one, according to V. Budaev's classification in [11]:

Type II  $\alpha(1+\beta) < \gamma, 2\sqrt{\alpha\beta}$  (for example, beryllium and barium titanate).

According to the radiation conditions the only possible way of spending cuts was obtained in work [6] and [7] and used in [8] and [9].

Thus, given that in case  $x_1 < -a$  calculations are similar, forming the General contour of integration, consisting of a circle of large radius in the lower complex half-plane, a segment of real axis and two loops using the Cauchy theorem and Lemma Jordan, come to equality:

$$\int_{-\infty}^{\infty} \Phi^{(m)}(\alpha) d\alpha = i \sum_{k=1}^N \operatorname{Re} s \Phi^{(m)}(\zeta) \Big|_{\zeta=\zeta_k^0} - \frac{1}{2\pi} \int_{L_1} \Phi^{(m)}(\zeta) d\zeta - \frac{1}{2\pi} \int_{L_2} \Phi^{(m)}(\zeta) d\zeta, \quad (20)$$

where

$$\begin{aligned} \Phi^{(1)}(\alpha) &= \sum_{n=1}^4 \frac{\tilde{D}_n A^{(n)}}{D_0^\varepsilon} e^{\gamma_n x_3 - i\alpha x_1}, \\ \Phi^{(2)}(\alpha) &= \sum_{n=1}^2 \frac{\hat{D}_n B^{(n)}}{D_0^\varepsilon} e^{-i\beta_n x_3 - i\alpha x_1} \end{aligned} \quad (21)$$

are functions to strip and half-plane, respectively,  $L_1, L_2$  are paths along the banks of the sections and encircling the branch point  $\alpha_1, \alpha_2$ :  $\beta_m(\alpha_m) = 0, m = 1, 2$ .

### III. ANALYSIS OF ENERGY FLOW

One of the main questions of the present study was the energy of received fields in both media. The dependence of energy characteristics from the properties of driving force and connection kind of the strip and half-plane was determined. General expression of the average period power stream supplied to the infinite layer on the half-plane was considered. The average period power stream  $\bar{W}$  loaded through normal forces pad  $|x_1| \leq a, x_3 = -h$  can be defined by the formula [12]:

$$\bar{W} = \frac{\omega}{2} \int_{-a}^a g(x_1) \operatorname{Im}[u_3^{(1)}(x_1, -h)] dx_1. \quad (22)$$

According to (22), to calculate  $\bar{W}$ , you need to know  $\operatorname{Im}[u_3^{(1)}(x_1, -h)]$  for  $|x_1| \leq a$ . To determine  $u_3^{(1)}(x_1, -h)$  the method of contour integration is applicable to the calculation of the integral (15) after finding out the properties of  $F(\alpha)$  which Fourier transformed from the specified function of the load:

$$F(\alpha) = \int_{-a}^a g(x_1) e^{i\alpha x_1} dx_1. \quad (23)$$

Formula (21) is not applicable when  $|x_1| \leq a$ , because the short circuit in the lower complex half-plane conditions of Lemma Jordan are not met. For output expression of the displacement vector in this case, one must provide transformant from the function loads (23) in the form of the sum, which is taken in the present study as a constant on the interval  $[-a, a]$  load  $g(x_1) = p$  of unit cost intensity ( $2pa = 1$ ), so it is

$$F(\alpha) = \frac{p}{i\alpha} e^{i\alpha a} - \frac{p}{i\alpha} e^{-i\alpha a}. \quad (24)$$

We will substitute  $F(\alpha)$  of (24) with the integral for the stripe at  $x_3 = -h$ , i.e. with integral

$$u_3^{(1)}(x_1, -h) = \frac{1}{2\pi} \int_{-\infty}^{\infty} \sum_{k=1}^4 \frac{\tilde{D}_k}{D_0} A_3^{(k)} e^{-\gamma_k h - i\alpha x_1} d\alpha. \quad (25)$$

Given  $F(\alpha)$  (24) and the fact that

$$\tilde{D}_k = (-1)^k D_k F(\alpha), \quad k = 1, \dots, 4, \quad (26)$$

result the representation of  $u_3^{(1)}(x_1, -h)$  as a sum of two non-native integrals. Given the above with respect to all the features of subintegral functions (25) and the types of sections, we present the final expression for  $\operatorname{Im}(u_3^{(1)}(x_1, -h))$ , which will be used further in the study of energy flow

$$\begin{aligned} \operatorname{Im}(u_3^{(1)}(x_1, -h)) &= \operatorname{Im} \left\{ i \sum_{m=1}^N \operatorname{res} [\Phi(\zeta_m^0) F(\zeta_m^0) e^{-i\zeta_m^0 x_1}] + p\Phi(0) + \right. \\ &+ \frac{1}{2\pi} \int_0^{\alpha_1} \Phi(\alpha) F(\alpha) e^{-i\alpha x_1} \Big|_{[\beta_1^-, \beta_2^-]} d\alpha - \frac{1}{2\pi} \int_0^{\alpha_1} \Phi(\alpha) F(\alpha) e^{-i\alpha x_1} \Big|_{[\beta_1^+, \beta_2^+]} d\alpha + \\ &+ \left. \frac{1}{2\pi} \int_{\alpha_1}^{\alpha_2} \Phi(\alpha) F(\alpha) e^{-i\alpha x_1} \Big|_{[\beta_1^-, \beta_2^-]} d\alpha - \frac{1}{2\pi} \int_{\alpha_1}^{\alpha_2} \Phi(\alpha) F(\alpha) e^{-i\alpha x_1} \Big|_{[\beta_1^+, \beta_2^+]} d\alpha \right\}. \end{aligned} \quad (27)$$

Here were introduced the following notation:

$$\begin{aligned} 0 \leq \alpha \leq \alpha_1, \quad \beta_1 = \beta_1^+ : \operatorname{Re}(\beta_1) > 0; \quad \beta_1 = \beta_1^- : \operatorname{Re}(\beta_1) < 0, \\ \alpha_1 \leq \alpha \leq \alpha_2, \quad \beta_1 = \beta_1^- : \operatorname{Im}(\beta_1) < 0; \quad \begin{cases} \beta_2 = \beta_2^+ : \operatorname{Re}(\beta_2) > 0, \\ \beta_2 = \beta_2^- : \operatorname{Re}(\beta_2) < 0, \end{cases} \end{aligned}$$

where  $\alpha_1, \alpha_2$  are branch points of  $\beta_1(\alpha), \beta_2(\alpha)$ , respectively ( $\alpha_1 < \alpha_2$ ).

When computing now the flow of energy, «uploaded» through the loading area (22), we considered this characteristic depending on a parameter  $a$  – half of the length of the segment of action of driving force In Fig. 1 one can see graphs of functions  $\bar{W}(a)$  for both types of connection media. Both, here and hereafter graphics corresponding to the rigid connection are shown in solid curve by sliding dotted line. Calculations showed that  $a$  in the values of  $\bar{W}(a)$  is monotonically decreasing. The General predominance of flow in the case of a rigid connection there is  $a$ , in which this difference is maximal. When  $a \rightarrow 0$ , we have the following ratio of flow:

$$\bar{W}(\text{rigid}) = 1.11 \bar{W}(\text{sliding})$$

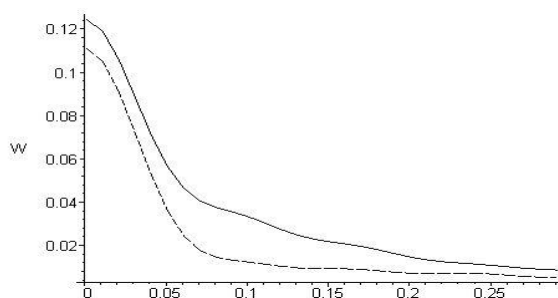


Fig. 1. Flow of energy, «uploaded» through the loading area.

Then the flow of energy through the cross-section of the strip ( $x_1 = \text{const}$ ) single width and height  $h$  was considered. As is known, this value is given by the formula (8):

$$\bar{W}_1 = \frac{i\omega}{4} \int_{-h}^0 \left( \overset{-}{\sigma}_{11} u_1 - \overset{-}{\sigma}_{11} u_1 + \overset{-}{\sigma}_{13} u_3 - \overset{-}{\sigma}_{13} u_3 \right) dx_3, \quad (28)$$

Included in (28) stress components are expressed through the infinite integral of the band solution. After counting the stress values  $\bar{W}_1$  has been obtained for  $x_1 > a$ . The behaviour of  $\bar{W}_1$  with growing  $a$  for each connection is shown in Fig. 2. Stream values are reduced to small ones when reaching a width of  $a$  of the order of the wavelength in the strip ( $a \sim \lambda = 0.15$ ). With a slight predominance of  $\bar{W}_1$  for sliding connection amplitudes take close values. When  $a \rightarrow 0$ , we have the following relation:

$$\bar{W}_1(\text{rigid}) = 0.91 \bar{W}_1(\text{sliding}).$$

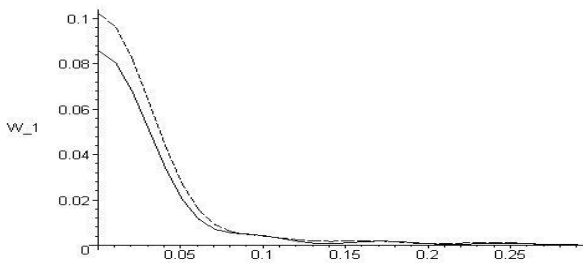


Fig. 2. Flow of energy through the cross-section of the strip.

Next, the flow of energy that propagates through the band to the half-plane is determined and the field in the half-plane is calculated based on the formula stationary phase. For this purpose the integral  $\overset{-}{u}^{(2)}$  of (16) was introduced through the sum of Fourier integrals:

$$\underline{u}_2 = \underline{V}_1 + \underline{V}_2, \quad (29)$$

where

$$\underline{V}_m = \int_{-\infty}^{\infty} \hat{\Phi}(\alpha) e^{-iRq_m(\alpha)} d\alpha;$$

$$R = \sqrt{x_1^2 + x_3^2}, \quad q_m(\alpha) = \alpha \sin \varphi + \beta_m \cos \varphi;$$

$$X_1 = R \sin \varphi, \quad X_3 = R \cos \varphi, \quad R \gg 2\pi/q_m, \quad m = 1, 2.$$

Using for  $\underline{V}_m$  of (29) the asymptotic:

$$\underline{V}_m \approx \sqrt{\frac{2\pi}{R|q_m''(\alpha_c^m)|}} \hat{\Phi}(\alpha_c^m) e^{-iRq_1(\alpha_c^m) - i\frac{\pi}{4} \text{sign} q_m''|_{\alpha=\alpha_c^m}}, \quad (30)$$

where  $\alpha_c$  is nondegenerate stationary point, which is the root of the equation

$$\frac{dq_m(\alpha)}{d\alpha} = 0, \quad \text{while} \quad \left. \frac{d^2q_1(\alpha)}{d\alpha^2} \right|_{\alpha=\alpha_c} \neq 0.$$

Further, by switching to polar coordinates, the relations

$$\hat{P}_R = -\frac{1}{2} \text{Re} \left\{ \sigma_{RR} \overset{-}{u}_R + \sigma_{R\varphi} \overset{-}{u}_\varphi \right\}, \quad \bar{W}_2 = 2 \int_0^{\pi/2} \hat{P}_R d\varphi$$

calculate radial component of the vector of the flow of energy  $\hat{P}_R$  and averaged over the period the energy stream  $\bar{W}_2$ , passing through the semicylindrical surface of the radius of  $R$ .

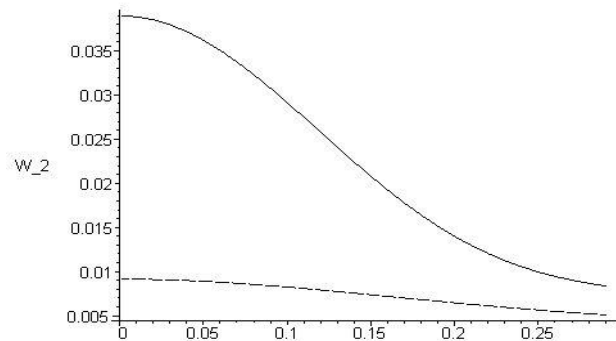


Fig. 3. Flow of energy through the band to the half-plane.

The graph of the function of the energy flow in the half-plane  $\bar{W}_2$  is based on the same parameter as shown in Fig. 3, where there is a predominance of flow for the hard connection. When  $a \rightarrow 0$  the ratio is:

$$\bar{W}_2(\text{rigid}) = 4.26 \bar{W}_2(\text{sliding}).$$

Taking the entire portable flow  $\bar{W}_1 + \bar{W}_2$  for 100% with concentrated indignation, the components are separated as follows:

$$\bar{W}_1(\text{rigid}) - 69\%; \quad \bar{W}_2(\text{rigid}) - 31\% = (15\% + 16\%);$$

$$\bar{W}_1(\text{sliding}) - 54\%; \quad \bar{W}_2(\text{sliding}) - 46\% = (30\% + 6\%).$$

For  $\bar{W}_2$  the distribution is given to the parts, corresponding to quasiparallel and quasioptical waves.

#### IV. RESULTS AND DISCUSSION

Thus, from the comparative analysis of properties of energy flows for two connection types it follows:

- 1) The total value of  $\bar{W}_1 + \bar{W}_2$  coincides with  $\bar{W}$ , which proves that the energy balance is taking place for the considered composite waveguide;
- 2) The available band is a barrier to the spread of the energy flow into the half-plane, so the most part of the «uploaded» power is transferred by the stripe;
- 3) By choosing the «moving» connection of materials the amount of power «uploaded» composite waveguide can be reduced by 10.5% when  $a \rightarrow 0$  as compared with «hard» connection;

4) It is shown that the choice of connection, can be adjusted to the distribution of the energy flow in the waveguide. In this example, the flow propagating in half-plane, while transiting from the sliding connection to the hard, increases in the band - reduces.

## REFERENCES

- [1] M. Babich, and A. B. Poskryakov, "About quasithin Rayleigh waves (case of anisotropic elastic body)," *Zap. the scientific. SEM. POMI*, vol. 332, pp. 7–18, 2006.
- [2] D. P. Morgan, "A history of surface acoustic wave devices," *Int. J. of High Speed Electronics and Systems*, vol. 10, no. 3, pp. 553–602, 2000.
- [3] V. K. Ignatovich, L. T. N. Phan, "Those wonderful elastic waves," *American J. of Physics*, vol. 77, № 12, pp. 1162–1172, 2009.
- [4] A. H. Nikitin, P. H. Vasin, T. I. Ivankina, A. A. Kruglov, and T. Lokajicek So, "Features passing quasiparabolic elastic waves through the interface of isotropic and anisotropic media: theoretical and experimental study," *Kristallografiya*, vol. 4, pp. 611–620, 2012.
- [5] E. Glushkov, N. Glushkova, and A. Krivonos, "Excitation and propagation of elastic waves in layered anisotropic composites," *Appl. Math. Mech.*, vol. 74, pp. 419–432, 2010.
- [6] A. B. Belokon, and O. A. Belokon, "Harmonic oscillations in anisotropic halfplane," *Izvestiya vuzov. The North Caucasus Region. Natural sciences*, vol. 4, 1999.
- [7] A. B. Belokon, and O. A. Belokon, "Method contour integration in the problems of harmonic oscillations of anisotropic half-plane," *Izvestiya vuzov. The North Caucasus Region – Natural Science. Region. Natural Sciences*, vol. 3, pp. 24–27, 2000.
- [8] A. B. Belokon, and M.Y. Remizov, "Harmonic oscillations of an infinite anisotropic strip rigidly connected with an anisotropic half-plane," *Dept. VINITI* from 29.12.00, vol. 3324.
- [9] M. Y. Remizov, "Forced oscillations of anisotropic strip rigidly associated with anisotropic half-plane," in *Abstracts of the International Conference of Modern Problems of Solid Mechanics*, 2000.
- [10] A. Sveshnikov, "The Principle of Radiation," *Dokl. The USSR Academy of Sciences*, 73, vol. 5, pp. 917–920, 1950.
- [11] V. Budaev, "The Roots of the characteristic equation and classification elastic anisotropic media classification," *Mechanics of solids*, vol. 3, 1978.
- [12] V. Grinchenko, and V. Meleshko, *Harmonic oscillations and waves in elastic bodies*. Kiev: Naukova dumka, 1981.



**Remizov Michael** received the Doctor's degree in Physics and Mathematics in 2003. He defended Doctoral Thesis "Energetic Field Analysis in Composed Anisotropic Half-Plane" in Southern Federal University, Rostov-on-Don, Russia. He is currently is an Associate Professor with the Technical Mechanics Department of Rostov-on-Don Civil Engineering University, Russia. Major areas of his research interests are: Elasticity Theory of Half-infinite Anisotropic Composed Media; Theory of Physical Diffractions. He is the author of 30 papers published in scientific journals and presented at international and Russian scientific conferences.

E-mail: remizov72@mail.ru

# Optimization Algorithms of Objective Control of Technical Objects

Genady Burov, *Riga Technical University*

**Abstract** – During the process of design, industrial production and operation of technical objects significant amount of information is accumulated. It can be used for the development of mathematical algorithms and programs for realization of automated computer control of technical objects. Because of the complexities in mathematical formalization of the aprioristic information difficulties arise, which do not always allow using it actively in mathematical models for the estimation of parameters obtained at separate stages of processing of the numerical information about measured transients. As the formed mathematical models are based on the theory of technical object identification, there is dependence of the computing stability of algorithms. Therefore, it is necessary to use equation systems with reasonably low orders. Such objective can be achieved due to the application of filtration of decomposition of autoregressive function. The algorithm of the objective control of technical objects is offered in the form of an algorithm by using the theory of pattern recognition. The recognition models as part of control algorithm may be built on the base of Fourier model. This results in efficiency of algorithms especially in test procedures.

**Keywords** – Characteristic polynomial, decomposition, discrete transfer function, regressive model, technical object transfer function.

## I. ANALYSIS OF ALGORITHM OF THE SOLUTION OF DIFFERENCE OF EQUATIONS

On the basis of measurements of signals of the technical object description of them can be developed in the form of difference equations (DE), which have been obtained during the design phase in the form of transfer functions (TF) (into the Laplace domain  $W(p)$ ). Obviously, this is a task for a mathematical model, which converts the digital measurements of signals at the input and output of the technical object into quantitative values of coefficients of its transfer function (TF)  $W(p)$ . The model of theoretical identification solves this task by solving a system of difference equations [3], [14]:

$$X\bar{\alpha} + Y\bar{\xi} = \bar{y} \quad (1)$$

$$U = [X \ Y];$$

$$U\bar{\theta} = \bar{y} \quad \bar{\theta} = U^{-1}\bar{y} = \begin{bmatrix} \bar{\alpha} \\ \bar{\xi} \end{bmatrix} \quad (2)$$

Vector  $\bar{\theta}$  connects the values of the input and output signals at specific time intervals and with factors of technical object TF  $W(p)$ . However, it consists of abstract values. The mathematical description of this connection is given in [13]. Thus, the

expression of generating operator of the system (1) can be derived:

$$D(z) = \frac{H(z)}{B(z)} = \frac{y(z)}{x(z)} \quad (3)$$

$$x(z) = \Phi_z(T)x(p)$$

$$y(z) = \Phi_z(T)y(p) \quad (4)$$

Here  $\Phi_z(T)$  denotes the quantization operation, known as operation Z-transform [2], [13]. It is implemented by decomposition (3) into the sum of elementary fractions and by applying Z-transform to each summand:

$$D(z) = \Phi_z(T)W(p) \quad (5)$$

$$D(z) = \frac{H(z)}{B(z)} = \sum_{i=1}^n \frac{Aw_i z}{z - \exp(-aw_i T)}$$

$$Aw_i = \frac{Rw(p = -aw_i)}{\prod_{j=1(j \neq i)}^n (aw_i - aw_j)} \quad (6)$$

As it can be seen from equations

$$\Phi_z(T)Qw(p) \Rightarrow B(z);$$

$$B(z) = \prod_{i=1}^n (z - \beta_i)$$

$$Qw(p) = \prod_{i=1}^n (p + aw_i) = \sum_{i=0}^n q_i p^i;$$

$$\beta_i = \exp(-aw_i T) \quad (7)$$

Let us consider an opportunity of realization of algorithm

$$\bar{\theta} \Rightarrow \bar{w} \quad \bar{w} \in W(p)$$

$$W(p) = \frac{Rw(p)}{Qw(p)} \quad (8)$$

We use operation inverse Z-of return transformation, applying expressions (3)–(7) upside-down:

$$\Phi_z^{-1}(T) \left\{ \widehat{D}(z) = \frac{\widehat{R}(z)}{\widehat{B}(z)} \right\} \Rightarrow \widehat{W}(p) \quad (9)$$

$$\bar{\alpha} \Rightarrow \widehat{R}(z) \quad \bar{\xi} \Rightarrow \widehat{B}(z) \quad (10)$$

The above polynomials are formed separately on the basis of the vector coefficients  $\bar{\alpha}$  and  $\bar{\xi}$ , in the vector  $\bar{\theta}$  composition. Therefore, for model (8) evaluation it is necessary to analyze the nature of computing operations (3)–(7). We must start by the characterizing polynomial (10) common denominator root definition

$$\widehat{B}(z) \Rightarrow \prod_{i=1}^n (z - \widehat{\beta}_i). \quad (11)$$

This analysis has shown that the individual root obtaining operation is imperative for any standardized computing algorithm. It may be impossible in the case of compressed information (impossible to distinguish between the calculated roots). At baseline analog poles for operator  $W(p)$  were well differentiated, as they were on the left plane of complex numbers and the distance between them was large enough. However, according to (7), these roots moved to the right complex plane in the restricted area at reduced distances. If the root finding operation cannot be carried out accurately, the next operation – the distribution of the vector  $\widehat{D}_M(z)$  sum of elementary fractions (9) and (10) cannot be carried out. It is concluded from the formula

$$V_i = \frac{\widehat{R}(z = \widehat{\beta}_i)}{\prod_{j=1; j \neq i}^n (\widehat{\beta}_j - \widehat{\beta}_i)}. \quad (12)$$

If for discrete pole splitting the Taylor series is one we obtain

$$\prod_{i=1(i \neq j)}^n (\beta_j - \beta_i) = T^{n-1} \cdot \prod_{i=1(i \neq j)}^n (a_j - a_i) \quad (13)$$

$$V_i \geq \frac{1}{T^{n-1}} \cdot \frac{\widehat{R}(z = a_i)}{\prod_{j=1; i \neq j}^n (a_j - a_i)}. \quad (14)$$

Further it is necessary to establish  $\widehat{D}(z)$  in (9) as a sum

$$\widehat{D}(z) \Rightarrow \sum_{i=1}^n \frac{V_i z}{z - \beta_i} \quad (15)$$

and to transform the summarized parts by using formula (7). These are nonlinear discrete-pole  $\beta_i$  operations for turning into analogues  $\mathcal{G}_i$

$$[\beta_i = \exp(-T \mathcal{G}_i)] \Rightarrow \left[ \mathcal{G}_i = \frac{\ln(\beta_i)}{T} \right]. \quad (16)$$

Using the formula

$$\Phi_z^{-1}(T) \left[ \frac{V_i z}{z - \beta_i} \right] \Rightarrow \frac{V_i}{p - \mathcal{G}_i} \quad (17)$$

expression (22) turns into the form

$$\Phi_z^{-1}(T) \widehat{D}(z) \Rightarrow \left\{ \widehat{W}(p) = \sum_{i=1}^n \frac{V_i}{p - \mathcal{G}_i} \right\}$$

$$\widehat{W}(p) = \frac{\widehat{R}w(p)}{\widehat{Q}w(p)}. \quad (18)$$

Therefore, model (8) computing operations are mathematically incorrect.

Abstract vector  $\bar{\theta}$  in (2) cannot modify parameters that characterize the physical state of the object

$$\Phi_z(T) \bar{\theta} \Rightarrow \widehat{W}(p). \quad (19)$$

## II. OPTIMIZATION OF ALGORITHM OF THE DECISION DIFFERENCE EQUATIONS

The system of the equations (2) contains a methodical error. It is designated as  $Yx(p)$

$$y(p) = Yw(p) + Yx(p) \quad (20)$$

We use decomposition

$$y(p) = x(p) \cdot W(p) = \sum_{i=1}^m \frac{Ax_i}{p + ax_i} + \sum_{i=1}^m \frac{Aw_i}{p + aw_i} \quad (21)$$

$$ax_i \in x(p); \quad aw_i \in W(p) \quad (22)$$

$$y(p) = \frac{R(p)}{Q^{(n)}(p)} = \sum_{i=1}^n \frac{A_i}{(p + a_i)} \quad (23)$$

$$y(t) = \sum_{i=1}^n A_i \cdot \exp(-a_i t). \quad (24)$$

We use operations (4)–(7)

$$\Phi_z(T) \left\{ y(p) = \frac{R(p)}{Q^{(n)}(p)} \right\} \Rightarrow y(z) \quad (25)$$

$$y(z) = \frac{R(z)}{B(z)}$$

$$\Phi_z(T) \left[ Q^{(n)}(p) = \prod_{i=1}^n (p + a_i) \right] = B(z) \quad (26)$$

$$B(z) = \prod_{i=1}^n (z - \beta_i) = \sum_{i=0}^n \xi_i z^{n-i};$$

$$\beta_i = \exp(-a_i \cdot T) \tag{27}$$

Vector  $\overline{w}^{-T}(t)$  of values  $y(t)$  on an interval

$$\overline{t}^{(n)} = [t \quad t+T \quad t+2T \quad \dots \quad t+nT]$$

can be written down as the sum of lines of the matrix

$$[H]_{i,j} = A_i \cdot \exp(a_i t) \cdot \beta_i^{j-1}. \tag{28}$$

Let us consider function of autoregression [15]

$$u(t) = y(t) + y[t-T] \cdot \xi_{n-1} + y[t-2T] \cdot \xi_{n-2} \dots + y[t-nT] \cdot \xi_0 \tag{29}$$

Here  $\xi_i$  are factors of transfer function of the filter

$$B\xi(z) = z^n + z^{n-1} \cdot \xi_{n-1} + z^{n-2} \cdot \xi_{n-2} + \dots + z^{n-k} \xi_{n-k}. \tag{30}$$

According to (30) expression (28) leads to a kind

$$H = D(\overline{dg})G; \quad \overline{dg}_i = A_i \cdot \exp(-a_i T); \tag{31}$$

$$G_{i,j} = \beta_i^j$$

Here the diagonal matrix is submitted by the vector of factors  $\overline{dg}$ . Then for  $k = 4$  we shall receive

$$H\overline{\xi} = Dg \begin{bmatrix} A_1 \exp(a_1 t) \\ A_2 \exp(a_2 t) \\ A_3 \exp(a_3 t) \\ A_4 \exp(a_4 t) \end{bmatrix} \cdot \begin{bmatrix} B\xi(z = \beta_1) \\ B\xi(z = \beta_2) \\ B\xi(z = \beta_3) \\ B\xi(z = \beta_4) \end{bmatrix} \tag{32}$$

$$\begin{bmatrix} B\xi(z = \beta_1) \\ B\xi(z = \beta_2) \\ B\xi(z = \beta_3) \\ B\xi(z = \beta_4) \end{bmatrix} = \begin{bmatrix} 1 & \beta_1 & \beta_1^2 & \beta_1^3 & \beta_1^4 \\ 1 & \beta_2 & \beta_2^2 & \beta_2^3 & \beta_2^4 \\ 1 & \beta_3 & \beta_3^2 & \beta_3^3 & \beta_3^4 \\ 1 & \beta_4 & \beta_4^2 & \beta_4^3 & \beta_4^4 \end{bmatrix} \cdot \begin{bmatrix} \xi_4 \\ \xi_3 \\ \xi_2 \\ \xi_1 \\ \xi_0 \end{bmatrix} \tag{33}$$

or in a brief form

$$H\overline{\xi} = \overline{dg} \otimes \overline{B\xi} = \begin{bmatrix} A_1 \exp(a_1 t) \\ A_2 \exp(a_2 t) \\ A_3 \exp(a_3 t) \\ A_4 \exp(a_4 t) \end{bmatrix} \overline{\exp(a_i t)} \otimes C$$

$$H\overline{\xi} = \overline{\exp(a_i t)} \otimes \overline{C}; \quad \overline{C} = \overline{A} \otimes \overline{B\xi} \tag{34}$$

$$B\xi_i = \prod_{j=1}^n (\beta_i - \mu_j)$$

$$F(\overline{\xi x})y(t) = \sum_{i=1}^n C_i \cdot \exp(-a_i t)$$

$$C_i = A_i B\xi_i \quad C_i = A_i \prod_{j=1}^n (\beta_i - \mu_j). \tag{35}$$

Using the received expressions for (29) it is received

$$u\xi(t) = \sum_{i=1}^n C_i \cdot \exp(a_i t) \tag{36}$$

$$C_i = A_i B\xi(z = \beta_i). \tag{37}$$

According to (32) the matrix (2) will be transformed to a kind

$$U\overline{\xi x} \Rightarrow [X = 0; Y^* = Y\overline{\xi x}]. \tag{38}$$

The transformed system of the equations is joint concerning a vector  $\overline{\xi w}$

$$Y\overline{\xi w} = 0 \quad \overline{\xi w} \in Bw(z). \tag{39}$$

The new model of algorithm does not contain the methodical error. Conditionality of the matrix is better because of the decrease in its order.

### III. OPTIMIZATION OF ALGORITHMS OF THE OBJECTIVE CONTROL OVER FOURIER MODELS

Restoration TF  $W(p)$  on algorithm (8) is connected to significant errors. The reason is that the roots of the analogue characteristic polynomial  $Q_w(p)$  denominator of the TF  $W(p)$  move from the left part of the infinite plane of complex numbers to its right part, to a narrow region of the right positive semi-circle. With the decrease of  $T$ , they contract in one multiple unit root. Therefore, large errors are characteristic of the recovery operations of discrete roots with the coefficients of the polynomial  $B(z)$  due to the constraints of the allocation of individual roots, since the distance between them can be compared to errors of computerized rounding of numbers. Therefore model (8) cannot be implemented because of the information compression of fragments  $W(p)$  due to sampling (4).

$$\overline{\theta} \Rightarrow [\hat{D}(z) = \hat{H}(z)/\hat{B}(z)] \tag{40}$$

$$\Phi_z^{-1}(T)\overline{\theta} \Rightarrow \hat{W}(p)$$

The results of computations in (4) are non-observable in nature. It indicates that for the identification of the dynamic characteristics of technical objects, it is appropriate to apply methods of pattern recognition theory rather than direct analytic transformations. Using the former, the measurements of the observed features are mapped into the measurements of non-observable patterns. For technical objects the task is simplified because the relationship between the features and patterns can

always be described using mathematical equations. It follows from the Weierstrass Theorem, according to which such a description can be obtained in the form of approximating polynomials [6]. In this case, the relationship is described by the Laplacian pattern

$$y(p) = W(p)x(p). \quad (41)$$

According to equation (12), for fixed test input  $x(p)$ , the matrix of vectors  $\bar{y}_i$  of values of transient processes  $My$  at intervals of fixed length is calculated. The relationship between matrices of vectors in the model

$$M = Mw \cup My \quad (42)$$

is described by the convolution equation. Therefore, the mapping of the set of vectors of features  $My$  onto the set of vectors of patterns  $Mw$  is isomorphism. The model of the objective control (MOC) is based on mapping

$$Mw \Leftrightarrow My. \quad (43)$$

The main task of the pattern recognition theory – classification of features and patterns in (13) – is fulfilled a priori [3] on the basis of isomorphism (14). According to the Weierstrass Theorem it is always possible to find mathematical description of the relationship between the elements not included in matrix (13)  $\bar{w}_i \notin Mw$ ,  $\bar{y}_i \notin My$  in the form of an approximating polynomial. Therefore, the decision function for the implementation of the transient process in the model of objective control may be formed in an analytical form to restore the numerical value of coefficient vector  $W_i(p)$  by the numerical value of the vector of transient process

$$\bar{y}_i \Rightarrow \bar{w}_i; \quad \bar{w}_i \in Mw; \quad \bar{y}_i \in My. \quad (44)$$

In [7] it is indicated that the decision function can be approximated by a function close to the linear one, by using the operation of endomorphism (by mapping models – matrices (13) “onto themselves”), in which their vectors can be decomposed into isomorphic basic systems,  $BzW^{(n)}$  and  $Bzy^{(n)}$ . They are formed on the basis of variations (12) in increments different from that in (13). The operation of endomorphism maps models in (13) onto the space of spectral vectors of the Fourier expansion of matrix elements (13) in the basic system

$$Fur(Bzy^{(n)})My^{(m)} \Rightarrow Cy^{(m)} \quad (45)$$

$$Fur(BzW^{(n)})Mw^{(m)} \Rightarrow Cw^{(m)} \quad (46)$$

$$Fur(Bzy^{(n)}; BzW^{(n)})(My \cup Mw) \Rightarrow (Cy^{(m)} \cup Cw^{(m)})$$

Isomorphism (14) is transformed into the isomorphism of the transformed model

$$(Mw \Leftrightarrow My) \rightarrow (Cw^{(m)} \Leftrightarrow Cy^{(m)}) \quad (47)$$

$$[Myw = My \cup Mw] \Rightarrow [Cyw = (Cy \cup Cw)]. \quad (48)$$

The corresponding algorithm is based on the operation of inversion of Gram matrices

$$Grw = (BzW^T BzW) \quad (49)$$

$$Gry = (Bzy^T Bzy); \quad (49)$$

$$\bar{w}_i = BzW \cdot Gry^{-1} (Bzy^T \bar{y}_i). \quad (50)$$

To form the model (13), expression  $W(p)$  of the transfer function of the object is required; it is derived from the DE system, which includes differential equations in the operator form (22). Coefficients of characteristic polynomial  $Qw(p)$  include the weight of the object.

The error of the OCM can be measured using the stationarity of changes of the vector of spectral coefficient. The nonlinear properties of operators of mapping deform the isometric properties of working spaces and are a source of methodical errors. Formally they represent a certain dynamic process generated by  $y(p) = W_i(p)x(p)$  on the interval  $t_0$ . According to (16) and (17) it is received

$$Cy_i = (Gry)^{-1} [Bzy^T \bar{y}_i(t)] \quad (51)$$

$$Cw_i = (Grw)^{-1} [BzW^T \bar{w}_i(t)]$$

$$Gry = Bzy^T Bzy \quad (52)$$

$$Grw = BzW^T BzW$$

$$\sigma_i = \sqrt{\frac{1}{N} \sum_{i=1}^N \|\bar{C}y_i - \bar{C}y_0\|} \quad (53)$$

$$N = (t_2 - t_1)/T.$$

This leads to the conclusion that for the estimation of algorithm usability characteristics of stationary of Fourier systems can be used. The accuracy of algorithm can be measured on the basis of the best approximation. For this purpose, let us use more accurate characteristics than the one used in [7]. It consists in the measurement of projections of vectors  $\bar{y}_i(t)$  and  $\bar{w}_i$  on the Fourier bases. Using the matrices of projection, we get

$$U = Bzy^T [Gry]^{-1} Bzy^T \quad (54)$$

$$S = BzW^T [Grw]^{-1} BzW^T. \quad (55)$$

Then the deviations of vectors from the subspaces of bases are:

$$u_i = (I - U)\bar{y}_i$$

$$s_i = (I - S)\bar{w}_i \tag{56}$$

Here the damped sinusoid had a frequency of 2.5 Gz, the object

From here we get angular values of deviations:

$$\varphi y_i = \arctg\left(\frac{\|(I - U_i)\bar{y}_i\|}{\|U\bar{y}_i\|}\right) \tag{57}$$

$$\varphi w_i = \arctg\left(\frac{\|(I - S_i)\bar{w}_i\|}{\|S_i\bar{w}_i\|}\right) \tag{58}$$

We shall note that the isometric properties of OCM algorithm can be received by the estimation

$$\Delta\varphi_i = \varphi y_i - \varphi w_i \tag{59}$$

These phase values and their discrepancy characterizes the isometric properties of the operator of mapping. The error of the OCM can be measured using the stationarity of changes of the vector of spectral coefficient. The nonlinear properties of operators of mapping deform the isometric properties of working spaces and are a source of methodical errors. Formally they represent a certain dynamic process generated by  $y(p) = W_i(p)x(p)$  on the interval  $t_0$ . According to (16) and (17) it is received

$$C y_i = (Gry)^{-1} [Bzy^T \bar{y}_i(t)]$$

$$C w_i = (Grw)^{-1} [Bzw^T \bar{w}_i(t)] \tag{60}$$

$$Gry = Bzy^T Bzy \quad Grw = Bzw^T Bzw \tag{61}$$

$$\sigma_i = \sqrt{\frac{1}{N} \sum_{i=1}^N \|\bar{C}y_i - \bar{C}y_0\|} \tag{62}$$

IV. EXAMPLE

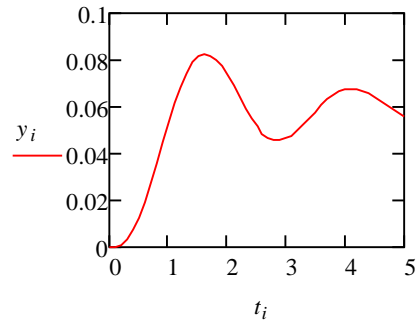
Below the results of a numerical experiment are presented which verify the accuracy to use OCM for identification of parameters of an object with TF

$$W(p) = \frac{p + \theta}{p^3 + q_2 p^2 + q_1 p + q_0} \tag{63}$$

Vectors  $\bar{w}_i \in Mw$  were given by deviations from the nominal value

$$\bar{w}_0^T = [\theta_0; q_{00}; q_{10}; q_{20}] = [0.5; 4; 1.863; 0.537]$$

in increments  $\varepsilon = 0.05$ ;  $\bar{w}_i = \bar{w}_0(1 + \varepsilon i)$ ; in interval  $i \in \overline{1.5}$ . The formation of OCM begins with the calculation of matrices for model (13). The accuracy of OCM (see  $\varepsilon q(\%)$ ) remained high. Due to the compression of information, an insoluble task to restore  $W(p)$ , formula (10) was solved on the basis OCM.



reaction  $y(t)$  is presented in Fig. 1.

Fig. 1. The object reaction  $y(t)$ .

Basic matrices  $Bzq$ ,  $Bzy$  (16) and  $My(Yx)$  were calculated as well as the matrix of transient processes  $Mw \Rightarrow My$  was calculated by formula  $y(p) = W(p)x(p)$ . Basic systems were used:

$$Bzy := \begin{pmatrix} 0 & 0 & 0 \\ 0.00024 & 0.00024 & 0.00024 \\ 0.0033 & 0.00327 & 0.00324 \\ 0.02258 & 0.02229 & 0.02203 \\ 0.12385 & 0.12201 & 0.12037 \\ 0.6259 & 0.61589 & 0.60703 \end{pmatrix}$$

$$Bzq := \begin{pmatrix} 4 & 3.45535 & 3.00526 \\ 10.6 & 10.04989 & 9.55372 \\ 6.4 & 6.20952 & 6.03636 \\ 1 & 1 & 1 \end{pmatrix}$$

To check the accuracy of OCM, a matrix

$$Mw^{(j)}(Qx) \in W^{(i)}(p)$$

was developed

$$Mw(Qx) := \begin{pmatrix} 4 & 2.772 & 2 & 1.489 & 1.139 \\ 10.6 & 9.279 & 8.249 & 7.424 & 6.749 \\ 6.4 & 5.94 & 5.575 & 5.278 & 5.032 \\ 1 & 1 & 1 & 1 & 1 \end{pmatrix}$$

The accuracy of its recovery from the matrix of transient processes  $My(Yx)$  was verified. Matrix  $Mw(Qx)$  was identified by matrix  $My(Yx)$  of the transient processes:

$$M_y(Yx) := \begin{pmatrix} 0 & 0 & 0 & 0 & 0 \\ 2.39 \cdot 10^{-4} & 2.36 \cdot 10^{-4} & 2.33 \cdot 10^{-4} & 2.31 \cdot 10^{-4} & 2.30 \cdot 10^{-4} \\ 3.30 \cdot 10^{-3} & 3.23 \cdot 10^{-3} & 3.17 \cdot 10^{-3} & 3.12 \cdot 10^{-3} & 3.08 \cdot 10^{-3} \\ 0.023 & 0.022 & 0.021 & 0.021 & 0.021 \\ 0.124 & 0.119 & 0.116 & 0.114 & 0.112 \\ 0.626 & 0.602 & 0.584 & 0.572 & 0.56 \end{pmatrix}$$

Matrices of spectral vectors  $[Cy]$  and  $[Cq]$  were also calculated (16)

$$C_y := \begin{pmatrix} 0.40709 & -1.02713 & -1.77714 & -2.18136 & -2.39909 \\ 1.3513 & 1.6911 & 1.38367 & 0.84219 & 0.23442 \\ -0.7597 & 0.33527 & 1.39125 & 2.33466 & 3.15762 \end{pmatrix}$$

$$C_q := \begin{pmatrix} 1 & 0.358 & 3.879 & 9.049 & 14.726 \\ 4.657 \times 10^{-10} & -1.31 & -10.806 & -23.362 & -36.685 \\ 1.164 \times 10^{-10} & 1.951 & 7.927 & 15.313 & 22.957 \end{pmatrix}$$

The matrix was identified

$$q_{x0} := \begin{pmatrix} 4.01447 & 2.74241 & 1.85357 & 1.20089 & 0.70314 \\ 10.63759 & 9.31091 & 8.35966 & 7.6462 & 7.09264 \\ 6.41046 & 5.95113 & 5.61632 & 5.36175 & 5.16204 \\ 0.99869 & 0.99924 & 0.99778 & 0.99549 & 0.99296 \end{pmatrix}$$

The accuracy of the algorithm OCM (%) is demonstrated in the matrix  $\varepsilon q(\%)$

$$\varepsilon q^{(j)} = \left\{ \left[ M_w^{(j)}(Qx) - q_{x0}^{(j)} \right] / M_w^{(j)}(Qx) \right\} 100\%$$

$$\varepsilon q(\%) := \begin{pmatrix} 0.00362 & -0.01075 & -0.07304 & -0.19372 & -0.38268 \\ 0.00355 & 0.00347 & 0.01342 & 0.02992 & 0.05098 \\ 0.00164 & 0.0019 & 0.00748 & 0.01593 & 0.02593 \\ -0.00131 & -0.00076 & -0.00222 & -0.00451 & -0.00704 \end{pmatrix}$$

Gram matrix is close to singular

$$\det(Gry) = 7.85 \times 10^{-21}.$$

Therefore, it is possible to implement the OCM only using special software [10], [12].

## V. CONCLUSION

Identification models based on conventional arithmetic equation solutions for signal measurements cannot be used for objective control. The arithmetic equation vectors  $\bar{\theta}$  are abstract. Their relation to physical parameters can be quantified

in analytical relationship. However, there are mathematically incorrect operations and results are not transparent. The operational computer software of automatic control and diagnostic systems of vector  $\bar{\theta}$  decrypting and the development of technical objects are doomed to failure. For the in-depth diagnosis of the object technical state, new methods must be used. Control models must include image recognition models that allow incorrect mathematical operations to provide the right solutions. The implementation of the image recognition system for Fourier models depends on the form of the basic information, which is not always sufficient and does not enable escape from significant errors.

## REFERENCES

- [1] G. Burovs, D. Varslavs, and M. Buikis, "Finite Difference Models of Identification of Dynamic Processes," *Scientific Proc. of Riga Technical University, Technologies of Computer Control*, vol. 5, pp. 66–76, 2001.
- [2] M. Buikis, and G. Burov, "Forecasting properties of recurrent relation," *Scientific Proc. of Riga Technical University, Technologies of Computer Control*, vol. 5, 2002.
- [3] G. Burov. 2002. "Structural disbalancement of regression models of identification," *Scientific Proc. of Riga Technical University in series Computer Science, Boundary field problems and computer simulation*, vol. 44, 2002.
- [4] J. Grundspenkis, and G. Burov, "The analysis of topological characteristics of information identification models," *Scientific Proc. of Riga Technical University in series Computer Science, Applied Computer Systems*, vol. 4, 2001.
- [5] J. Grundspenķis, and G. Burovs, "Topological properties of recurrent relations in models of identification," *Scientific Proc. of Riga Technical University in series Computer Science, Applied Computer Systems*, vol. 5, 2002.
- [6] G. Burovs, "Imitācijas modeļu izmantošana parametru kontroles algoritmos," *Pārskats ZPD NAA VPSN-02/02-2013*, pp. 7–17, 2013.
- [7] G. Burov, "The Computer Diagnosing of Technical Objects with the Use of Pattern Recognition Principles," *Scientific Journal of Riga Technical University, Boundary field problems and computer simulation*, vol. 52, 2013.
- [8] G. Burovs, "Tehnisko objektu datorizēta diagnosticēšana, izmantojot attēlu atpazīšanas principus," *Pārskats ZPD NAA VPSN-02/02-2013*, pp. 18–43, 2013.
- [9] M. Buikis, and G. Burovs, "Matemātiska un programmu nodrošināšana datorizēto sistēmu diagnosticēšanas algoritmiem," *Pārskats ZPD NAA VPSN-02/02-2013*, pp. 49–57, 2013.
- [10] G. Burov, "Combinatorial methods of formation of parallel algorithms of the signals processing," *Scientific Proc. of Riga Technical University in series Computer Science, Boundary field problems and computer simulation*, vol. 45, 2003.
- [11] G. Burov, "Principles of formation of parallel algorithms of the information processing in dynamic objects," *Scientific Proc. of Riga Technical University in series Computer Science, Technologies of computer control*, vol. 3, 2003.
- [12] G. Burovs, "Symbolical Combinatory Model of Parallel Algorithm of Identification That Uses Method of Least Squares," *Scientific Proc. of Riga Technical University in series Computer Science, Boundary field problems and computer simulation*, vol. 37, 2008.
- [13] J. M. Smith, *Mathematical modelling and digital simulation for engineers and scientists*. New York, Chichester: Wiley, 1980.
- [14] D. Graupe, *Identification of Systems*. New York: IEEE Press, 1976.
- [15] G. E. P. Box, G. M. Jenkins, *Time Series Analysis: Forecasting and control*. USA, University of Wisconsin: Holden-Day, 1970.

**Genady Burov** was born 1937 in St. Petersburg, Russia. He received the Doctoral degree in 1966. Genady Burov is currently a Leading Researcher with the Environment Modeling Center of Riga Technical University.  
E-mail: emc@cs.rtu.lv

# Appliance of Pumping Data of Wells for Obtaining Transmissivity Distributions of Aquifers for Hydrogeological Model of Latvia

Aivars Spalvins<sup>1</sup>, Inta Lace<sup>2</sup>,  
<sup>1-2</sup>Riga Technical University

**Abstract** – In 2010 – 2012 the hydrogeological model (HM) of Latvia called LAMO was developed by the scientists of Riga Technical University (RTU). LAMO generalizes geological and hydrogeological information accumulated by the Latvian Environment, Geology and Meteorology Centre (LVGMC). The commercial program Groundwater Vistas (GV) was used for running LAMO. In 2013 – 2014 LAMO was considerably upgraded. Density of the hydrogeological network (rivers and lakes) was increased, cuttings of river valleys into primary geological strata were accounted for, transmissivity distributions for aquifers were refined. To improve transmissivity data of HM aquifers, information provided by pumping tests for wells was used. The refined transmissivity data were applied to create the permeability maps of aquifers as the variable initial data for the GV system. To accomplish these task methods of numerical interpolation and digital image processing were used.

**Keywords** – Hydrogeological model, numerical interpolation, pumping tests for wells, transmissivity of aquifers.

## I. INTRODUCTION

In 2010 – 2012 the HM LAMO was developed and in 2013 – 2014 it was upgraded [1] by the scientists of RTU. LAMO comprises the active groundwater zone that provides drinking water. The location of LAMO is shown in Fig. 1. As it follows from the vertical schematization of HM (Fig. 2), the current version of LAMO simulates 27 geological layers, 12 of which are aquifers. As see in Fig. 3 and Fig. 4, most of the layers are outcropping.



Fig. 1. Location of LAMO.

They are not continuous and, for this reason, they are not present everywhere in the HM area. After emerging at the surface such layers have zero thickness  $m = 0$ . To avoid in GV calculations “the division by zero”,  $m = 0$  must be replaced by small  $\varepsilon > 0$  (for LAMO,  $\varepsilon = 0.02$  meters). It is explained later that the presence of the  $m = 0$  areas causes problems when the permeability maps for aquifers are obtained.

To understand the aquifer transmissivity role for HM, basic mathematical expressions of numerical hydrogeological modelling [2] must be considered.

Vector  $\varphi$  of the piezometric head is the numerical solution of the boundary field problem which is approximated in nodes of the HM  $xyz$ -grid by the following algebraic expression:

$$A\varphi = \beta - G\psi, \quad A = A_{xy} + A_z \quad (1)$$

where  $A$  is the symmetric sparse matrix of the geological environment which is presented by the  $xy$ -layer system containing horizontal ( $A_{xy}$  – transmissivity  $T$ ) and vertical ( $A_z$  – vertical hydraulic conductivity) elements of the HM grid and  $\psi$  and  $\beta$  are the boundary head and flow vectors, respectively;  $G$  is the diagonal matrix (part of  $A$ ) assembled by elements linking the nodes, where  $\varphi$  must be found with the points where  $\psi$  is given.

The transmissivity elements  $a_{xy}$ , of  $A_{xy}$ , of the HM  $xy$ -planes are computed, as follows:

$$a_{xy} = k_i m_i = T_i, \quad m_i = z_{i-1} - z_i, \quad m_i = > 0, \quad i = 1, 2, \dots, p \quad (2)$$

where

- $z_{i-1}$  and  $z_i$  elevations, accordingly, of the top and bottom surfaces of the  $i$ -th geological layer;
- $p$  number of surfaces (for LAMO,  $p = 28$ );
- $z_0$  ground surface elevation  $\psi_{rel}$  map;
- $k_i, m_i$  elements of the digital  $km$ -maps of the  $i$ -th layer permeability and computed thickness.

The  $m$ -maps are obtained from the  $z$ -maps and the elements  $T_i$  are also computed within the GV system [3]. For this reason, it is difficult to change the  $m$ -maps and one has to apply the variable permeability  $k$ -maps to control elements  $T_i = a_{xy}$ .

The matrices  $A_{xy}$  (transmissivity  $T$ ) for aquifers are very important, because they control the horizontal groundwater flow regime.

For aquitards  $a_{xy} \sim 0$ , because their permeability  $k$  is very small and the effect of  $A_{xy}$  is insignificant.

In the Appendix, as an example, obtaining of the *k*-maps for the D3pl aquifer is explained.

No of HM plane		Name of layer	Geological code	HM plane code
1.		Relief	relh	relh
2.	■	Aeration zone	aer	aer
3.		Unconfined Quaternary	Q4-3	Q2
4.	■	Upper moraine	gQ3	gQ2z
5.		Confined Quaternary or Jura	Q1-3 J	Q1#
6.	■	Lower moraine or Triass	gQ1-3 T	gQ1#z
7.		Perma Karbons Skerveles Ketleru	P2 C1 D3šķ D3ktl	D3ktl#
8.	■	Ketleru	D3ktl	D3ktlz
9.		Zagares Svetes Tervetes Muru	D3žg D3sv D3tr D3mr	D3zg#
10.	■	Akmenes	D3ak	D3akz
11.		Akmenes Kursas Jonisku	D3ak D3krs D3jn	D3krs#
12.	■	Elejas Amulas	D3el D3aml	D3el#z
13.		Stipinu Katlesu Ogres Daugavas	D3stp D3ktl D3og D3dg	D3dg#
14.	■	Daugavas Salaspils	D3dg D3slp	D3slp#z
15.		Plavinu	D3pl	D3pl
16.	■	Plavinu Amatas	D3pl D3am	D3am#z
17.		Amatas	D3am	D3am
18.	■	Upper Gauja	D3gj2	D3gj2z
19.		Upper Gauja	D3gj2	D3gj2
20.	■	Lower Gauja	D3gj1	D3gj1z
21.		Lower Gauja	D3gj1	D3gj1
22.	■	Burtnieku	D2brt	D2brtz
23.		Burtnieku	D2brt	D2brt
24.	■	Arikula	D2ar	D2arz
25.		Arikula	D2ar	D2ar
26.	■	Narvas Narvas	D2nr2 D2nr1	D2nr#z
27.		Pernavas	D2prn	D2pr

■ - aquitard  
# - united aquifer; #z – united aquitard

Fig. 2. Vertical schematization of LAMO.

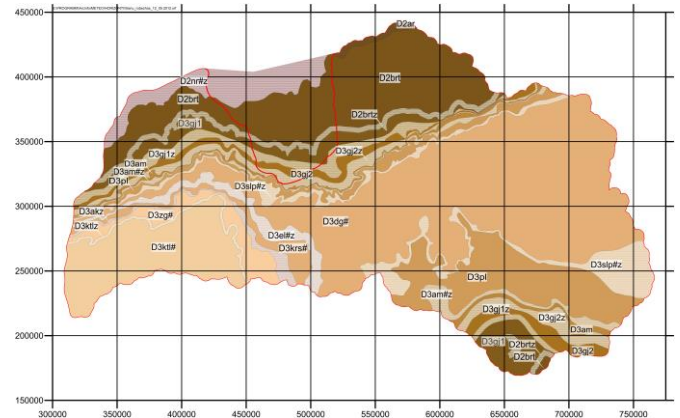


Fig. 3. Boundaries of primary geological strata.

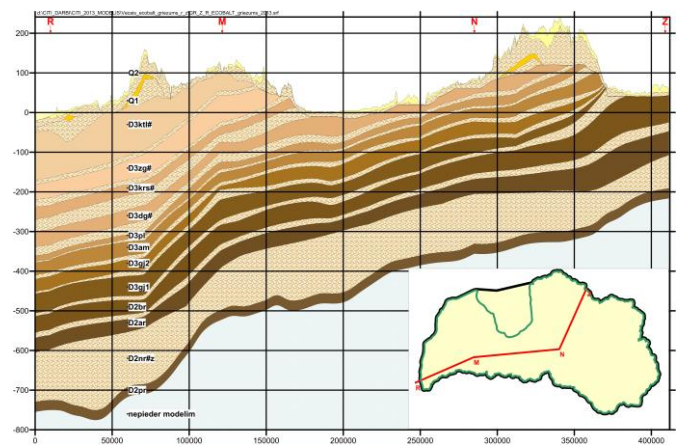


Fig. 4. Geological cross section.

II. APPLICATION OF PUMPING TEST RESULTS FOR REFINING TRANSMISSIVITY DATA

For the well pumping test in the confined aquifer the discharge rate *Q* was applied and the drawdown *S* of the groundwater head was observed. Mathematically the test is presented by the expression [4]:

$$S = \frac{Q}{2\pi T} (\ln(R/r) + \xi), T = km \tag{3}$$

where *R* are *r*-radiuses, accordingly, of the well depression cone and screen,  $\xi$  is additional hydraulic resistance that accounts for the partial penetrating factor of a well. From (3) one can obtain:

$$T = \frac{q}{2\pi} (\ln(R/r) + \xi), q = Q/S \tag{4}$$

where *q* is the well specific capacity of the well.

If *q* and *T* have the dimensions, [litre/(sec.meter)], and [(meter)<sup>2</sup>/day], respectively, then

$$T = 13.75q(\ln(R/r) + \xi). \tag{5}$$

All aquifers of LAMO for the primary strata are leaky and confined. Then  $R = 1.12B$  [5]:

$$B = \sqrt{\frac{km}{k_1/m_1 + k_2/m_2}} \quad (6)$$

where  $B$  is the leakage factor,  $T = km$  – transmissivity of the aquifer,  $k_1, m_1$ , and  $k_2, m_2$  are permeability and thickness of the leaky confining aquitards, accordingly, located above and below the aquifer. In Table I values of  $B, R$  and  $\ln(R/r)$  are given for a typical leaky confined aquifer of LAMO when  $r = (0.05 - 0.1)$  meter.

TABLE I  
COMPUTED VALUES OF  $B, R, \ln(R/r)$

$km$	$k_1, k_2$	$m_1, m_2$	$B$	$R$	$r$	$\ln(R/r)$
100	$10^{-4}$	10	1 581	1 771	0.1	9.78
100	$10^{-4}$	5	2 236	2 504	0.1	10.13
100	$10^{-4}$	10	1 581	1 771	0.05	10.47
100	$10^{-4}$	5	2 230	2 504	0.05	10.82

By exploiting the fact that in Table I  $\ln(R/r) \sim 10$ , one can approximate formula (5). If  $\xi = 0$  then the following formula roughly provides the minimal value  $T_{\min}$  of transmissivity for the confined aquifer:

$$T_{\min} = 137.5q. \quad (7)$$

In [4] the following formula is presented for computing of the resistance  $\xi$ :

$$\xi = (1/a - 1)(\ln 1.47ab - 2.65a), \quad a = l/m, \quad b = m/r \quad (8)$$

where  $m$  is the thickness of aquifer and  $l$  and  $r$  are, accordingly, the length and radius of the well screen. The formula can be used if  $m/r > 100, l/m \geq 0.1$ . In Table II the results given by (8) are presented.

TABLE II  
VALUES OF THE WELL HYDRAULIC RESISTANCE  $\xi$

$l/m$	$m/r$			
	100	200	500	1000
0.1	21.80	28.04	36.29	42.53
0.2	11.40	14.18	17.84	20.61
0.3	6.98	8.60	10.73	12.35
0.4	4.52	5.56	6.93	7.98
0.5	2.97	3.66	4.58	5.27
0.6	1.92	2.41	3.00	3.46
0.7	1.19	1.49	1.88	2.17
0.8	0.63	0.83	1.06	1.24
0.9	0.28	0.35	0.46	0.53
1.0	0.00	0.00	0.00	0.00

If one uses the geometrical well data  $l/m$  and  $m/r$  then the resistance  $\xi$  can be applied to refine the transmissivity  $T$ , as follows:

$$T = T_{\min}(1 + \xi/10) = cT_{\min}. \quad (9)$$

For LAMO, the typical values of  $l/m$  and  $m/r$  are within the limits:  $0.5 > l/m > 0.2; 500 > m/r > 100$ . Then, as it follows from Table II, the correction  $c$  may be within the limits:  $2.78 > c > 1.29$ .

### III. OBTAINING OF PERMEABILITY MAPS

It was explained before that the variable permeability  $k$ -maps must be used to control the  $T$ -maps of the GV system:

$$k = T/m \quad (10)$$

where  $T$  is the transmissivity derived from the well pumping data,  $m$  is the aquifer thickness which is computed and used by the GV system to obtain  $T = km$  of (2).

By using the EXCEL program [6] the set of the specific capacity  $q$  [litre/(sec.meter)] must be extracted from the well pumping data. As a rule the  $q$ -set contains very low and also very high values. In order to normalize the set, minimal and maximal values of  $q$  are fixed. The  $q$ -set contains  $n$  pointwise data. For LAMO  $n > 1000$  for practically all aquifers. Due to the large  $n$  the very fast gridding method of “inverse distance to power” is applied by the SURFER program [7]. This method computes the interpolated value  $\sigma_o$  at the node by using the available neighboring pointwise data  $\sigma_i = 137.5 q_i, i = 1, \dots, n$ , as follows [8]:

$$\sigma_o = \left( \sum_{i=1}^n \sigma_i \tau_i \right) / \sum_{i=1}^n \tau_i$$

$$\tau_i = (1/d_{oi})^p, \quad d_{oi} = \sqrt{(x_o - x_i)^2 + (y_o - y_i)^2} \quad (11)$$

where  $\tau_i$  weight of  $\sigma_i; d_i$  distance between the grid node  $o$  and the  $\sigma_i$  data location point;  $p$  weighting power;  $x_o, y_o; x_i, y_i$  coordinates, respectively, of the  $o$ -th grid node and the  $i$ -th point. The value  $p = 2$  is used, to prepare the data for LAMO.

The interpolation result of (11) is rather rough and, to smooth it, the moving digital “inverse distance” low-pass filter of size  $11 \times 11$  was used [9]:

$$\sigma_{oo} = \left( \sum_{i,j} \sigma_{ij} \tau_{ij} \right) / \sum_{i,j} \tau_{ij}, \quad \tau_{ij} = (1/D_{ij})^p, \quad D_{ij} = \sqrt{i^2 + j^2} \quad (12)$$

where  $\tau_{ij}$  filter weight;  $p$  the power ( $p = 0.5$  is applied);  $i$  and  $j$  the grid row and column local indices for the neighboring nodes with respect to the central node  $oo$  of the filter;  $D_{ij}$  the distance between the nodes  $oo$  and  $ij$ .

In Table III the first quadrant of the  $\tau_{ij}$  matrix of the filter (12) is shown. The filter contains four symmetrical quadrants, because negative  $i$  and  $j$  indices are also applied.

TABLE III  
WEIGHTS  $T_{ij}$  FOR THE FIRST QUADRANT OF THE 11×11 SIZE FILTER

$j$						
5	0.444	0.443	0.431	0.414	0.395	0.376
4	0.500	0.492	0.473	0.447	0.420	0.395
3	0.577	0.562	0.527	0.485	0.447	0.414
2	0.707	0.669	0.595	0.527	0.473	0.431
1	1.000	0.841	0.669	0.562	0.432	0.443
0	2.000	1.000	0.707	0.577	0.500	0.444
	0	1	2	3	4	5
						$i$

One can conclude from the values of  $\tau_{ij}$  given in Table III that smoothing provided by the filter is rather moderate in comparison with the corresponding averaging filter ( $p \rightarrow 0$ ) where all weight  $\tau_{ij} = 1.0$ . To preserve the information provided by pumping of wells, only one pass of filtering was done.

The “inverse distance” interpolation and filtering do not account for discontinuity of aquifers that include the  $m = 0$  areas. Therefore, for all nodes of the  $601 \times 751$  size grid of LAMO, interpolated and smoothed values of transmissivity  $T_{ij}$  are obtained. To obtain the permeability  $k$ -map from the  $T$ -grid, the formula (10) must be used where the thickness  $m$ -map is the divider. Only at the aquifer existing area where  $m > 0$ , reasonable values of the aquifer permeability  $k$  can arise when the operation (10) has been done. To mend the  $k$ -map produced by (10), the large values of  $k$  that are caused by the dividers  $\varepsilon = 0.02$  have to be replaced by the largest value of  $k_{\max}$  that can be found within  $m > 0$  area of the aquifer. The final  $k$ -distributions are obtained by applying the filter of (12). For the GV system the digital  $k$ -map is presented, as the following product:

$$k = k_{\text{norm}} k_{\text{mean}}, \quad k_{\text{norm}} = k / k_{\text{mean}}, \quad k_{\text{mean}} = \sum_{i=1}^n k_i / n \quad (13)$$

where  $k_{\text{norm}}$  – normalized  $k$ -map;  $k_{\text{mean}}$  and  $n$  – the mean value of  $k$  and the number of grid nodes at the  $m > 0$  area, accordingly.

TABLE IV  
SUMMARY OF CHARACTERISTIC PARAMETERS OF THE PRIMARY AQUIFERS OF LAMO

$C$	$L_C$	$m_{\text{mean}}$	$k_{\text{mean}}$	$k_{\text{min}}$	$k_{\text{max}}$	$T_{\text{min}}$	$T_{\text{max}}$	$(l/m)_{\text{mean}}$
D3ktl	5.44	62.89	2.12	0.5	4.5	82.66	214	0.15
D3zg	7.53	50.43	3.64	1.5	8.0	125.38	330	0.24
D3krs	9.34	22.71	5.95	2.3	10.0	121.17	263	0.36
D3dg	32.84	30.76	5.58	0.7	10.0	127.82	474	0.34
D3pl	44.10	22.98	6.11	1.3	20.0	146.9	513	0.55
D3am	46.52	22.11	4.69	1.5	8.5	94.87	212	0.53
D3gj2	51.17	26.55	5.58	2.2	10.0	136.00	282	0.49
D3gj1	56.66	31.79	5.24	1.6	10	145.62	244	0.51
D2brt	68.96	45.30	1.91	0.6	3.5	79.02	129	0.40
D2ar	68.96	41.00	2.13	0.65	4.0	80.64	133	0.50

In Table IV the summary of characteristic parameters for the primary aquifers of LAMO are presented. The data for the  $k$  and  $T$  values are preliminary, because they have been obtained due to rather rough approximations without accounting for the hydraulic resistances of individual wells. No checking of pumping data correctness has been done.

In Table IV the following acronyms are used:  $C$  is the code of aquifer;  $L_C$  is the area of aquifer [thous.km<sup>2</sup>];  $m_{\text{mean}}$  is the mean thickness [meter];  $k_{\text{mean}}$ ,  $k_{\text{min}}$ ,  $k_{\text{max}}$  are mean, minimal, maximal permeability [meter/day];  $T_{\text{mean}}$ ,  $T_{\text{max}}$  are mean, maximal transmissivity [(metre)<sup>2</sup>/day];  $(l/m)$  is mean parameter that can be used to compute the resistance  $\xi$  that is applied for the correction (9).

#### IV. CONCLUSION

Formerly, the constant values represented the permeability  $k$ -maps of LAMO. By using the information of well pumping, the upgraded variable  $k$ -maps have been created. To obtain them, the digital interpolation and image processing methods were applied. Currently the new  $k$ -maps are used in LAMO that results in refined transmissivity distributions of the HM primary aquifers. To make these results better the well geometrical data will be accounted for and the initial pumping data will be checked and corrected.

#### ACKNOWLEDGMENT

In 2010 – 2012 the hydrogeological model of Latvia LAMO has been developed within the framework of the project “Creating of Hydrogeological Model of Latvia to be Used for Management of Groundwater Resources and for Evaluation of their Recovery Measures”. The project was co-financed by the European Regional Development Fund.

#### APPENDIX

##### APPLICATION OF WELL PUMPING DATA FOR CREATING OF THE D3PL AQUIFER $k$ -MAP.

In Fig. 1a the location of wells is shown. They are not distributed evenly within the area of aquifer. Number of wells  $n = 1730$ ;  $5.0 > q > 0.3$ .

In Fig. 2a the interpolated and smoothed isolines of transmissivity are shown when the “inverse distance” method (11) and the filtering (12) have been applied. The results are existing in all nodes of the full LAMO area grid.

The  $m$ -map of the aquifer thickness is shown in Fig. 3a. One can notice that the map includes rather deep incisions of the Daugava and Saka river valleys.

In Fig. 4a the initial and filtered  $k$ -maps are shown. Filtering has eliminated the wrong uplift of the  $k$  values at the places of incisions of the Daugava and Saka river valleys.

Formerly the  $k$ -map for the D3pl aquifer was a constant value. The upgraded  $k$ -distributions of Fig. 4a are rather variable and, for this reason, the parameter  $k_{\text{mean}}$  is used as a part of the product (13) for the GV system.

The final refined  $T$ -map which is currently used by LAMO is shown in Fig. 5a. Due to filtering of the  $k$ -map at the location of incisions of the Daugava and Saka river valleys the transmissivity is correct.

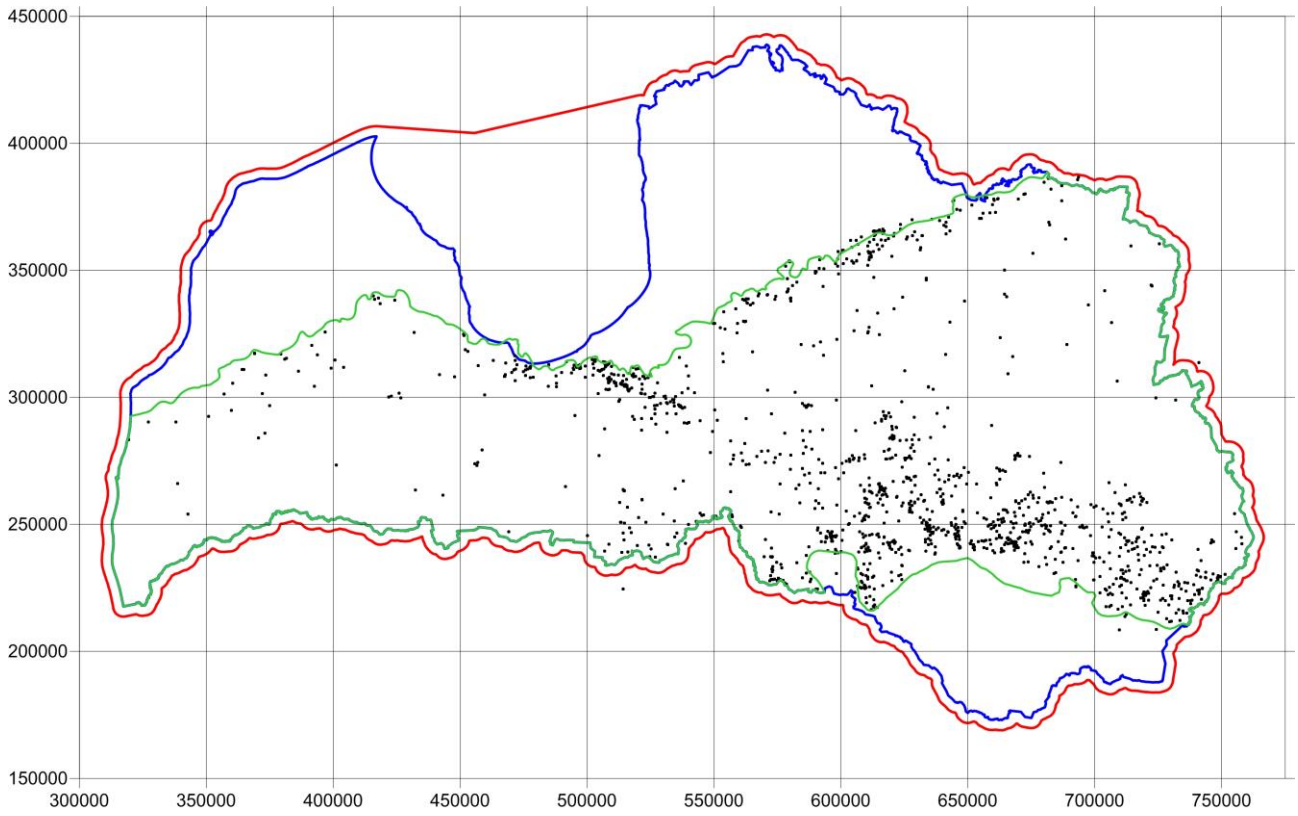


Fig. 1a. Location of wells for the D3pl aquifer.

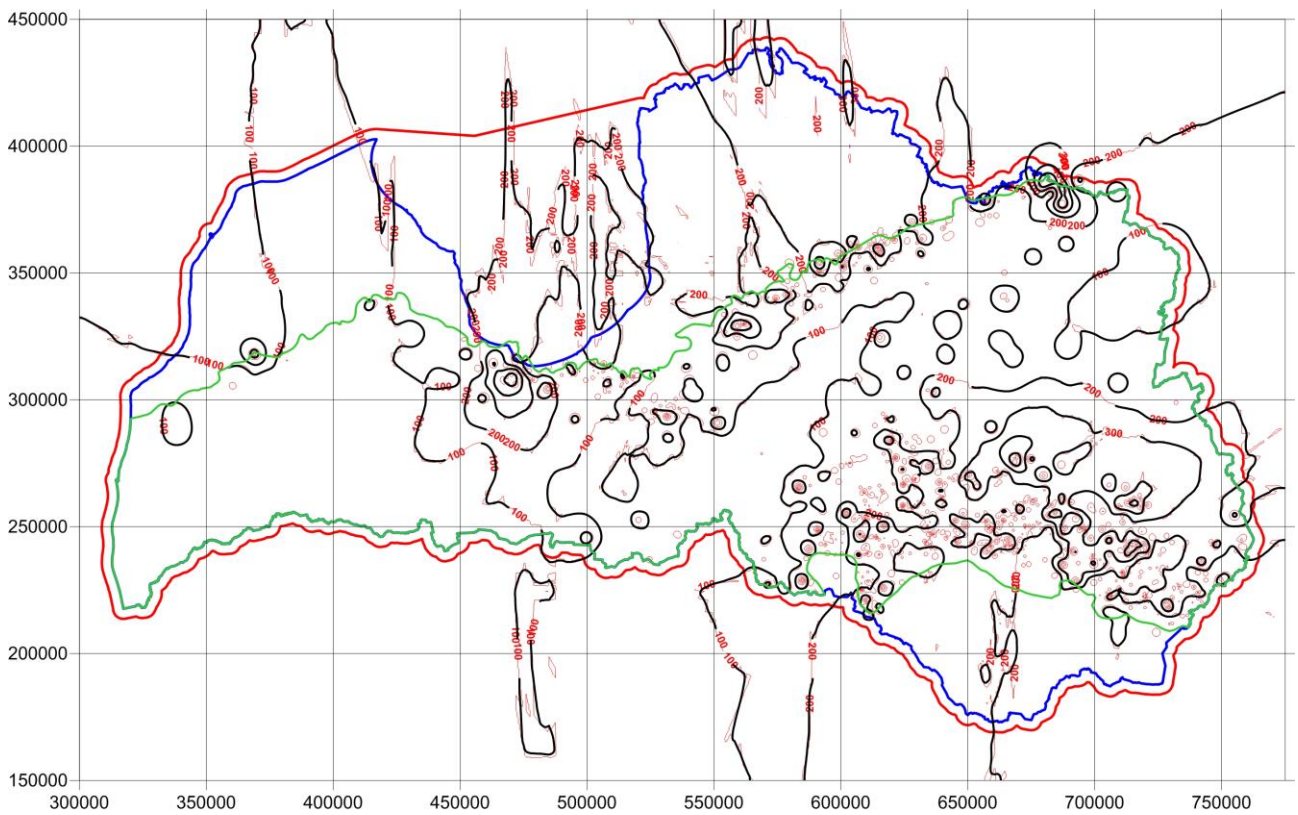


Fig. 2a. Interpolated (red) and smoothed (black) isolines of transmissivity.

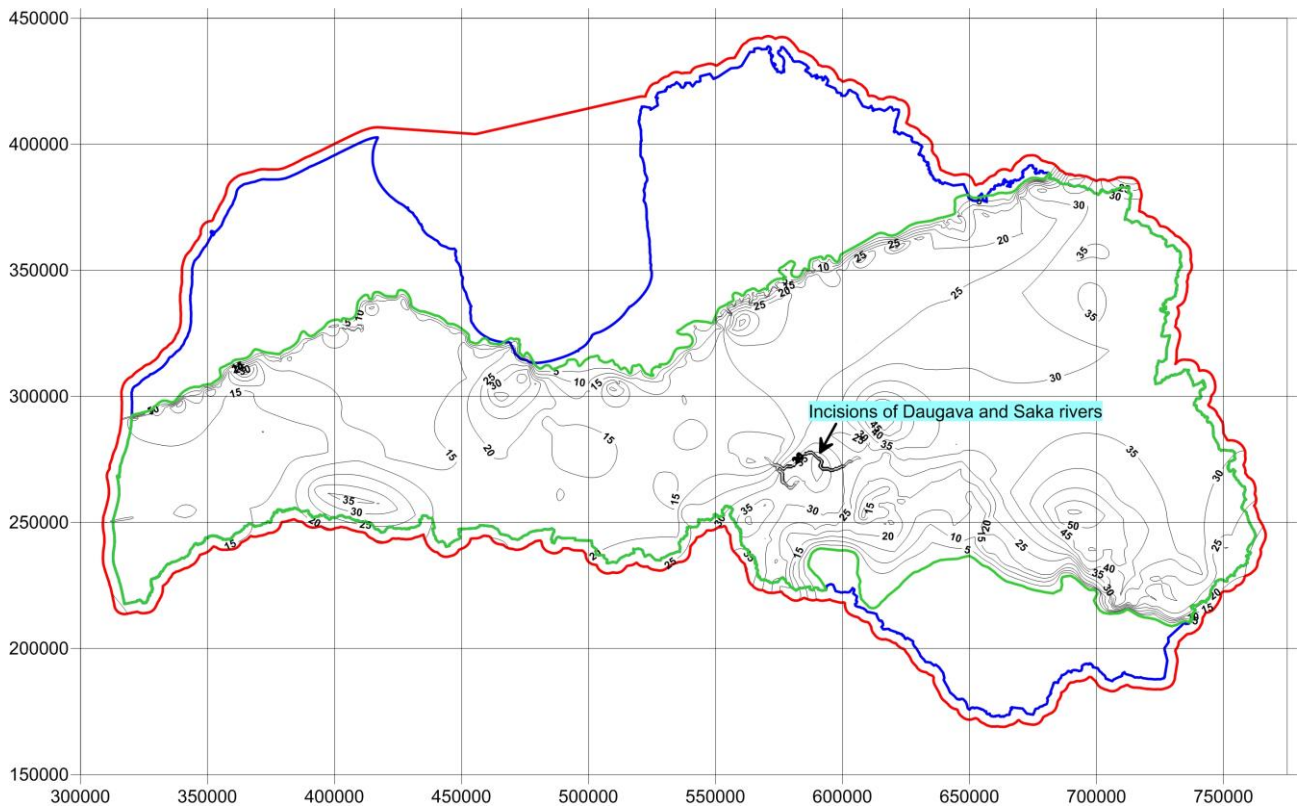


Fig. 3a.  $M$ -map for the aquifer thickness; incisions of the Daugava and Saka river valleys.

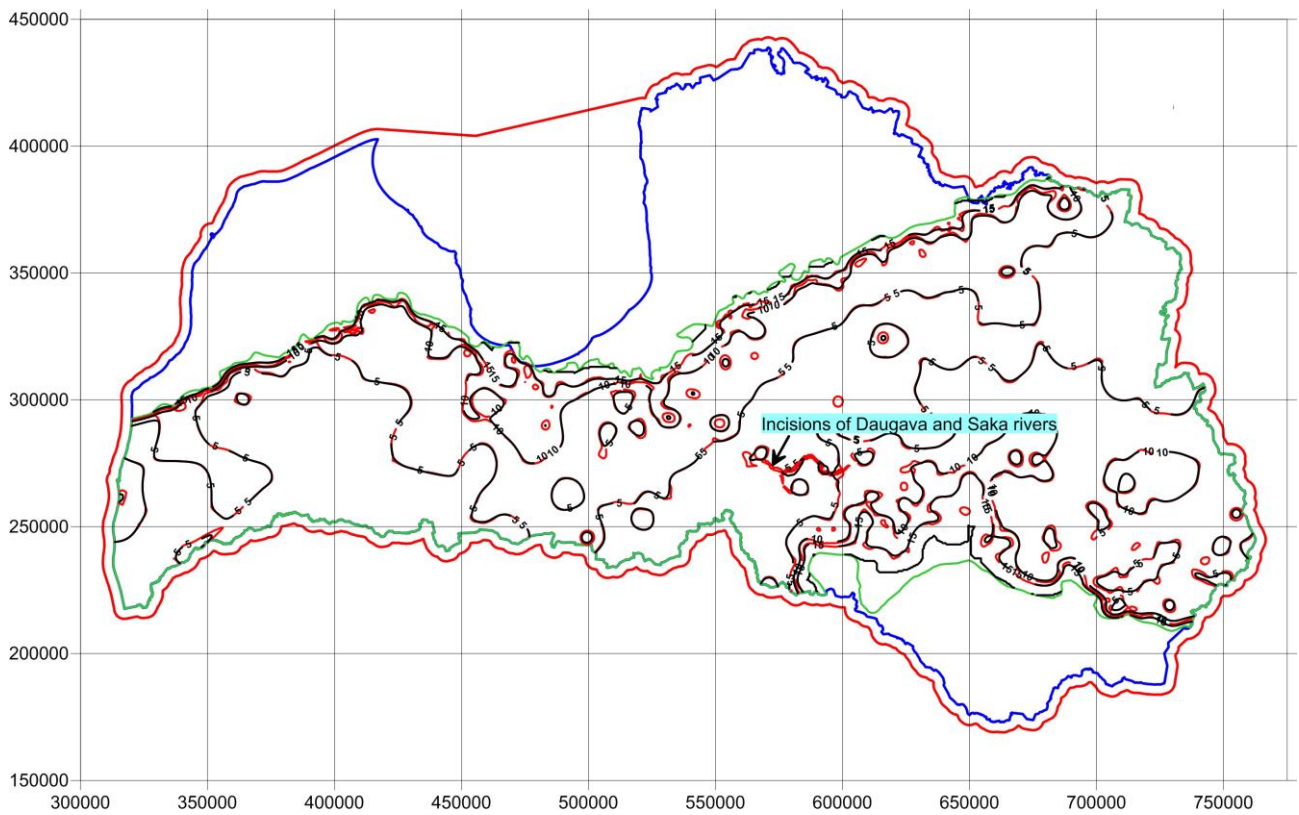


Fig. 4a. Initial and filtered  $k$ -maps (initial and filtered lines are red and black); filtering has eliminated the wrong uplift of the  $k$  values at the places of incisions of the Daugava and Saka river.

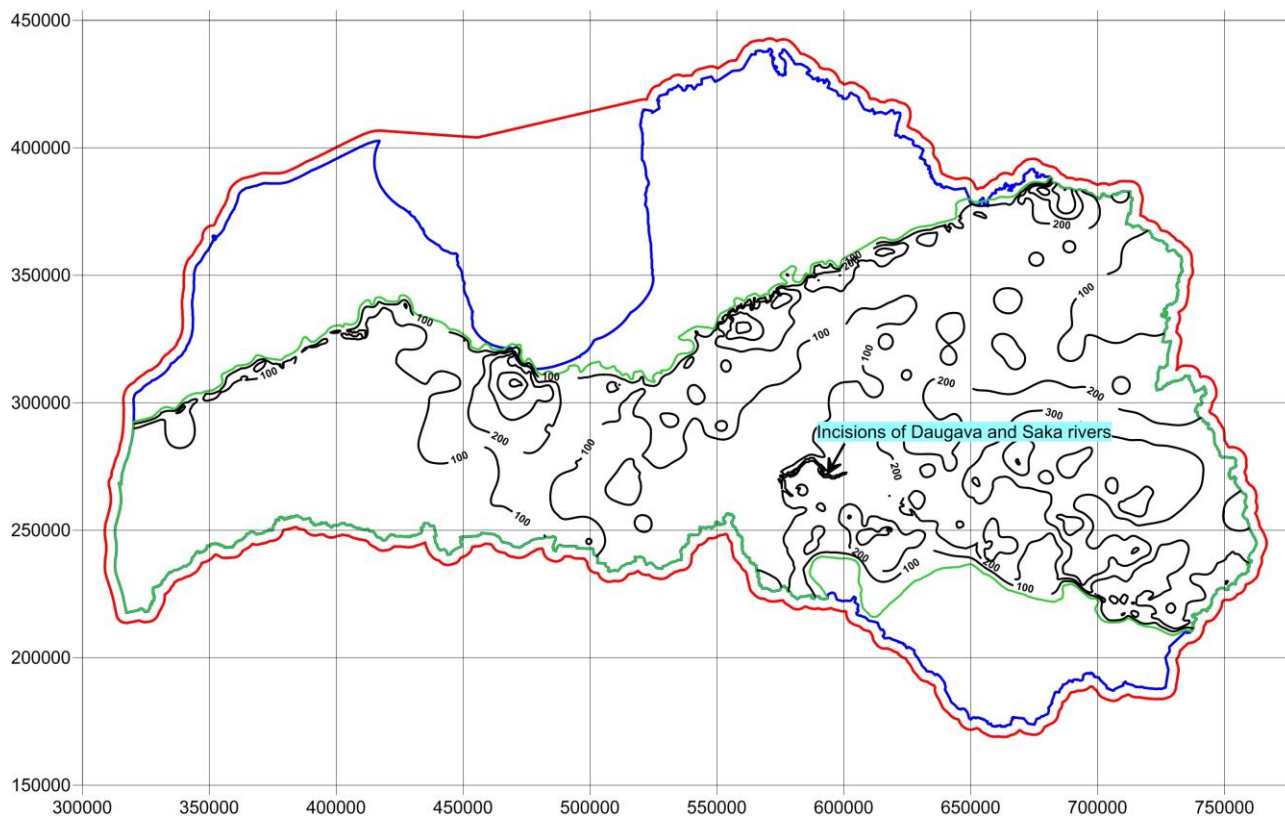


Fig. 5a. Final  $T$ -map. Places of the Daugava and Saka river incisions and transmissivity drops.

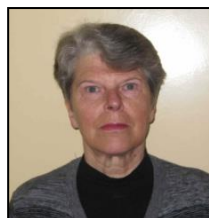
#### REFERENCES

- [1] A. Spalvins, J. Slangens, I. Lace, K. Krauklis, V. Skibelis, O. Aleksans, and I. Eglite, "Hydrogeological model of Latvia after increasing density of its hydrographical network," *Scientific Journal of Riga Technical University, Boundary Field Problems and Computer Simulation*, vol. 53, pp. 12–24, 2014.
- [2] A. Spalvins, J. Slangens, I. Lace, K. Krauklis, V. Skibelis, O. Aleksans, and N. Levina, "Hydrogeological model of Latvia, first results," *Scientific Journal of Riga Technical University, Boundary Field Problems and Computer Simulation*, vol. 53, pp. 4–13, 2012.
- [3] Environmental Simulations, Inc., "Groundwater Vistas. Version 6, Guide to using," 2011, [Online]. Available: [http://www.groundwatersoftware.com/groundwater\\_vistas.htm](http://www.groundwatersoftware.com/groundwater_vistas.htm) [Accessed: Sept. 5, 2012]
- [4] N. Verigin, *Methods Used for Finding Permeability of Geological Strata*. Moscow: Gosstroizdat, 1962 (in Russian).
- [5] N. Bindeman, and I. Jazvin, *Evaluation of Groundwater Resources*. Moscow: Nedra, 1982 (in Russian).
- [6] J. Walkenback, *Excel-7 Bible*. Indianapolis, Indian: Wiley Publishing, Inc., 2007.
- [7] Golden Software, Inc., "SURFER-11 for Windows, Users manual, Guide to Using," 2012. [Online]. Available: <http://www.goldensoftware.com/products/surfer> [Accessed: Sept. 23, 2012]
- [8] R. Franke, "Scattered Data Interpolation: Test of Some Methods," *Mathematics of Computations*, vol. 33, pp. 181–200, 1982.
- [9] I. Ditas, *Digital Image Processing Algorithms and Applications*, New York: John Wiley and Sons, 2000.



**Aivars Spalvins** was born in Latvia. In 1963, he graduated from Riga Polytechnical Institute (Riga Technical University since 1990) as a Computer Engineer. He is currently Head of the Environment Modelling Center of RTU. His research interests include computer modelling of groundwater flows and migration of contaminants.

E-mail: emc@cs.rtu.lv



**Inta Lace** was born in Latvia. In 1971, she graduated from Riga Polytechnical Institute (Riga Technical University since 1990) as a Computer Engineer. In 1995, she received the Master's degree in Applied Computer Science. Since 1991, she is a Researcher with the Environment Modelling Center, Faculty of Computer Science and Information Technology, RTU.

E-mail: emc@cs.rtu.lv

# Improvement of Teaching Methodology of Mathematics in Riga Technical University by Using Video Lectures

Sarmite Cernajeva, *Riga Technical University*

**Abstract** – Improvement of teaching methodology of mathematics by using video lectures is a current issue in Riga Technical University because teaching methodology largely determines the quality of studying. The aim of the article is to explore the possibilities of how, based on students' motivation, to improve the teaching methodology of mathematics and to promote active studies of mathematics. The material "E-learning materials made by Riga Technical University" was worked out to achieve the set goal which will help secondary school pupils to prepare themselves for studies at the university.

**Keywords** – Active studies, methodology of mathematics, video lectures.

## I. INTRODUCTION

The long-term goal for the development of Latvia is to have educated, creative and enterprising people. Nowadays the world needs specialists able to analyze complicated phenomena, determine the essence of problems and their solutions, synthesize and integrate various elements and can use information effectively and constructively cooperate with other people. Engineers are valued and needed specialists in labor market, which is why quality education in the professional activity for new engineers have important role in the future of the country. Experience shows that it is easier to study if one has accumulated good basic knowledge in sciences [7]. That is why YouTube channel was created in Riga Technical University, where learning videos were added that could help secondary school pupils to prepare for studies in university. Practical testing of this methodological material was done, paying special attention to promotion of the methodology of acquisition of mathematics [1]–[4].

Using method of theoretical literature analyses, psychological understanding of the adults was described in the article, as well as necessity of education for adults and motivation to study was discussed.

## II. PSYCHOLOGICAL ASPECTS OF ACQUISITION OF MATHEMATICS. MATERIALS AND METHODS

The theoretical ground for learning mathematics was worked out within Mathematics Education (ME).

At the beginning ME research was developed within cognitive psychology. Constructivism as a theoretical ground appeared in 1985 – 1995 and became a dominant theory, based on which ME research was carried out and justified [6], although, it should not be forgotten that traditional teaching of

mathematics is based on the grounds of behaviorism. The essence of ME theoretical ground is:

- Behaviorism – based on the observed changes in human behavior. New behavior model is repeated until it becomes automatic.
- Cognitivism – based on thinking process, which occurs in behavior. Changes in thinking are evaluated by changes in human behavior.
- Constructivism – based on each individual's individual organization of experience in report system, which serves for understanding the world. Facing a problem creates opportunity to save the change in the created report system.

Theoretical grounds of learning mathematics also determine the lecturer's role in the learning process.

In Behaviorism lecturer is thinking more about the teaching outcome than about the process. The learning process is isolated and not connected with other subjects. The methods used in work are one-way methods: from lecturer to student, the feedback is minimal.

In Cognitivism lecturer prefers evaluation methods that require constructive answers, projects, summaries, and tasks with several steps – everything that can reveal person's conceptual understanding better than tests or short answer tasks. Lecturer activates all stages of students' cognitive process – detection, realization, remembering and using.

The role of the lecturer seriously changes in Constructivism, because one of the main principals of constructivism claims that knowledge can never be transferred directly from one person to another. The only way that people can gain knowledge is either create, or construct it themselves. Thus, the task of the lecturer is to change the environment of students, so that they can construct themselves such cognitive forms which the lecturer wants to give them.

## III. SIGNIFICANCE OF UNDERSTANDING OF PSYCHOLOGICAL PECULIARITIES OF ADULTS IN ACQUISITION OF MATHEMATICS

Nowadays adult learning is becoming a lifestyle. Exploring the data from the employment statistics and their relationships with the educational level in European countries, we get proof that lifelong wholesome realized learning provides personality's fruitful action in professional and social life. As the role of mathematics increases not only in scientific-research but also in school, while working with various

computer programs, great attention must be paid to the quality of studies of mathematics in university study programs.

In adult education it must be taken into consideration that part time students gain education parallel to taking care of family and work obligations. Such students are not always psychologically ready to restart intensive study process; there are steady pictures in their minds about their abilities and knowledge that not always correspond with the reality. Pedagogue's first task is to assure students of their positive abilities and give the necessary knowledge about the study process in general. During the study process the lecturer is the person who is responsible for the students to gain or take over his/her experience or knowledge. Lecturer ensures quality study process through his/her own life experience, professional competence and arsenal of methodological techniques. Student is a person who wishes to gain this experience or knowledge and to take the opportunity in order to improve, to become creative in taking independent decisions and actions.

The pedagogue must create appropriate teaching plan and teaching methods for each specific group, where the stress is put on cooperation, positive motivation and perspective. The adult's personality and chosen goals must be taken into account during the contact.

As experience shows, the greatest problem for the applicants is the big amount of repetition material, which is why the lecturer must successfully organize both, usage of visual consumables, and atmosphere of positive contact, which would encourage the cognition in students and willingness to achieve good results. To facilitate the repetition process for the participants, great attention must be paid to usage of visual learning materials.

It is advised that the learning materials for studies are visualized as much as possible, giving the opportunity to see the material both as a whole, and in details. Parallel to the example of the task solving, theoretical grounds and explanations must be given. Students, who are combining studies with work and are able to attend only part of the offered classes, want to receive short and specific information. Their attitude towards obligatory homework is negative, thus they want to receive learning material that is appropriate for independent work – concise, understandable and with ready examples of problem solving. To create the interest, lecturer must be not only knowledgeable but also organize lectures so that students are not bored and they do not lose attentiveness. Nowadays pedagogy suggests that most important is the correlation of the lecturer and the student that involves psychological and practical preparation for action, realization of action and evaluation. The mastery of lecturer is in the ability to choose such teaching methods that evoke activity in students and create positive atmosphere in the study process. During the process of educational changes methods have more significant role than study programs, textbooks or teaching computer programs, because textbooks, or computer programs do not promote the quality of education, if the pedagogue does not have the necessary skills to use them.

Nowadays a significant place in the list of teaching methods

is for e-learning. UNESCO experts define e-learning as „studies with the help of the Internet and media” [12]. E-learning can easier be defined as the usage of the Internet and digital technologies to create experience that requires improving learning methods in education.

The usage of technologies during the study process allows differentiating creation of skills of problem solving during the lessons. It gives a chance for a teacher to demonstrate also his/her own creativity and talents. H. Borko and A. Vitkombms mention an important aspect of the teachers' knowledge of language, which in multicultural environment is especially important [12].

ICT usage is approved in all countries, thus, data from international surveys state that ICT is being rarely used in mathematics lessons. Wider research and data about positive influence of ICT usage in teaching mathematics could promote and push it to an effective use. Each student is a personality with his own skills, information acquisition speed, abilities and interests. That is why study programs of mathematics and didactics must be improved based on ICT (devoting more attention to the use of mathematics, including using ICT), creating learning materials based on modern technologies and ensuring access to them in internet. It provides the opportunity to:

- Facilitate lecturers' work during the classes and in preparation for them through using ICT to visualize learning materials and in continuous improvement of them;
- Place the materials in internet, which would significantly facilitate studies for those students that work and are not able to regularly attend lectures;
- Gain skills and habits to use ICT widely in students' everyday work when acquiring e-materials.

Thus, by using ICT possibilities during the implementation of the study programs of mathematics, we will not only facilitate the work of lecturers and make adult study process more interesting and effective, but also significantly improve the quality of the higher education and the level of training of specialists for labor market.

Although the development of technologies has promoted the progress of this type of teaching, technology cannot be considered an end in itself, but as a tool for better and easier learning. It is confirmed by Hannafin, Land and Oliver [13], suggesting that technological tools must be used under psychological and pedagogical preconditions. Mioduser, Nachmias, Oren and Lahav [15] warn about the tendency “for technology to go one step forward, but pedagogy – two steps back”.

#### IV. NECESSITY OF THE ADULT EDUCATION AND MOTIVATION TO STUDY

Mathematics has many practical applications both in our everyday life and also in fields of modern science and technology. Mathematical models are used in many economic and social processes of our lives, they are more and more included in technical and social artifacts and that is why often become „invisible” for ordinary people [14].

For the work of mathematics lecturer to be effective, he/she must know the subject well and must understand how to teach it. Positive attitude towards mathematics and self-confidence in the acquisition of it is also connected with better results in mathematics. These motivating aspects influence the decisions about involvement in the learning trends or educational programs with deeper acquisition of mathematics. As the motivation to acquire mathematics is a set of motives that create and keep an active learning process in the acquisition of mathematics, learners should be helped to structure and plan studies to motivate them. One of the conditions to find out the most effective ways to motivate the learners to actively acquire mathematics is relying on peculiarities of the age of students.

Methodology of teaching greatly determines the quality of learning. Pedagogue's task is to help students to acquire knowledge and skills, the most important of which is – the skill to learn.

The word “method” comes from the Greek language and in direct translation means „road to something”. Teacher's and student's didactic cooperation system is the teaching method, with the help of which students gain new knowledge, skills and abilities at the same time developing also their own cognitive skills [9]. Teaching method means teachers and students joint methods of activity during the learning process that help to carry out certain tasks.

There is no single comprehensive classification of teaching methods, different authors group them differently. Voldemar Zelmenis [10] suggests the following division:

- By types of cognition (mutual, visual and practical methods);
- By main tasks of methods (knowledge gaining, creation of skills and abilities, development of abilities and methods of evaluation);
- By the activity of students' cognition and independency in studies (dogmatic, reproductive, problematic and research methods).

It is important to evaluate the level of learning motivation in the acquisition of mathematics of learners, because, only after the pedagogue knows it he/she can better organize the educational process for students. Professor J. Mencis points out that during the process of acquisition of mathematics minimal level can be distinguished, and reaching it has the crucial role in whole further mathematical development. The minimal level refers to understanding and remembering separate mathematical concepts, as well as to creation of the separate „node” abilities. Professor J. Mencis stresses that the acquisition of mathematics can happen only if students actively think along during the solving process of tasks [11]. Moreover, to achieve the minimal necessary level basic exercises have crucial role.

“Learning mathematics is a road from the known to the unknown, from understanding to the not yet understood, from question to answer. A system that gives opportunity to save efforts and achieve as much as possible is needed here,” that is what professor E. Ģingulis writes in [5].

## I. EXPERIMENTAL VERIFICATION OF HANDOUTS

The author carried out a survey of groups of students in RTU where she works. In the beginning of the semester students were informed about the research, about its significance in the further activation of the cognition process of learning and what students will gain from it.

## V. RESULTS OF SITUATION ANALYSIS

The task of the pedagogue is to keep the interest of the learner with pedagogical methods. The subjects that are not closely connected with the future profession or other life plans of the learner must be offered in the way that is acceptable, so that it does not cause aversion. The video material [8] that was made and tried out in practice by the author helped learners to understand separate mathematical questions, gave support for individual work in the acquisition of mathematics, helped to prepare for the tests and, as a result, promoted motivation of learners for active studies of mathematics.

## REFERENCES

- [1] D. Āboltiņa, D. Kriķis, and K. Šteiners, *Matemātika 10. klasei*. Rīga: Zvaigzne ABC, 2011.
- [2] D. Āboltiņa, D. Kriķis, and K. Šteiners, *Matemātika 11. klasei*. Rīga: Zvaigzne ABC, 2013.
- [3] D. Āboltiņa, D. Kriķis, and K. Šteiners, *Matemātika 12. klasei*. Rīga: Zvaigzne ABC, 2013.
- [4] D. Kriķis, *Matemātika 11. klasē. Skolotāja grāmata*. Rīga: Zvaigzne ABC, 2013.
- [5] E. Ģingulis, *Kā saprast un iemācīties matemātiku*. Rīga: RaKa, 2005.
- [6] B. Handal, “Teachers' Mathematical Beliefs: A Review,” *The Mathematics Educator*, vol. 13, no. 2, pp. 47–57, 2003.
- [7] A. D. Semushin, *Iz opyta prepodovaniya matematiki v shkole*. Moskva: Prosveshhenie, 1978.
- [8] RTU eMācībās. [Online]. Available: [http://www.youtube.com/results?search\\_query=rtu.emacibas.lv](http://www.youtube.com/results?search_query=rtu.emacibas.lv) [Accessed May 23, 2014]
- [9] *Pedagoģijas terminu skaidrojošā vārdnīcā*. Rīga: Zvaigzne ABC, 2000.
- [10] V. Zelmenis, *Pedagoģijas pamati*. Rīga: RaKa, 2000.
- [11] A. Šmite, *Izglītības iestādes vadība I daļa. Pedagoģis. Organizācija. Pārmaiņas*. Rīga: RaKa, 2004.
- [12] H. Borko, and A. Whitcomb, “Teachers, Teaching and Teacher Education: Comments on the National Mathematics Advisory Panel's Report,” *Educational Researcher*, vol. 37, 2008.
- [13] P. Rabardel', *Ljudi i tehnologii (kognitivnyj podhod k analizu sovremennyh instrumentov)*. Moskva: Institut psihologii RAN, 1999.
- [14] M. J. Hannafin, S. Land, and K. Oliver, “Open learning environments: Foundations, methods, and models,” in *Instructional-design theories and models*, 2 edition, C. M. Reigeluth, Ed. Mahwah, NJ: Erlbaum, 1999, pp. 138–140.
- [15] D. Mioduser, R. Nachmias, A. Oren, and O. Lahav, “Web-based learning environments: Current states and emerging trends,” in *Proceedings of EdMedia'99*, Seattle, Washington, 1999, pp. 753–758.



**Sarmite Cernajeva** received the Diploma in Mathematics from the University of Latvia in 1984, and the Master's degree in Education Sciences from the Pedagogical Academy of Liepaja in 2003. Since 2008 she has been a Doctoral student with the Latvia University of Agriculture. She currently is a lecturer with the Department of Engineering Mathematics at Riga Technical University.

Her research interests include issues of mathematical pedagogy. She is a member of the Latvian Mathematical Society.

E-mail: sarmite.cernajeva@rtu.lv